Characterizing the Immune Cell Transcriptomic Response to Sustained Low Dose Ionizing Radiation Exposure

Bryan Marr

Supervisors: Seung-Hwan Lee, PhD & Arvind Mer, PhD

A thesis submitted to the University of Ottawa in partial fulfillment of the requirements for the MSc degree in Microbiology and Immunology

Department of Biochemistry, Microbiology and Immunology

Faculty of Medicine

University of Ottawa

Abstract

This study investigates the effects of sustained low dose ionizing radiation (LDIR) exposure on the murine immune system, focusing on the molecular mechanisms and cellular responses to low dose rate whole-body γ-radiation. Female C57BL/6 mice were continuously exposed to low dose rate ^{60}Co γ-radiation over a period of 7 days, resulting in cumulative absorbed doses of 10 mGy and 100 mGy. Immediately following the exposure period, hematological analysis, flow cytometry, bulk RNA-sequencing, and single-cell RNA-sequencing were employed to comprehensively assess immune cell populations and their gene expression profiles.

Our findings indicate that the LDIR exposure model employed induced, at most, minimal perturbations to the immune system. Hematological metrics showed no significant changes in the abundance of hematopoietic cells in blood. Flow cytometry revealed no significant differences in the proportion of immune cell subsets in the spleen, thymus, and bone marrow across radiation conditions. Transcriptomic analyses identified minimal differentially expressed genes of low magnitude. Unsupervised single-cell RNA-seq analysis further confirmed the absence of significant perturbations to immune cell transcriptomes.

These results suggest a preservation of immune cell homeostasis under sustained low dose-rate exposure conditions. This study represents the first single-cell transcriptomic investigation of immune cells following whole-body exposure to low dose ionizing radiation. It contributes to a broader understanding of radiation biology, emphasizing that the effects of low-dose radiation on the immune system can be limited at very low dose-rates in mice. These findings may inform future research on radiation exposure and contribute to assessing the risks associated with chronic low-dose radiation in various contexts, from medical treatments to occupational exposures.

Acknowledgements

I wish to extend my profound gratitude to my supervisor, Dr. Seung-Hwan Lee, whose guidance and benevolent mentorship have profoundly shaped both my academic and personal growth. I am deeply grateful for your passionate commitment to my scientific training, imparting me with your expertise, entrusting me with challenges, and fanning the flames of my curiosity. Your support has been the keystone of my journey, continuously inspiring me to pursue excellence.

Additionally, I would like to express my appreciation to the members of my SH Lee lab family, especially Dr. Abrar Khan, Shelby Kaczmarek, Donghyeon Jo, Simin Ahmadvand, Safa Ghaziasgar, and Oksu Shin. Your camaraderie, mentorship, and collaboration have rendered my graduate studies productive and imbued them with enjoyment.

I wish to further extend my gratitude to Dr. Abrar Khan, whose partnership has been pivotal in shaping this thesis project. As a collaborator, you have propelled my research forward, imparted deep expertise, and served as a source of inspiration. Your commitment to a productive and dedicated scientific practice has set a high standard, motivating me to strive for excellence in my training.

I want to express my sincere appreciation to the members of my thesis advisory committee. I am grateful for the guidance of my co-supervisor Dr. Arvind Mer on this project. Furthermore, I am thankful that he helped cultivate my interests in computational biology, broadening my training and research horizons. Additionally, I would like to thank Dr. Jim Sun and Dr. Scott McComb for advising my studies and providing kind and motivational support that bolstered my confidence and perseverance.

The realization of this thesis project would not have been possible without the collaboration and support of the Canadian Nuclear Laboratories (CNL). Therefore, I extend my thanks to Holly Laakso and Melinda Blimkie for their indispensable contributions to our low-dose radiation research endeavors. Your expertise and assistance have been essential in shaping the intellectual design and execution of this study.

Special acknowledgment is reserved for Dr. David Cook, whose generous mentorship enriched both my research projects and personal growth. Sharing your technical expertise has empowered me to

explore new directions in science, and I have gleaned valuable insights from our discussions about your passions and professional experiences.

I would also like to extend a profound gratitude to the Mitacs Accelerate Fellowship program. This fellowship empowered me to live happily and healthily as a graduate student, relieving pressures of graduate studies. I am honored to be supported and recognized by this prestigious award.

I am deeply grateful to my friend Alexis, whose support and intellectual partnership have been instrumental throughout my university journey. Our exchange of motivation and collaboration remains a powerful force driving success in our academic endeavors.

With profound love and gratitude, I extend my deepest appreciation to my family. To my beloved husband, Chris, it is my greatest joy to share life at your side. Your love, infectious laughter, and adventurous spirit make every moment brighter. Moreover, your confidence and intelligence greatly inspire me to approach life with conviction. Together, we have applauded the victories and weathered the storms of our academic pursuits, and this year we celebrate the achievement of academic milestones. While I eagerly anticipate the possibilities that await us, I am confident that we will continue to share a pursuit of joy and silliness hand in hand. I am grateful for our cat, Oliver, who habitually sits right next to or directly on top of my keyboard as I pore over papers and analyze data. By proxy to my studies, Oliver may himself meet the requirements for this Master's degree.

I extend my deep gratitude to my mother, without whom my academic pursuits would not have been possible. Thank you for being a pillar of love and encouragement. Your support gives me a sense of security I cherish. Your commitment to work and family has set a high standard I hope to match someday. To my brother, thank you for your steadfast companionship. Your visits to Ottawa, routine calls, and late-night video gaming are cherished moments in my life. My mother and brother have been my unwavering cheerleaders, powering my drive forward.

To my dad, while your treatment journey represents an overwhelmingly difficult experience, it also ignited my passion for science, propelling me into university studies and fueling my determination to contribute to biomedical science. I am forever captivated by the way you embraced every moment and

lived with boundless energy and love for life. You are forever, in my heart. This thesis is dedicated to your memory and the enduring legacy of your strength and joy.

Preface

During my master's research, I undertook a significant project characterizing the effects of chronic low-dose radiation on the immune system. This thesis project aimed to comprehensively unravel the response of various immune cell populations to sustained low-dose radiation exposure. This research is crucial for addressing several critical knowledge gaps and understanding the broader implications of radiation exposure, holding significant potential for improving public health and safety.

Additionally, I had the privilege to continue a project initiated during my undergraduate studies. This project focused on potentially enhancing CAR NK cell functionality by overexpressing the IL-2 receptor alpha subunit. Given the extensive time and effort invested in this endeavor, and valuable preliminary results, my thesis advisory committee and I agreed on the importance of documenting this project within the appendix of my thesis.

By including a detailed account of this work in the appendix, I aim to highlight the breadth of my research activities and provide a comprehensive overview of my contributions to the fields of both radiation biology and cancer immunotherapy. Moreover, it is my firm belief that documenting the preliminary results and proposed experiments of this secondary project is essential for future scientific progress. This detailed record serves not only as a testament to the work accomplished during my tenure but also as a valuable resource for future researchers who may wish to build upon this foundation.

Therefore, this thesis comprises two major components: the primary investigation into the effects of chronic low-dose radiation on the immune system and a short appendix detailing the CAR NK cell engineering project. Together, these sections encapsulate the full scope of my research efforts and underscore the multifaceted nature of my academic pursuits. I am grateful for the guidance and support of my advisory committee, whose encouragement has been instrumental in the completion of this body of work.

Table of Contents

List of Abbreviations

ARS	Acute Radiation Syndrome
ATM	Ataxia-Telangiectasia Mutated
ATR	Ataxia-Telangiectasia And Rad3-Related
BER	Base Excision Repair
CAR	Chimeric Antigen Receptor
CBA	Cytokine Bead Assay
CDK	Cyclin-Dependent Kinase
CDP	Common Dendritic Cell Progenitors
CHK	Checkpoint Kinase
CKI	Cyclin-Dependent Kinase Inhibitor
CNL	Canadian Nuclear Laboratories
CNSC	Canadian Nuclear Safety Commission
CRS	Cytokine Release Syndrome
CTD	C-Terminal Domain
DDR	DNA Damage Repair
DEG	Differentially Expressed Gene
DNA-PK	DNA-Dependent Protein Kinase
DSBs	Double Stranded Breaks
EMR	Electromagnetic Radiation
ERR	Excess Relative Risk
FBS	Fetal Bovine Serum
GMP	Granulocyte-Monocyte Progenitors
GO	Gene Ontology
Gpx	Glutathione Peroxidase
GSEA	Gene Set Enrichment Analysis
GSH	Glutathione
GST	Glutathione S-Transferase
Gy	Gray
HDIR	High-Dose Ionizing Radiation
HR	Homologous Recombination
ICANS	Immune Effector Cell-Associated Neurotoxicity Syndrome
ICRP	International Commission On Radiation Protection
IL	Interleukin
IR	Ionizing Radiation
LDIR	Low Dose Ionizing Radiation
LDRT	Low-Dose Radiation Therapy
LET	Linear Energy Transfer
LNT	Linear No-Threshold
LSS	Lifespan Study
MC	Mitotic Catastrophe
MCH	Mean Corpuscular Hemoglobin
MDIR	Moderate Dose Ionizing Radiation
MDP	Monocyte-Dendritic Cell Progenitors
MEP	Megakaryocyte-Erythroid Progenitors

MOMP	Mitochondrial Outer Membrane Permeabilization
MPS	Million Person Study
MRN	Mre11-Rad50-Nbs1
NADPH	Nicotinamide Adenine Dinucleotide Phosphate
NAS	National Academy Of Sciences
NHEJ	Non-Homologous End-Joining
Nrf2	Nuclear Factor (Erythroid-Derived 2)-Like 2
NTE	Non-Targeted Effects
PARP1	Poly(ADP-Ribose) Polymerase 1
PBMC	Peripheral Blood Mononuclear Cell
Pol	Polymerase
pSTAT5	Phosphorylated Signal Transducer And Activator Of Transcription 5
RBC	Red Blood Cell
RIBE	Radiation Induced Bystander Effect
RIL	Radiation Induced Lymphopenia
ROS	Reactive Oxygen Species
RPA	Replication Protein A
SAC	Spindle Assembly Checkpoint
scRNA-seq	Single-Cell RNA Sequencing
SOD	Superoxide Dismutase
SSBR	Single Stranded Break Repair
SSBs	Single Stranded Breaks
Sv	Sievert
TBI	Total Body Irradiation
Trp53	Transformation related protein 53
TGFb	Transforming Growth Factor Beta
UMAP	Uniform Manifold Approximation and Projection
UMI	Unique Molecular Identifier
UNSCEAR	United Nations Scientific Committee On The Effects Of Atomic Radiation
UT	Untreated
WBC	White Blood Cell
XRCC1	X-Ray Repair Cross-Complementing Protein 1
γH2AX	Phosphorylated H2AX

List of Figures

1 Introduction

Across the modern world, ionizing radiation (IR) is widely used across various sectors. It powers vital medical diagnostics, fuels the engines of energy production, drives industrial tools and processes, and is wielded in weapons of mass destruction. In Canada, about 15% of the country's energy is derived from 22 nuclear power plants[1]. As the application of this energy increases, so does the population exposed to anthropogenic IR, particularly among the growing working population occupationally exposed to it. Therefore, understanding the interplay between ionizing radiation and our cellular machinery is imperative. This thesis investigates the effects of sustained low-dose ionizing radiation (LDIR) exposure on the murine immune system, addressing a critical need to elucidate these effects. The findings hold significant implications for public health policies, occupational safety standards, and medical practices.

1.1 What is Ionizing Radiation?

The term 'Radiation' encompasses a broad spectrum of physical phenomena, ranging from electromagnetic waves to particulate radiation. Radiation can be defined simply as energy in the form of moving waves or streams of particles. This highlights a core concept in radiation physics: wave-particle duality. This phenomenon posits that particles, such as photons and electrons, can exhibit both wave-like and particle-like behaviour. This duality is quantified by the de Broglie wavelength, which is inversely proportional to the particle's momentum, indicating that particles with higher momentum exhibit shorter wavelengths and more particle-like behaviour[2]. The type, energy, and quantity of radiation, whether in the form of high-energy gamma rays or lower-energy radio waves, determine how it interacts with matter, influencing the potential biological and chemical impacts of exposure.

Electromagnetic radiation (EMR) is classically defined as energy propagating through space in the form of transverse waves of oscillating electric and magnetic fields. From a quantum perspective, electromagnetic radiation can be described as streams of photons, where photons are massless, uncharged fundamental particles of light carrying discrete energy and having momentum. These dual

perspectives aid in the description of wave-like EMR behaviour, such as interference and diffraction, and particle-like EMR behaviour such as the photoelectric effect. The energy of electromagnetic radiation is directly proportional to the frequency and inversely proportional to the wavelength of the associated wave[2]. The electromagnetic spectrum categorizes electromagnetic radiation based on frequency and wavelength, ranging from low-frequency, low-energy radiation such as radio waves, microwaves, and visible light to high-frequency, high-energy radiation such as X-rays and gamma rays.

Particle radiation consists of atomic or subatomic particles that are ejected during nuclear processes. These particles have mass and can be organized into electrically charged or non-charged particles. Charged particle radiation, such as emitted alpha particles and beta particles, will interact with matter differently than non-charged neutron radiation. Unlike electromagnetic radiation, particle radiation is not typically described as waves because the particles involved (such as electrons, protons, and neutrons) have significant mass and interact with matter primarily through collisions and ionization processes, rather than through wave-like properties.

The category ionizing radiation (IR) encompasses a subset of radiation that possess sufficient energy to displace electrons in the material through which it passes. This type of radiation is potent enough to break the bonds holding electrons within an atom, which is a fundamental characteristic that differentiates it from non-ionizing radiation. It is generated from various sources, including natural sources such as cosmic rays from space and radioactive materials in the Earth's crust, as well as anthropogenic sources such as medical imaging equipment, nuclear reactors, and certain types of industrial equipment. In these contexts, ionizing radiation is generated during nuclear processes and reactions, such as nuclear decay, fission and fusion, and the acceleration of subatomic particles.

In nuclear decay, unstable high-energy atomic nuclei lose energy by emitting radiation to achieve a more stable lower-energy state. Several types of nuclear decay exist. In alpha decay, a large heavy nucleus typically made unstable by electrostatic repulsions between a large number of protons will release an alpha particle (consisting of two protons and two neutrons), resulting in a new element with a lower atomic number. Beta decay occurs when a nucleus with an imbalance between protons and neutrons. In beta-plus decay, a proton in an unstable, proton-rich nucleus is transformed into a neutron

while emitting a positron (the antimatter counterpart of an electron) and a neutrino. In beta-minus decay, a neutron in an unstable, neutron-rich nucleus is transformed into a proton while emitting an electron (known as a beta particle) and an antineutrino. Gamma rays are emitted when an excited atomic nucleus releases excess energy to transition to a lower-energy state. This typically occurs following beta or alpha decay, or during nuclear fission and fusion reactions, where the resulting nucleus is often left in an excited state. Cobalt-60 is a man-made isotope frequently used in biological radiation research. It is also commonly used in medical applications, such as radiotherapy for cancer treatment, and in industrial applications, including radiography and sterilization. It decays through beta-minus decay transforming into nickel-60. The resulting nickel-60 nucleus is often left in an excited state and subsequently emits gamma rays to reach its ground state.

Beyond nuclear decay, both nuclear fission and fusion reactions release ionizing radiation. Utilized in power plants, nuclear fission involves the bombardment of a heavy nucleus with a neutron, splitting the nucleus into two smaller ones and releasing neutrons and high-energy photons in the process. Those neutrons can go on to cause fission of other atoms nearby, leading to a chain reaction of fissions. The photons are generated by the daughter nuclei, which can be left in an excited state following fission and release a gamma ray to reach ground state or be a radioactive isotope which will go through beta decay, releasing gamma rays. In the sun, elements are created via nuclear fusion when light atomic nuclei combine to form a heavier nucleus, releasing energy in the process. Ionizing radiation from these solar reactions reaches the earth in the form of ultraviolet light and high-energy particles.

The ionization process from ionizing radiation exposure occurs through multiple mechanisms[3,4]. In the photoelectric effect, a low-energy photon is completely absorbed by an atom, transferring all its energy to an orbital electron. This causes the electron to be ejected from the atom, leading to ionization. The photoelectric effect is more pronounced at lower photon energies and in materials with higher atomic numbers, where electrons are more tightly bound. In contrast, the Compton effect occurs predominantly at higher photon energies, such as those from gamma rays. In this process, a high-energy photon collides with an orbital electron, transferring part of its energy to the electron and ejecting it from the atom. The photon is then deflected with a reduced energy, continuing its path as scattered

radiation. This scattering effect contributes significantly to ionization in biological tissues exposed to high-energy radiation.

Charged particle ionization occurs through Coulomb forces, where particles such as alpha or beta particles (which are charged) interact with the electrons of an atom. Charged particles lose energy and slow down as they pass through matter due to collisions with atoms involving electrical forces of attraction or repulsion. These forces can ionize atoms by separating orbital electrons. Part of the energy is used to overcome the electron's binding energy, while the remainder is transferred to the ejected electron as kinetic energy. In some cases, charged particles penetrate the orbital electron cloud and interact with the nucleus, potentially causing nuclear reactions.

Once an atom is ionized, the ejected electrons (primary ionization) can have sufficient energy to ionize other atoms in their path, leading to a cascade of secondary ionizations. These secondary ionizations amplify the initial ionization event, increasing the overall ionizing potential of the radiation. When ionizing radiation interacts with atoms and ejects electrons, it leads to the formation of ions and free radicals. These charged particles and reactive species can cause significant chemical changes within biological tissues.

Linear Energy Transfer (LET) is a measure of the energy transferred by ionizing radiation to the material it traverses per unit length (keV/ μm)[4]. It is a crucial factor in determining the extent and type of biological damage caused by radiation. Charged particles, such as alpha particles and neutrons, have high LET, depositing more energy along its path. Low LET radiation, such as gamma rays and X-rays, deposits energy sparsely along its path. The difference in energy deposition patterns between low and high LET radiation influences the type and severity of damage. Low LET radiation is more likely to cause widespread but less severe damage, while high LET radiation results in concentrated, severe damage in the affected area.

In radiation dosimetry, the Gray (Gy) and the Sievert (Sv) are two essential units used to quantify radiation dose[3,4]. The Gray is a unit of absorbed dose and is defined as the absorption of one joule of radiation energy per kilogram of matter. It measures the amount of energy deposited by ionizing radiation in a substance, providing a straightforward way to gauge the potential for physical and

biological damage. In contrast, the Sievert is a unit of dose equivalent that accounts for the biological effects of radiation. While the Gray quantifies the physical dose, the Sievert considers the type of radiation and its impact on specific tissues, incorporating weighting factors to reflect the varying biological harm caused by different types of ionizing radiation. Dosimeters measure radiation exposure by detecting and quantifying the amount of energy absorbed, the amount of ionization formed, or the amount of free radicals formed.[3] They work by using materials that react to radiation, such as thermoluminescent crystals that emit light when heated or semiconductor detectors that measure changes in electrical conductivity.

1.2 Cellular & Molecular Responses to Ionizing Radiation

1.2.1 Radiation Damages Biomolecules

At the cellular level, ionizing radiation deposits energy as it traverses through the cell, causing ionizations and excitations of atoms neighbouring its trajectory, which can lead to chemical modifications of biomolecules that trigger cell responses. Direct effects occur when ionizing radiation directly interacts with biomolecules, leaving them chemically modified[3,4]. Direct damage is the predominant consequence of higher LET radiation.[4] Indirect effects of ionizing radiation are mediated through the radiolysis of water, which constitutes the bulk of the cellular environment, comprising about 80% of the mass of a living cell[3,4]. Therefore, a significant proportion of radiation energy deposited will be absorbed in cellular water. Indirect effects are the predominant consequence of low LET radiation. The process of water radiolysis involves the absorption of energy from ionizing radiation, which splits water molecules into various reactive oxygen species (ROS)[3,5]. Initially, ionization results in the formation of ionized water (H_2O^+), which subsequently dissociates into hydroxyl radicals (·OH) and hydrogen radicals (H·) or can react with another water molecule to generate a hydronium (H_3O^+) and hydroxy radical. The freed electron can be captured by another water molecule to generate a hydroxyl anion and hydrogen radical. The radicals and ions formed in the primary reactions can further react with each other or with other water molecules, leading to a variety of products including, hydrogen peroxide, molecular hydrogen and additional radicals. These ROS have high reactivity towards biomolecules and are capable of diffusing

away from their site of origin, leading to indirect damage to distant cellular structures. Therefore, the indirect mechanism of radiation significantly amplifies the direct damage caused by ionizing radiation. The ROS generated from ionization events will trigger cellular ROS-producing systems that exacerbate these oxidative reactions, including activation of nicotinamide adenine dinucleotide phosphate (NADPH) and the electron transport chain[4,5]. This propagation can lead to increased cellular damage, but it also plays roles in signalling for DNA repair, apoptosis, and other stress responses. Most of the cellular damage from gamma radiation is due to indirect effects rather than direct ones.

Nucleic acids are highly susceptible to IR damage. The interaction of IR with DNA can result in various lesions, including base modifications, single-strand breaks (SSBs), double-strand breaks (DSBs), and DNA cross-links. Hydroxyl radicals are particularly effective at abstracting hydrogen atoms from the deoxyribose sugar in the DNA backbone, resulting in the formation of carbon-centred and alkoxy radicals, which undergo other reactions leading to the cleavage of phosphodiester bonds[4,5]. This reaction leads to SSBs, which if occur in proximity on complementary strands, can result in a DSB. Base modifications arise from the interaction of ROS with the nitrogenous bases of DNA.[4,5] These highly reactive species can attack DNA bases, causing oxidation, alkylation or deamination. For example, guanine can be oxidized to form 8-oxo-7,8-dihydroguanine, a common oxidative lesion that can mispair with adenine during DNA replication, leading to G to T transversion. When radiation causes a variety of DNA lesions within proximity, this is referred to as complex DNA damage[3,4]. Complex DNA damage is a hallmark of high LET IR and is considered more lethal to a cell as it is difficult to repair. Chromatin architecture also influences DNA damage. Euchromatin is decondensed and more prone to DNA damage as it is less protected. On the other hand, the condensed and protein-covered nature of heterochromatin protects it from radiation damage. In summary, radiation-induced DNA damage can result in mutations, genomic instability, and, if not properly repaired, cell death generally occurs.

In addition to nucleic acids, incident IR will also impact proteins which constitute the bulk of organic content within the cell[4,5]. Both direct and indirect effects can damage proteins at their amino acids and backbones. Radicals released from radiolysis can remove hydrogen atoms from both the backbone and side chains of amino acids, leading to the formation of highly reactive carbon-centred radicals that will

react with oxygen to form peroxyl or phenoxyl radicals causing oxidative modifications, fragmentation, and cross-linking of proteins. Oxidation of amino acid residues and their side chains frequently introduces carbonyl groups to the side chains of amino acids, an irreversible modification that leads to acyl-modified amino acids, protein backbone lesions, and increased protein degradation. Methionine and cysteine are uniquely modified by oxidative processes due to their sulphur-containing side chains, which provide specific reactivity not seen in other amino acids. Methionine is primarily oxidized to methionine sulfoxide and sulfone, while cysteine undergoes a range of modifications, including sulfenic acid formation and disulfide bond formation. In summary, due to modifications to amino acids and the protein backbone, IR can alter protein structure, impairing its function, and promoting fracture and aggregation. Due to their high abundance, oxidation of proteins is likely the main target of radiation-induced ROS.[4]

Upon exposure to ionizing radiation, cellular lipids, particularly polyunsaturated fatty acids (PUFAs) within membrane structures, undergo a series of oxidative reactions known as lipid peroxidation.[5] ROS generated by radiation, such as hydroxyl radicals, initiate this process by abstracting electrons from PUFAs, converting them into lipid peroxyl radicals. These radicals propagate a damaging chain reaction, which eventually culminates in the formation of lipid hydroperoxides. Although more stable than lipid radicals, lipid hydroperoxides are prone to decomposition in the presence of transition metals, yielding additional ROS, including alkoxyl and hydroxyl radicals. This decomposition releases toxic aldehyde by-products, such as malondialdehyde and 4-hydroxy-2-nonenal, which react with cellular proteins and DNA, forming adducts and cross-links that compromise cellular function. In the lipid bilayer, the integration of lipid hydroperoxides and reactive aldehydes disrupts membrane integrity by increasing permeability, altering fluidity, and impairing protein function, leading to ion imbalance and loss of cellular homeostasis. In addition to these effects, ionizing radiation induces significant changes in sphingolipid metabolism, notably by activating sphingomyelinases that hydrolyze sphingomyelin to produce ceramide.[5] Elevated ceramide levels promote the formation of ceramide-enriched membrane domains, which reorganize membrane structure and serve as platforms for cell death signalling pathways.

1.2.2 Antioxidant Response

In response to the oxidative stress induced by IR, cells utilize antioxidant defence mechanisms to neutralize reactive oxygen species (ROS) and mitigate further biomolecular damage.[4–6] Superoxide dismutase (SOD) converts superoxide anions into hydrogen peroxide (H2O2), while catalase breaks down hydrogen peroxide into water and oxygen, reducing oxidative stress. Glutathione peroxidase (GPx) catalyzes the reduction of hydrogen peroxide and organic hydroperoxides using glutathione, a major cellular antioxidant. Additionally, low-molecular-weight antioxidants such as reduced glutathione (GSH), ascorbate (vitamin C), melatonin, lipoic acid, ubiquinone, and vitamin E target water radiolysis products directly. As a reducing equivalent for enzymes and as a free radical scavenger, GSH is maintained at very high levels in the cytosol. Oxidative stress promotes activation of transcription factors like nuclear factor (erythroid-derived 2)-like 2 (Nrf2), leading to the increased expression of ROS detoxifying enzymes, including catalase, SOD, and GPx. It also promotes GSH synthesis and recycling via the upregulation of enzymes like glutathione S-transferase (GST). These enzymatic, non-enzymatic and transcriptional antioxidant responses are central to promoting cell survival during the oxidative stress of radiation exposure.

1.2.3 DNA Damage Response

Genomic stability is vital for the proper functioning of cells. DNA damage, if not properly managed, can lead to mutations, transformation, genomic instability and cell death. The amount of DNA damage inflicted by radiation is startling. A radiation dose of 1-2 Gy typically induces around 1,000 base damages, approximately 1,000 SSBs, and about 40 DSBs, in the DNA of a cell.[3] Therefore, when DNA is damaged, cells must deploy sophisticated DNA damage repair (DDR) mechanisms to respond to this damage.

The initial detection of DNA damage is mediated by sensor proteins that recognize abnormalities in DNA structure and begin to propagate the DDR signalling cascade.[6,7] Detection of radiation-induced DSBs is critical because even one unrepaired DSB can result in cellular lethality.[4] The Ku70/Ku80 heterodimer is a prominent DSB sensor, central to the non-homologous end-joining (NHEJ) repair

mechanism. Ku70/80 has a high affinity for exposed DNA ends where it will bind to prevent further degradation and recruit other DDR proteins. The Mre11-Rad50-Nbs1 (MRN) complex is another first-line sensor of DSBs, it has a high affinity for exposed DNA ends and plays a central role in homologous recombination (HR). For SSBs, the primary sensor is poly(ADP-ribose) polymerase 1 (PARP1). This protein rapidly binds to SSBs and catalyzes the addition of ADP-ribose polymers to itself, facilitating the recruitment of SSB repair factors.

Once DNA damage is recognized, a cascade of signalling events is initiated to amplify the damage signal and coordinate downstream responses. DNA-dependent protein kinase (DNA-PK), a key component of the NHEJ repair pathway, is activated by binding to the DNA ends through its interaction with the Ku heterodimer.[8] DNA-PK phosphorylates various substrates involved in NHEJ and modulates the activity of repair proteins at the break site. Ataxia-Telangiectasia Mutated (ATM) is one of the most important proteins involved in DDR, phosphorylating hundreds of substrates in response to DNA damage. The MRN complex is important for recruiting and activating ATM. However, MRN independent means of ATM activation also exist. MRN will recruit and activate many important checkpoint and repair proteins. Importantly, upon the occurrence of a DSB, H2AX a variant of the core histone protein H2A is rapidly phosphorylated by ATM, forming γH2AX. This modification serves as an early marker of DNA damage and recruits other repair proteins to the damage site. In the absence of ATM, DNA-PK can also generate γH2AX. Ataxia-telangiectasia and Rad3-related (ATR), on the other hand, are activated in response to single-strand DNA regions generated by replication stress.[8] When radiation-induced SSBs cause the replication fork to stall, Replication Protein A (RPA) stabilizes the region and recruits ATR-interacting protein to activate ATR. Subsequently, ATR phosphorylates and activates cell cycle arrest and DNA repair.

Cell cycle checkpoints are critical control mechanisms that ensure the integrity of the genome by halting cell cycle progression in response to DNA damage.[6,9,10] These checkpoints provide the necessary time for DNA repair before the cell resumes division, thereby preventing the propagation of damaged DNA and cell death. The G1/S checkpoint is primarily regulated by the p53-p21 pathway and serves to prevent DNA synthesis when DNA damage is present. p53 gets activated and accumulates in

the nucleus downstream of ATM, checkpoint kinase (CHK)-2 and Ku/DNA-PKC. Accumulated p53 induces the transcription of p21, a cyclin-dependent kinase inhibitor (CKI) that inhibits the activity of Cyclin E/CDK2 required for the G1 to S phase transition. Furthermore, ATM-driven activation of CHK-2 inhibits Cell Division Cycle 25A (CDC25A), which blocks the Cyclin E/CDK2 complex, further reinforcing the block on S phase entry. DSBs are not resected to generate significant amounts of RPA-ssDNA in G1 thus, the involvement of ATR in this checkpoint is thought to be minimal. The intra-S checkpoint prevents the replication of damaged DNA. ATR and ATM both play central roles in this checkpoint by phosphorylating and activating CHK1 and CHK2, respectively. Phosphorylation of CDC25A phosphatases by CHK1 and CHK2 phosphorylate leads to it's degradation or sequestration in the cytoplasm, preventing the activation of Cyclin A/CDK2 complexes and thereby stalling DNA synthesis. The G2/M checkpoint prevents cells with damaged DNA from entering mitosis. ATM and ATR phosphorylate and activate CHK1 and CHK2, which in turn phosphorylate CDC25C, leading to its inactivation. This inhibits the activation of Cyclin B/CDK1 complexes, preventing the cell from progressing into mitosis. Additionally, p53 can induce the transcription of genes involved in G2 arrest, DNA repair and apoptosis at this stage.

Cells utilize several pathways tailored to different types of lesions to repair DNA damage. Single Stranded Break Repair (SSBR) and Base Excision Repair (BER) are essential for repairing SSBs and base modifications resulting from oxidation, alkylation, or deamination. Upon detection of an SSB, PARP1 binds to the break and undergoes auto-ADP-ribosylation, recruiting SSBR repair factors to the damage site.[7] After PARP1 binding, XRCC1 (X-ray repair cross-complementing protein 1) is recruited as a scaffold for other proteins like DNA ligase 3 (LIG3), DNA polymerase β, and polynucleotide kinase 3'-phosphatase (PNKP). These proteins coordinate the filling of the DNA gap and ligation to complete the repair process. In the case of damaged bases, specific DNA glycosylases act as a sensor to detect the specific base modification and remove it, leaving an abasic (AP) site. Subsequently, AP endonuclease 1 (APE1) cuts the DNA backbone, creating an SSB. Following the creation of an SSB, BER shares downstream repair proteins with SSBR, including PARP1 and XRCC1.

NHEJ is crucial for repairing DSBs.[4] This mechanism involves the direct ligation of the broken DNA ends without the need for a template. The process begins with the recognition and binding of the Ku heterodimer to the DNA ends. Ku recruits and activates DNA-PK, which phosphorylates and regulates various repair proteins. The DNA ends are processed by nucleases, such as Artemis, to remove damaged nucleotides and create compatible ends. Special DNA polymerases (Pol), including Pol μ and Pol λ, fill in the gaps without requiring a template, helping bridge small gaps and mismatches. DNA ends are finally ligated by the XRCC4-Ligase IV complex, with the help of XLF. NHEJ's direct ligation without a template makes it a rapid but error-prone repair mechanism.

Homologous Recombination is another pathway for repairing DSBs, particularly those occurring during the S and G2 phases of the cell cycle when a sister chromatid is available as a template.[4] This error-free repair process begins with the resection of DNA ends to generate 3' single-stranded DNA overhangs. This resection is mediated by the MRN complex, CtIP and the exonuclease EXO1. The ssDNA is then initially coated by RPA for stabilization. Later RPA is replaced by RAD51, facilitated by BRCA2. RAD51 forms nucleoprotein filaments that search for and invade the homologous DNA sequence on the sister chromatid, forming a displacement loop (D-loop). DNA synthesis is then initiated using the homologous strand as a template, followed by resolution of the D-loop and ligation to restore the intact DNA molecule. HR is considered an error-free repair because its use of the homologous template guides accurate repair, replacing the original sequence at the break.

The decision between NHEJ and HR for DNA DSB repair is regulated through several factors, primarily influenced by cell cycle phase, DNA end resection, and the involvement of regulatory proteins.[11,12] DNA end resection is a pivotal process in determining the choice between HR and NHEJ. The resection generates ssDNA at the break site, which is essential for HR but incompatible with NHEJ. End resection is promoted by S/G2 CDKs which phosphorylate key proteins, particularly CtIP, enabling it to initiate resection at DSBs. To preserve NHEJ, end resection is tightly blocked. NHEJ-promoting factors, such as 53BP1 and the shieldin complex, bind to the DNA ends, stabilizing the break site and physically obstructing the initiation of resection.

1.2.4 Cellular Consequences of Radiation Damage

In some cases, cells may successfully defend against oxidation, block their cell cycle progression, repair their genomic lesions, and thereby cope with biomolecular damage. In that case, the cell will eventually re-enter the cell cycle and resume its usual function. In other cases, a cell may not be able to cope with the biomolecular damage and suffer consequences.

If not repaired properly, IR-induced DNA damage leads to DNA mutations, structural variations and chromosomal aberrations. Mutations in the protein-coding regions from failed repair mechanisms can lead to loss of that protein's expression, or expression of an aberrant version of that protein. DNA lesions which escape repair can cause replication forks to stall or collapse, generating further damage and inducing stress responses. NHEJ is an error-prone process that can cause structural variants, including insertions, deletions or translocations. For example, two DSBs on different chromosomes can be incorrectly joined, leading to chromosomal translocations. Misrepair can also cause chromosomal aberrations, such as dicentric, acentric and ring chromosomes.

Intrinsic apoptosis may be induced in cells experiencing extensive oxidative stress and damage from radiation. When DNA damage, particularly DSBs are detected, sensor proteins like ATM and ATR drive the stabilization and activation of the tumour suppressor protein p53. While p53 is involved in cell cycle arrest, buying time for repair, its accumulation signals a shift towards apoptosis. Activated p53 transcribes pro-apoptotic genes, including PUMA, NOXA, and BAX, promoting mitochondrial outer membrane permeabilization (MOMP) and the release of cytochrome c. This triggers the formation of the apoptosome and the activation of caspases, ultimately leading to apoptosis. Mitochondrial apoptosis can be triggered by other stress signals, such as the accumulation of ceramides.[4,5] As mentioned previously, IR radiation promotes ceramide formation at the plasma membrane via activation of acid sphingomyelinase and mitochondrial ceramide via de novo synthesis. Ceramide is held as an important mediator of radiation-induced cell death as it can trigger several processes culminating in apoptosis.[4,5,13,14]

Cells that evade immediate apoptosis and retain substantial DNA damage can sometimes aberrantly progress into mitosis. Here, the Spindle Assembly Checkpoint (SAC) plays a critical role, ensuring cells

do not proceed to anaphase until all chromosomes are correctly attached to the mitotic spindle and aligned at the metaphase plate. Radiation-induced chromosomal abnormalities often interfere with proper spindle attachment, activating the SAC and pausing cell division. Cells stopped in metaphase with abundant DNA damage can trigger apoptosis.

However, in cells with extensive instability, the SAC may fail, allowing cells to proceed to anaphase with misaligned or unattached chromosomes. This results in segregation errors such as anaphase bridges, where dicentric chromosomes are pulled towards opposite poles, forming bridges that frequently snap, causing further DNA breaks. Unattached chromosomes will be missegregated, and chromosomes with multiple centromeres can generate multipolar spindle attachment. These events often culminate in mitotic catastrophe (MC), where the cell is unable to complete mitosis successfully. This can trigger apoptosis in the mitotic phase, killing the cell due to its failed mitosis.

In some cases, despite mitotic catastrophe, cells complete erroneous division, resulting in structurally abnormal progeny. These cells often display micronuclei (small extranuclear bodies containing missegregated chromosomal fragments), multiple nuclei, or become polyploid. Such abnormalities generate strong signals for cellular stress, leading to apoptotic cell death shortly after mitosis due to structural disorganization and genomic instability. In some cases, apoptosis may be delayed until the subsequent G1 phase, at which point mitochondrial pathway-driven apoptosis, mediated by p53 and other death signals initiates.

Some cells complete mitosis with less overt but still significant chromosomal defects. These cells survive with genomic instability, a condition where underlying chromosomal abnormalities increase the risk of further mutations and DNA damage in future cell divisions. This instability is particularly hazardous because it perpetuates a cycle of damage and repair, making the cell more vulnerable to additional chromosomal aberrations. Over time, such cells accumulate mutations that progressively disrupt cellular functions, often triggering apoptosis or necrosis due to accumulated damage.

Finally, senescence is a permanent form of cell cycle arrest that can be induced in response to radiation.[4,15,16] Activation of DDR in response to IR is meant to temporarily induce cell cycle arrest and allow repair. However, in some cases of persistent DDR activation, sustained activation of p53–p21–

retinoblastoma protein (RB) and p16INK4A–RB pathways cause prolonged cell cycle arrest. Despite prolonged DDR and activation of p53, apoptosis is avoided when the balance of pro-apoptosis and anti-apoptosis signals are insufficient to pull the trigger on active cell death. Over time, the prolonged cell-cycle arrest leads the cell to adopt a senescent phenotype, characterized by morphological alterations, accumulation of cyclin D1, increased senescence-associated β-galactosidase activity, formation of senescence-associated heterochromatin foci and activation of the senescence-associated secretory phenotype. Notably, the specifics of senescence induction and phenotype expression can vary depending on the irradiated cell type and its state.

1.2.5 Cellular Radiosensitivity

Cellular radiosensitivity refers to the susceptibility of cells to damage or death upon exposure to ionizing radiation. This sensitivity varies widely across cell types and activation states, reflecting a complex interplay of intrinsic and extrinsic factors. Key determinants include genetic background, cell cycle phase, DNA repair efficiency, redox status, and the influence of the surrounding microenvironment. These factors collectively shape cellular responses to radiation, influencing the extent of DNA damage, the activation of stress response pathways, and ultimately, cell fate.

When cells divide, they are particularly vulnerable to radiation-induced damage because the process of mitosis involves critical stages like DNA replication and chromosome segregation, which, if disrupted by radiation, can lead to cell death. Cells that undergo division more frequently will exhibit the effects of radiation damage more rapidly, as radiation-induced damage is realized during the process of cell division.[44]With cell cycle checks behaving as a radiation executioner, differences in cell cycle stages create differences in cell radiosensitivity.[3,4,17–20] While the precise molecular mechanisms remain partially understood, studies using synchronized cell cultures prior to irradiation reveal distinct radiosensitivity profiles depending on cell cycle phase. Generally, differences in DNA repair pathways and the timing of checkpoint activation contribute to these variations. Experimental evidence indicates that cells irradiated in the G1 phase exhibit moderate sensitivity to radiation. Cells in early G1 tend to be more resistant, likely due to their increased distance from the S phase, which limits immediate DNA

replication stress. Conversely, cells irradiated later in G1 show higher sensitivity as they may attempt to enter the S phase with unresolved DNA damage. Additionally, cells with an extended G1 duration demonstrate greater resistance compared to those with a shorter G1 phase. During the S phase, cells exhibit elevated resistance, particularly in late S phase, where abundant sister chromatids are available to facilitate efficient DNA repair through homologous recombination. In contrast, cells in the G2 and M phases are markedly more sensitive to radiation. This heightened sensitivity is attributed to the lethal consequences of entering mitosis with unrepaired DNA damage, which can lead to catastrophic mitotic events. Generally, cells in the G0 phase or those in a state of senescence, which are non-proliferative, display the highest levels of radiation resistance.

The susceptibility of proliferating cells to radiation has long been recognized. In 1906, Bergonié and Tribondeau proposed a principle stating that tissues tend to be more radiosensitive when their cells are less differentiated, possess a high proliferative potential, and undergo rapid division.[4,21] However, this law is not universally true. Instead, radiosensitivity is governed by a complex interplay of molecular and cellular mechanisms. Consequently, some highly proliferative cancers exhibit greater radioresistance than their healthy tissue counterparts. Moreover, certain cell types, such as resting lymphocytes, are highly susceptible to radiation-induced interphase cell death despite their low proliferative activity. Therefore, while applicable in certain instances, the Law of Bergonié and Tribondeau is too generalized.

Cell-type specific expression of DDR and antioxidant proteins likely governs in-part the radiosensitivity or cell populations. Cells which express greater pro-apoptotic genes at baseline or following irradiation more easily trigger apoptosis in comparison to cells expressing more anti-apoptotic proteins.[22,23] Cell type specific expression of DNA repair mechanisms may also explain the variation in cell survival following radiation exposure. Furthermore, differential binding of genomic regions to proteins such a p53 may explain variation in radiation response.[24] Genotype may also contribute to radiosensitivity, with non-pathologic variants in important DDR genes existing amongst the population.[25] Genetic defects in various genes can also manifest in changes to radiosensitivity.[4] For example, mutations in the ATM gene lead to increased radiosensitivity, as seen in Ataxia-Telangiectasia (A-T) syndrome. These cells exhibit impaired DNA repair and heightened chromosomal instability. Mutations

in p53 can disrupt its ability to induce cell cycle arrest and apoptosis in response to DNA damage, leading to increased radioresistance in some cancers.

One major mechanism governing radiation sensitivity is hypoxia, which limits the radiosensitizing effect of oxygen.[4] Directly, radiation exposure polarizes or radicalizes biomolecules, such as DNA, creating transient disturbances that are typically reversible. Oxygen, however, sequesters excited electrons from these unstable molecular states, converting transient radicals into fixed, irreparable forms. Indirectly, radiation generates reactive water-derived radicals that further damage biomolecules. Oxygen readily binds with these radicals, forming stable peroxides that inhibit cells from neutralizing the radicals, effectively impeding the cell's repair mechanisms. In hypoxic conditions, this fixation effect is absent, allowing antioxidants to mitigate radical damage more effectively and thereby enhancing cellular radioresistance. Consequently, oxygen amplifies radiation-induced damage by stabilizing fleeting radical intermediates into persistent, non-repairable lesions, underscoring hypoxia as a protective state that facilitates cellular repair in response to radiation-induced stress.

[4]Interestingly, it has been documented that cells become more resistant to subsequent radiation exposures after being exposed to a low, "priming" dose of radiation.[4] This “induced resistance” or “priming effect” has been demonstrated by exposing cells to an initial low dose of radiation, which is thought to induce protective mechanisms that make cells less sensitive to a subsequent exposure of higher doses compared to cells which were not primed. The precise mechanisms underlying this response are not fully characterized, but it is thought to involve the upregulation of antioxidant responses through pathways like Nrf2, enhanced DNA repair via ATM/ATR pathways, and improved cell cycle regulation by activating checkpoints that allow more time for DNA repair.[26] These mechanisms collectively reduce oxidative damage, enhance DNA repair efficiency, and prevent apoptosis, thereby protecting cells from the damaging effects of higher radiation doses.

1.2.6 Non-Targeted Effects of Radiation Exposure

In the 1990s, scientists began to report that ionizing radiation exposure could impact cells that were themselves not impacted directly by an ionizing radiation track. Since then, these non-targeted effects

(NTE) have been analyzed in more detail and categorized into different effects[4]. However, many questions remain regarding molecular mechanisms underlying NTE.

The radiation-induced bystander effect (RIBE) refers to the "ability of irradiated cells to transport manifestations of damage to other cells which were not directly targeted by irradiation."[4] This concept challenges the traditional view that radiation only affects cells directly damaged by radiation. Instead, RIBE shows that cells not directly exposed to ionizing radiation can undergo significant biological changes. The first report of such effects was in 1992, made by Nagasawa and Little, who irradiated Chinese hamster ovary cells with alpha particles.[27,28] Although only 1% of nuclei were directly traversed by alpha particles, 30% of cells exhibited an increase in the frequency of sister chromatid exchange.

Since its discovery, scientists have worked to describe the mechanisms underlying RIBE. Eventually, it was revealed that intercellular communication via gap junctions was of critical importance to bystander responses.[28] Formed by connexin proteins, gap junctions allow the passage of small molecules and ions between cells. Inhibiting gap junctions has been shown to greatly reduce the bystander effect. ROS, NO, calcium ions, and Ip3 have all been shown to traverse gap junctions to mediate the bystander response.

In addition to direct cell-to-cell communication, irradiated cells release soluble factors that diffuse through the extracellular medium, affecting neighbouring cells. This phenomenon is well-demonstrated by medium transfer experiments, where the culture medium from irradiated cells is introduced to non-irradiated cells, causing them to exhibit bystander responses.[29,30] Cytokines such as IL-1, IL-6, TNFα and TGFβ have been implicated as soluble factors mediating RIBE. ROS reaction products such as H_2O_2 or peroxynitrite are also likely involved. Furthermore, it is suspected that exosomes and microvesicles may play a role in communication between irradiated and non-irradiated cells.[31]

The influx of these signals from irradiated cells can trigger various cellular responses in non-irradiated bystander cells.[4] Among these effects, bystander cells may exhibit DNA damage, chromosomal aberrations, micronucleus formation, and apoptosis, all hallmarks similar to those seen in directly irradiated cells. Additionally, elevated ROS levels in bystander cells contribute to oxidative

stress, which further perpetuates biomolecular damage. Cytokines released by irradiated cells, can also induce inflammatory pathways in bystander cells.

1.3 Effects of High-Dose Ionizing Radiation Exposure

The cellular and molecular responses to ionizing radiation can manifest into health effects which vary significantly depending on the context of exposure. The understanding that ionizing radiation has health effects evolved through a series of historical discoveries, beginning in the late 19th and early 20th centuries[4]. Initially, people were fascinated by the ability of X-rays to visualize bones and radium's luminescent properties, which quickly led to medical and industrial applications. However, harmful effects of radiation were beginning to be observed among researchers and radiologists. For example, the physician responsible for taking the first clinical x-ray in 1896, Dr. Hall-Edward's, would go on to develop cancer of the hands from radiation exposure in his practice[4]. The tragic case of the "Radium Girls" in the 1920s, where factory workers suffered severe radiation poisoning from painting watch dials with radium-laced paint, highlighted the need for protective measures[4,32]. Eventually, in response to accumulating knowledge and use of radiation, international efforts were made to establish safety standards, starting with the formation of the International Commission on Radiation Protection (ICRP) in 1928, followed by the United Nations Scientific Committee on the Effects of Atomic Radiation (UNSCEAR) in 1955.[4] The Canadian Nuclear Safety Commission (CNSC) was founded in 2000, succeeding the Atomic Energy Control Board, which was originally established in 1946 to regulate nuclear energy in Canada.[33] These organizations all play crucial roles in regulating radiation and protecting both workers and the public from harmful effects.

High-dose ionizing radiation (HDIR) exposure refers to exposure at levels that exceed the thresholds typically associated with medical or environmental exposure. This includes exposures seen in nuclear accidents, war and radiotherapy. Specifically, HDIR is often defined as doses above 0.5 Gy to 1 Gy delivered at a high-dose-rate that result in both severe immediate and long-term health consequences.[34] To put that in context, total body irradiation (TBI) at 8 Gy or above is completely lethal within a couple

weeks[34]. On the other hand, TBI of 1-2 Gy will result in acute symptoms and long-term risks. The clinical manifestation and severity will vary with the absorbed dose and dose rate of the exposure.

Acute Radiation Syndrome (ARS) can occur within hours after irradiation of the entire body (or most of it) with acute absorbed doses of 2+ Gy penetrating radiation. It is characterized by a sequence of phases, each presenting distinct clinical manifestations and severity depending on the dose received[32,34]. The prodromal phase initiates within 1–3 days post-exposure and is characterized by symptoms such as nausea, vomiting, anorexia, fever, headache, and early skin erythema. Following the prodromal phase is the latent phase, during which symptoms may temporarily subside, giving a false impression of recovery. This phase can last from a few hours to several weeks, with higher doses shortening its duration. The manifest illness phase marks the culmination of ARS, manifesting as distinct syndromes hematopoietic, gastrointestinal, and cerebrovascular, each dictated by the absorbed radiation dose.

Hematopoietic syndrome occurs at doses exceeding 1 Gy and primarily affects the bone marrow[32,34]. Hematopoietic cells are highly sensitive to radiation, and their destruction via radiation reduces the output of hematopoietic cells from the bone marrow. This leads to pancytopenia, anemia, thrombocytopenia, malaise, increased risk of infection, and bleeding. Symptoms of hematopoietic syndrome typically appear within 1 to 6 weeks post-exposure. Without medical intervention, this syndrome can be fatal. Gastrointestinal syndrome arises at higher doses, between 6 and 15 Gy, resulting from damage to the rapidly dividing epithelial cells lining the gastrointestinal tract[32,34]. Symptoms include severe nausea, vomiting, diarrhea, dehydration, and electrolyte imbalance. The loss of mucosal integrity leads to bacterial translocation into the bloodstream, increasing the risk of sepsis. Symptoms appear within a few hours to a few days post-exposure and can lead to death within 2 weeks without intensive medical care. Neurovascular syndrome occurs at doses above 20 Gy, causing severe damage to the central nervous system and cardiovascular system[32,34]. This damage includes endothelial cell damage, increased intracranial pressure, and a systemic inflammatory response. Symptoms, which can appear within minutes to hours, include severe headaches, cognitive impairment, loss of

coordination, seizures, and ultimately, loss of consciousness. Death typically occurs within 1 to 2 days post-exposure due to the rapid progression of neurological and cardiovascular collapse.

Radiation exposure can also cause more stochastic long-term health consequences. In radiation epidemiology, disease risk is often reported as the relative risk (RR), which is calculated as the ratio of the incidence of a health outcome in an exposed population to that in an unexposed population. To express the additional risk attributable to exposure, the excess relative risk (ERR) is commonly used. ERR is derived by subtracting 1 from the RR, where an ERR of 0 indicates no excess risk, and positive values indicate an increased risk due to exposure. ERR is frequently modeled per unit of radiation dose, typically per gray (Gy), to quantify how risk changes with increasing exposure levels. This is to be distinguished from rate ratios, which compare incidence rates rather than cumulative risk. A rate ratio (also called an incidence rate ratio, IRR) is calculated as the incidence rate in the exposed group divided by the incidence rate in the unexposed group and accounts for person-time at risk. In contrast, RR compares cumulative incidence, measuring the proportion of individuals affected over a fixed period. While these measures may be similar when follow-up times are equal or when the outcome is rare, they diverge when disease incidence is high or when individuals contribute different amounts of time at risk.

Initiated in 1950, one of the most consequential epidemiological studies of radiation exposure is the long-term follow-up of Japanese Atomic Bomb survivors (Life Span Study – LSS)[35,36]. The LSS includes over 100,000 individuals who were present at various distances from the explosion hypocenters and who were guarded by different levels of shielding, thereby leaving them with varying absorbed doses of ionizing radiation. A control group of citizens who were at such a distance that their exposures were exceedingly small has been followed for comparison. The LSS found significant excess relative risk (ERR) for both leukemias and solid cancers amongst atomic bomb survivors.[35–38] Analyzing leukemia mortality from 1950-2000, individuals exposed to radiation doses of 2 Gy or more have a risk ratio of 17.3 (90% CI: 11.2, 26.7) compared to control[37]. In the 1–<2 Gy group, the risk ratio was 6.7 (90% CI: 4.4, 10.4). Significant excess relative risk was observed for solid cancers of the bladder, breast, lung, brain, thyroid, colon, esophagus, oral cavity, stomach, liver, and skin (excluding melanoma)[36,38]. [36]The

LSS is strong evidence for excess cancer risk being one of the foremost long-term consequences of HDIR exposure[35,36].

Beyond cancer, radiation-induced cataracts and circulatory diseases manifest from tissue reactions to radiation and represent significant health effects, especially in the higher dose range.[4] Despite extensive research, no significant hereditary effects have been detected in the children of atomic bomb survivors[35,36]. Studies have shown no increased risk of stillbirths, malformations, neonatal death, or cancers in these children. Therefore, despite the radiosensitivity of germ cells and results of animal studies, concerns about transgenerational effects have not been seen to manifest in the literature.

When analyzing epidemiology of HDIR exposure, one can observe several factors potentially influencing an individual's susceptibility to the health effects of ionizing radiation exposure. Notably, children are considered to be more susceptible to the health effects of radiation exposure. For example, the excess risk for leukemia in the immediate years following the atomic bombs was much higher for those exposed at <10 years of age compared to adults[37]. Sex differences have been frequently observed across epidemiological studies, with “ERR… estimates for solid cancers [being] about 50% higher for women than for men,” amongst the LSS cohort.[36] Genetic predispositions, such as DNA repair deficiencies, would also increase susceptibility to radiation-induced damage and health consequences.[4,39]

1.4 Low-dose Radiation Exposure Effects

1.4.1 Context of Low-Dose Radiation Exposures

While the dramatic and more deterministic effects of HDIR exposure are largely understood with scientific consensus, the biological effects and health risks of LDIR exposure continue to be highly contested. LDIR is defined by the National Academies of Science in the USA as exposures resulting in absorbed doses as near zero to 0.1 Gy (100 mGy).[40] Low dose rate radiation is typically defined as being under 0.5 mGy/hr.[40] This level of exposure is significantly lower than doses typically associated with radiation therapy or ARS.

People frequently encounter LDIR from a variety of sources in their daily lives. Common exposures include natural background radiation, medical procedures and occupational exposures.[40] Natural background radiation comes from cosmic rays, terrestrial sources such as radon gas, and internal sources within the human body. According to the CNSC, the average natural background radiation exposure in Canada is 1.8 mSv absorbed dose per year[41]. However, in certain locations, increased cosmic rays or radon can contribute to above-average background exposure; for instance, background radiation in Northern Iran can reach 260 mSv per annum[41]. LDIR exposure is frequently encountered in medical diagnostics, with a typical bitewing dental x-ray resulting in 0.005mSv while a typical chest CT scan results in 7 mSv.[40] Higher occupational exposures occur in various industries such as space exploration, mining, nuclear energy, radiology, science, and aviation. An astronaut is exposed to an average 150 mSv per year on the space station.[42] The CNSC claims nuclear energy workers (NEW) receive 1-2 mSv of ionizing radiation exposure per year in excess of background.[42] The World Nuclear Association claims the average nuclear energy worker or uranium miner receives 1.5 – 2.5 mSv per year.[43] There is great variation in exposure depending on the nature of nuclear energy work, with a publication from the million person study analyzing US NEWs reporting a mean cumulative career dose of 52.6 mSv, and a maximum dose of 1.32 Sv and only around 15% of workers with career exposures over 100 mSv.[44] The public limit for radiation exposure from power plants in Canada is 1 mSv per year, and the occupational limit for those in the nuclear industry is 50 mSv per year or 100 mSv per 5 years.[45]

1.4.2 Models of Low-Dose Radiation Effects

Several models have been proposed to explain the molecular responses and health effects of low-dose radiation exposure.[19] The Linear No-Threshold (LNT) model posits that the risk of cancer and other health effects increases linearly with radiation dose, with no threshold beneath which risk is eliminated. The LNT is also often applied to describe the biomolecular damage and responses inflicted by radiation exposure such as DSBs or p53 upregulation. Despite some controversy, the LNT model remains widely used in radiation protection guidelines, with committees recognizing that accumulating epidemiological evidence in the low dose range continues to support the LNT model.[46,47] However, other scientists

dispute its accuracy, citing contexts where the LNT model does not fit molecular responses and health consequences.

Conversely, the threshold model suggests that there is a dose below which no adverse health effects are observed, implying that the body can tolerate low levels of radiation without significant harm. This model aligns with findings demonstrating the absence of adverse health effects or molecular responses beneath certain doses. Notably, while some molecular events induced by radiation exposure, such as DSBs, may adhere to a LNT model, a threshold may still be required for these molecular changes to amount into a discernible health effect. Contrastingly, the hypersensitivity cellular model posits that at low doses, cells may exhibit an exaggerated response, potentially increasing the chance of certain health outcomes more than predicted by linear models.

Finally, the hormesis model proposes that low doses of radiation may have a beneficial effect on cellular biology and health. This model aligns with observations of LDIR exposure stimulating protective biological mechanisms that could improve health. Within the scope of this model falls low-dose radiation therapy (LDRT), which has been explored in the lab and clinic for treating cancer and non-cancer diseases.

These differing models underscore the complexity of radiation biology and the ongoing debate about the most accurate representation of low-dose radiation effects on health and cell biology. There is evidence which supports each of these models across different exposure contexts and measured outcomes, highlighting the need for ongoing research to better understand LDIR effects.

1.4.3 Cellular and Molecular Responses to Low-Dose Radiation Exposure

A critical area of investigation in the radiation biology field is the differential cellular and molecular responses between HDIR and LDIR exposure. As discussed in section 1.2, there are canonical descriptions of radiation-induced DNA damage, oxidative stress, DDR, cell death, etc. However, the extent of biomolecular damage and the nature of the cellular response vary significantly amongst exposure levels and sometimes in a non-linear fashion. Therefore, there remains a continued effort to elucidate LDIR responses at the cellular and molecular level. The studies below are not meant to

represent a comprehensive review of differences in molecular response to LDIR and HDIR; rather, they highlight that LDIR can impact cellular behaviour in unexpected and significant ways.

When comparing LDIR and HDIR exposures, there are differences in both the quantity and quality of DNA damage. Current evidence supports that double stranded DNA damage induction is linear with dose.[48] In-vitro, Rothkam et al. could detect DSBs above baseline at doses as low as 1.2 mGy by measuring γ-H2AX foci with immunofluorescent imaging.[49] Importantly, they found a linear relationship between the number of γ-H2AX foci at high-doses to low doses over a large range of 1.2 mGy to 200 Gy. In humans, γ-H2AX foci can also be found in peripheral blood immediately following CT scans in a dose-dependent manner.[50,51] DNA damage can also increase in complexity at higher doses (even with low LET), as more DNA damage can be located together in proximity.[4] Furthermore, Sanchaz et al. demonstrated that protracted low-dose radiation exposure in mice led to cumulative DNA damage marked by γ-H2AX foci formation.[52]

Interestingly, DDR may be less responsive to low-dose radiation than high-dose radiation. In confluent non-dividing cell cultures exposed to LDIR, limited $\gamma\mathrm{H2AX}$ foci persist, whereas higher doses reduce $\gamma\mathrm{H2AX}$ foci more quickly.[53,54] This suggests that a threshold of biomolecular damage is needed to trigger sufficient NHEJ (the primary mechanism amongst non-dividing cells). This could be recapitulated in an in-vivo experiment using TBI of 10 mGy, showing delayed loss of $\gamma\mathrm{H2AX}$ foci in various tissues compared to TBI at 100 mGy or 1 Gy.[54] Interestingly, pre-treating cells with H_2O_2 results in a loss of the delayed effect. The authors argue that the increased ROS helped the LDIR treatment reach a sufficient threshold of biomolecular damage to trigger DNA repair. In contrast, Asaithamby et al. used 53BP1 foci dynamics in-vitro to show that repair was equally efficient at low doses as it was at higher doses, supporting a model where DDR mechanisms, particularly NHEJ, can operate effectively regardless of radiation intensity. [48]

HDIR may favour error-prone NHEJ over HR for DSB repair. Belov et al. explored the kinetics of Rad51 and γH2AX foci, finding that they correlated temporally at lower doses rather than high-doses.[55] The stronger temporal alignment of Rad51 and $\gamma\mathrm{H2AX}$ foci suggests cells preferentially engage in HR at low doses. On the other hand, it is possible that NHEJ increases with dose due to a reduction in G2-

phase cell availability. However, experiments on G2-phase-enriched cell populations exposed to increasing doses of IR have shown a switch from HR to NHEJ.[56–58] This indicates that HR's contribution to DSB repair is limited at higher doses, where NHEJ predominates. The switch from HR to NHEJ may be caused by the overwhelming of HR resources, shifting the repair burden to NHEJ to manage the DNA damage burden.

Of particular interest to researchers is whether the DDR and oxidative stress responses are sufficiently activated in response to LDIR. Maccullum et al. could still find elevated Trp53 (transformation related protein 53) levels in the spleen and liver following TBI as low as 0.01 Gy, with increasing levels as the dose increased.[59] Shimura et al. could find increased Nrf2 in peripheral blood mononuclear cells (PBMC) following TBI as low as 0.1 Gy.[60] These findings suggest that DDR and oxidative stress responses are still activated even from low-dose radiation exposure in vivo.

In Sampadi et al., phosphoproteomics was used to investigate how mouse embryonic stem cells respond to in-vitro low (0.1 Gy) and high-doses (1 Gy).[61] Their findings reveal that while DDR scales proportionally with the dose, activating key DDR kinases like ATM, other cellular responses vary significantly between low and high doses. LDIR primarily activated oxidative response pathways like NRF2, ERK1/2 and mTOR , which showed phosphorylation patterns that implied activation of antioxidant and redox-regulated signalling. LDIR enhanced phosphorylation on glycolysis-related proteins, such as GAPDH and PKM2, and mitochondrial proteins, aligning with a metabolic shift. Conversely, HDIR predominantly triggered DDR and cell cycle arrest genes, with a focus on mitigating the extensive damage from the higher dose. The authors suggest that these findings demonstrate that LDIR prompts a coordinated response focused on oxidative stress management and metabolic adaptation, while high-dose radiation activates extensive DDR and cell cycle arrest mechanisms.

The cell cycle response may also be different when comparing low and high-dose radiation responses. In general, it is thought that while HDIR forces strong upregulation of cell checkpoint molecules, causing long persistent cell cycle pause, leading to apoptosis, LDIR causes more mild upregulation of checkpoint molecules, causing shorter duration of cell cycle pause allowing cells to repair limited damage and reenter the cell cycle.[62] For example, Yunis et al. used RNA-seq to investigate

how low (0.1 Gy) versus moderate (1 Gy) doses of X-rays impact gene expression in a three-dimensional skin model.[63] Note that the term moderate-dose ionizing radiation (MDIR) is not a standardized classification but is sometimes used in experimental contexts to describe radiation doses that exceed the low-dose range yet remain below levels typically associated with acute radiation syndrome (ARS). The precise boundaries of MDIR vary between studies, but it generally refers to doses high enough to induce measurable biological effects without causing the severe, immediate health consequences seen at high-dose exposures. In cells exposed to LDIR, the immediate response favoured survival, such that within minutes, anti-apoptotic pathways were upregulated. By the 3-hour mark, these cells displayed a sustained G1/S checkpoint arrest, regulated by key genes such as p21, Rb, and p130, stalling the cell cycle to allow time for DNA repair. DNA repair pathways were moderately active, promoting careful progression toward recovery. By 24 hours, LDIR-exposed cells suggested a readiness to re-enter mitosis after successful repair. Thus, the response to LDIR emphasized controlled damage repair and survival.

In contrast, cells exposed to MDIR rapidly activated DDR and apoptosis pathways, indicating recognition of more severe DNA damage.[63] This stronger stress response was marked by early upregulation of pro-apoptotic genes such as Fas, DR5, GADD45α, and caspase-9, pointing to a cellular decision to eliminate damaged cells rather than prioritizing recovery. By 3 hours post-irradiation, MDIR-exposed cells had bypassed the G1/S checkpoint and instead engaged a robust G2/M checkpoint arrest. The upregulation of G2/M regulators like cyclin B1, CDK1, and PLK1 reinforced the G2/M arrest, halting the cell cycle until the damage was either sufficiently repaired or deemed irreparable. By 24 hours, MDIR-exposed cells still largely remained in G2/M arrest, with strong apoptotic signalling present, highlighting a cell-death-focused response that contrasts with the survival and repair emphasis in LDIR-exposed cells. The study underscores the nuanced, non-linear response of skin cells to different doses of ionizing radiation. LDIR appears to enable protective adaptation and survival strategies, allowing cells to "assess" and repair damage. MDIR induces immediate DDR and apoptosis pathways and relies more on the G2/M arrest point.

Recognizing the need to further explore molecular mechanisms of LDIR response, Wang et al. used in-silico modelling of radiation energy deposition in cell culture.[64] Their in-silico simulations propose that there is considerable heterogeneity in the dose received per cell when cultures are exposed to LDIR. As simulated dose increases, the energy distribution across cells becomes more uniform. Therefore, their modelling indicated that HDIR results in more consistent exposure across a cell culture. To explore the biological implications of these findings, the researchers applied single-cell RNA-sequencing to analyze the response of BEAS-2B cell lines to 10 mGy,100 mGy or 1 Gy of in-vitro gamma radiation. Their bioinformatic analysis focused on identifying genes whose expression patterns correlated with the in-silico microdosimetric energy distribution. In other words, the researchers identified genes whose expression variability reflected the energy distribution patterns at different doses; specifically, genes were chosen if their expression variability across cells decreased with increasing radiation dose. At low doses, genes involved in cellular stress responses, ribosomal function, and mitochondrial processes were upregulated. At high doses, pathways related to DNA damage response, apoptosis, and mitochondrial stress were more prominent, indicating that cells experience more significant stress, leading to DDR or apoptosis. This integrative approach stresses substantial heterogeneity amongst cells exposed to LDIR and highlights unique stress responses, including ribosomal function as implicated following low-dose radiation exposure.

In another study, human lung fibroblasts exposed to LDIR (0.05 Gy) showed temporary activation of the Raf and Akt signalling pathways, promoting cell proliferation.[65] Blocking these pathways halted the proliferation, underscoring their key role in a growth response to LDIR. In contrast, HDIR did not trigger Raf and Akt-mediated proliferation; instead, it activated the DDR and apoptosis. This further highlights the potential existence of non-linear responses to LDIR.

It is thought that the involvement of non-targeted radiation effects is central to the low-dose cellular response.[66] The rationale is that in the low dose range, cells unexposed to direct DNA damage can experience phenotypic changes and responses, ultimately contributing to a population-level response greater than the number of cells directly affected. In contrast, high-dose exposures lead to more cellular

and molecular damage, overshadowing non-targeted effects due to the high probability of DNA damage and cytotoxicity in heavily irradiated cells.

Liu et al. investigated NTE in human cells exposed to LDIR using a medium transfer approach.[29] In this experiment, they irradiated a set of cells and then transferred the culture medium from these irradiated cells to non-irradiated bystander cells, allowing the researchers to observe effects solely from signalling molecules without direct DNA damage. They found three distinct response phases: (1) a protective effect at doses below 2 mGy, where bystander cells exposed to the medium showed better survival compared to directly irradiated cells, (2) a dose-dependent decline in bystander cell survival between 2 mGy and 0.5 Gy, and (3) a plateau effect above 0.5 Gy, where bystander effects saturated and did not worsen with higher doses. These outcomes suggest that NTEs, driven by signalling rather than direct radiation damage, are predominant in the low dose range and behave differently from traditional dose-linear radiation effects.

In summary, LDIR exposures cause milder biomolecular damage and are thus associated with more minimal radiation responses (at the population and single-cell level). These studies collectively emphasize that LDIR can induce DNA damage measured in excess of the background radiation and that DDR can still be activated in a low dose range. However, there are interesting differences in the quantity and quality of DNA damage, the mechanism and kinetics of repair, as well as the transcriptional pathways activated when comparing LDIR and HDIR. These LDIR responses likely manifest differently across cell types, cell states, tissues and organs. Indeed, Shin et al. emphasize the organ-specific nature of cellular responses, noting distinct responses depending on the tissue affected.[67] Together, these findings emphasize the complexity of radiation biology and the need for an improved understanding of both the cellular and molecular events triggered by LDIR exposure specifically.

1.4.4 Health Effects of Low-Dose Radiation Exposure

To date, epidemiological studies have researched valuable cohorts exposed to LDIR, such as atomic bomb survivors, nuclear industry workers, radiologists, patients exposed to frequent diagnostic

procedures and people living in high background radiation. These studies are invaluable in assembling an understanding of the health effects and risks associated with LDIR exposure.

Depending on distance and shielding from the atomic bomb hypocenter, many participants in the LSS cohort were positioned at such a distance from the atomic bomb blast center that they received acute LDIR exposure.[68] By analyzing the LSS data, insights have been gleaned regarding the health effects of LDIR exposure[35–38]. For solid cancers, studies found a significant dose-response relationship even at low doses (0 to 0.20 Gy), with an estimated ERR per Gy of 0.56 (95% CI: 0.15, 1.04).[38] Leukemia, particularly acute myeloid leukemia, showed a positive ERR of 0.15 (95% CI: -0.01, 0.31) at 100 mGy. While this result was not statistically significant, it suggests a potential association at low doses. These results suggest that acute LDIR has measurable cancer risks.

Another major study is the INWORKS study, which aimed to assess cancer risks associated with LDIR exposure among nuclear power plant workers, thereby providing an estimate of the association between protracted low-dose radiation exposure and cancer. The study pooled data from nuclear workers in France, the United Kingdom, and the United States, covering a total of 308,297 workers followed over 35 years. These workers received an average cumulative exposure between 17.7 mGy to 20.9 mGy (weighted colon dose). [69–71] INWORKS found a statistically significant association between cumulative radiation dose and mortality from many cancers. The ERR for leukemia (excluding CLL) was 2.96 per Gy (90% CI 1.17-5.12)[71]. Notably, this risk remained significant even when the analysis was restricted to cumulative doses below 300 mGy. Excluding leukemia, the ERR for all other cancers was 0.48 per Gy (90% CI 0.20-0.79) and 0.47 per Gy (90% CI 0.18-0.79) for solid cancers specifically[70]. This excess risk remained significant when the analysis was restricted to cumulative doses under 200 mGy and even 150mGy[69,72]. INWORKs also found significant positive ERR for mortality from cerebrovascular and ischemic heart disease. The ERR for all circulatory mortality remained significant when restricting the dose range down to under 300 mGy cumulative exposure, beneath which they remained positive but not significant.[73] A study of low dose rate exposed workers in the UK also found a significant risk for heart disease, however, the risk was not significant under 100mSv cumulative exposure.[74]

The SELTINE French cohort of 80,348 nuclear workers also found a significant risk for leukemia death.[75] However, they found no significant ERR for circulatory diseases. Interestingly, they found a significant risk for death from dementia and Alzheimer's in the study cohort. The authors stress that the result should be "interpreted with caution," recommending follow-up studies to investigate this new finding that has not been consistently observed in other studies.

Beyond nuclear power cohorts, there have also been important studies of medical exposures. [72] One meta-analysis investigated the effects of exposure to medical radiation in children. The analysis reported a significantly increased risk for leukemia with a pooled ERR of 26.9 per Gy for postnatal CT exposure.[76] There was however a large 95% CI of 2.7-57.1. The study also found a significantly increased risk for brain tumours with a pooled ERR of 9.1 per Gy (95% CI 5.2-13.1) for postnatal CT exposure. Following sensitivity calculations to add robustness to the findings, the authors concluded that there is excess risk of cancer associated with childhood CT scans. The meta-analysis included a large-cohort Netherlands study including 170,000 people who received CT scans. The study found an ERR per Gy of 8.6 (95% CI: 2, 22) for brain tumours, with a cumulative average dose of 38.5mGy to the brain and found uncertain estimates of excess risk for leukemia.[77]

Epidemiological research has also analyzed disease incidence in individuals living at high natural background radiation. [72] Many such studies have reported mixed results, with some finding no association between dose and risk, others finding excess risk and some reporting reduced risk. Overall, a couple of reviews have concluded that drawing conclusions based on the epidemiological evidence available at the time was difficult. It is clear that if changes to risk do exist, they are likely minor. If there is no excess risk, this could be especially interesting since such populations are exposed to greater cumulative radiation than other cohorts who have seen excess cancer risk, potentially indicating the presence of an induced protective mechanism.

One major meta-analysis conducted by the US National Cancer Institute in 2020 examined studies involving occupational, environmental and medical exposures under 100 mGy. Focusing on studies which passed a bias assessment, this meta-analysis revealed that, for solid cancers, 16 out of 22 studies reported positive ERR per unit dose, rejecting the hypothesis that the median ERR equals zero.[78] After

excluding four studies with potential positive bias, 12 out of 18 studies still reported positive ERRs. For leukemia, 17 out of 20 studies reported positive ERRs, with significant evidence of increased risk even after excluding studies with potential biases. The findings indicate a statistically significant increase in cancer risks from low-dose radiation exposure. The meta-ERR at 100 mGy for solid cancers was 0.029 and 0.16 for leukemia in adults, while for childhood exposure, the meta-ERR for leukemia was notably higher at 2.84[78].

Another large review of LDIR epidemiology posited that "substantial evidence was found from epidemiological studies of exposed groups of humans that ionizing radiation causes cancer at acute and protracted doses above 100 mGy, and growing evidence for doses below 100 mGy."[72] Furthermore, they suggest studies demonstrate that "significant radiation-related solid cancer risks observed at doses of several 100 mGy of protracted exposures (observed, for example, among nuclear workers) demonstrate that doses accumulated over many years at low dose rates do cause stochastic health effects. On this basis, it can be concluded that doses of the order of 100 mGy from recurrent application of medical imaging procedures involving ionizing radiation are of concern, from the viewpoint of radiological protection."

In review of radiation epidemiology, the LNT model continues to be supported by committees for radiation protection. [46,47] Notably, a US National Council on Radiation Protection analysis reviewing 29 studies of occupational, medical and environmental LDIR exposure found that despite their being challenges in quantifying risk in the low-dose range, most studies showed at least weak-to-moderate support for the LNT model.[79] Therefore, they concluded the LNT model continues to be prudent for radiological protection. To date, the CNSC claims the LNT "model plays a key role in how the CNSC approaches radiation protection."[80]

Today, The Million Person Study (MPS) is ongoing to assess the health impacts of prolonged low-dose radiation exposure[81]. The MPS includes over a million individuals across various cohorts, such as nuclear power plant workers, industrial radiographers, medical workers, and atomic veterans. Some preliminary results have been published from the MPS. In the cohort of approximately 135,000 U.S. nuclear power plant workers (mean bone marrow exposure: 37.9 mGy; max: 953 mGy) followed from

1957 to 2011, a notable increase in leukemia risk was observed, with an ERR at 100 mGy of 0.15 (90% CI: -0.001 to 0.31)[44]. However, for solid cancers and other outcomes, such as lung cancer and ischemic heart disease, the findings were less conclusive, with minimal or no observed radiation associations. The ERR at 100 mGy for all solid cancers was 0.01 (95% CI: -0.03 to 0.05), indicating a weak relationship between radiation dose and solid cancer incidence in this cohort. Among the 109,000 medical radiation workers (mean bone marrow exposure: 12.9mGy; max: 1187mGy) monitored between 1965 and 2016, the ERR at 100 mGy for leukemia was 0.10 (95% CI: -0.34 to 0.54). For lung cancer, an ERR of 0.15 (95% CI: 0.02 to 0.27) was reported. [82]

In summary, many epidemiological studies suggest that there exists mounting evidence of excess risk for both incidence and mortality of cancer and non-cancer diseases following exposure to LDIR. Still, more work needs to be done to accurately quantify ERR in the ultra-low dose range, however one can assume these risks would be low based on the available evidence today. Furthermore, epidemiology has not offered any insights as to how dose-rate or quality affects risk, and there is little understanding of what factors may predispose someone to increased risk for radiation-induced health effects. There is however, evidence that the health risks of LDIR are more severe for children than adults. Sex-specific differences in ERR have also been recorded and require follow-up.

There exists harsh criticism of this epidemiological literature, citing biases, poor statistical methodology, and uncertainties in dosimetry. Critics argue that studies, such as the LSS yield modest and highly uncertain estimates in the low-dose range, leaving them significantly vulnerable to confounding factors.[83,84] The INWORKS study, which aimed to assess cancer risks in nuclear workers, has been criticized for not adequately controlling for smoking, stressing that when the study excludes all smoking related cancers, the study showed no statistically significant positive ERR.[83]

Furthermore, opponents of LDIR health risks cite studies which fail to find a correlation between LDIR exposure and health risks, and even studies which find beneficial responses of LDIR exposure.[83–87] Proponents of radiation-induced hormesis claim that LDIR stimulates protective antioxidants, stimulates anti-cancer immunity and suppresses inflammation. Given these claims, LDIR health effects and the LNT model are “considered at least doubtful (and often-obsolete) by certain researchers.[84]

Although this thesis does not focus on the direct assessment of disease risk following LDIR exposure, the epidemiological evidence discussed above frames the biological relevance of LDIR exposure. While contested, this body of research demonstrates that LDIR is not necessarily biologically inert. Even at low doses, ionizing radiation has been shown to induce measurable biological changes that manifest over time as various health outcomes, primarily cancer but also non-cancer diseases. These findings, observed at the population-level, highlight the capacity of LDIR to perturb cellular processes sufficiently to culminate in disease. Therefore, LDIR may pose quantifiable risks to human health, affirming the need to study the underlying biological processes that may lead to those outcomes.

1.5 Ionizing Radiation and the Immune System

It is well-established that ionizing radiation significantly impacts the immune system. The earliest report was published just 10 years following the initial description of x-rays, when Heinke "report[ed] changes in lymph follicles in the spleen and lymph glands [and] a decrease in circulating lymphocytes post x-irradiation."[88,89] The aftermath of the Hiroshima and Nagasaki bombings further illustrated this, as survivors near the hypocenter suffered from ARS, which included hematopoietic syndrome. Specifically, "at the LD_{50} level, bleeding and infection due to immunodeficiency resulting from bone marrow depletion [were] the main causes of death."[90] These historical observations laid the foundation for decades of research exploring the complex effects of ionizing radiation on immune homeostasis, ranging from acute damage to long-term immunomodulatory consequences.

As previously mentioned, hematopoietic syndrome characterized by pancytopenia and susceptibility to infection are major consequences of HDIR exposure. Advancements in single-cell RNA sequencing (scRNA-seq) have enabled the profiling of bone marrow radiosensitivity. In a recent study, mice were subjected to 6 Gy total body irradiation (TBI) prior to conducting gene expression analysis on various bone marrow cell types.[91] The study identified hematopoietic stem and progenitor cells (HSPCs), granulocyte-monocyte progenitors (GMPs), and B cells as the most radiosensitive populations. As anticipated, the highly proliferative HSPCs and GMPs exhibited significant radiosensitivity, while more differentiated cells in non-proliferative states demonstrated increased radioresistance. Radiosensitive clusters exhibited notable shifts in gene expression related to DNA damage response and apoptotic

pathways, correlating with a rapid decline in cell numbers post-irradiation. The authors observed that B cells showed reduced expression of survival pathways, including those regulated by NFKB and AMPK. Conversely, radioresistant populations such as neutrophils displayed minimal alterations in gene expression, suggesting intrinsic protective mechanisms against radiation-induced damage. Nevertheless, despite their resistance, neutrophils and other short-lived hematopoietic cells rapidly deplete in the absence of progenitors and stem cells, leading to conditions such as neutropenia, anemia, and thrombocytopenia. These findings highlight the previously recognized radiosensitivity of bone marrow to ionizing radiation and underscore the heterogeneity in radiosensitivity among its diverse cell populations.

A recent multi-omic study of rhesus macaques has helped comprehensively describe molecular and cellular events occurring within peripheral blood following whole-body HDIR exposure.[92] Their model employed hematology analysis, RNA microarrays and proteomics to understand the impact of 4 Gy total body irradiation, with emphasis in describing the pancytopenia following HDIR exposure. It was observed that lymphocyte levels plummeted within 23 hours post-exposure, with RIL persisting for approximately 27 days in macaques. Conversely, neutrophils and monocytes exhibited a transient increase after exposure, likely due to demargination, followed by a dramatic drop to nearly undetectable levels, only beginning recovery around day 24. The transcriptomic and proteomic data highlighted immediate inflammatory responses and activated pathways for DNA repair and cell cycle arrest, peaking within the first week. From Day 7 onward, cell repair and regeneration processes became dominant, facilitating a gradual restoration of blood cell counts and cellular maintenance functions by four weeks post-exposure. This study provides a detailed characterization of the strong impact of HDIR on the immune system in the acute response, implicating inflammation and hematopoietic syndrome as central processes.

The pronounced radiosensitivity of lymphocytes is especially noteworthy. For patients undergoing radiation therapy, Radiation-induced Lymphopenia (RIL) is a consequence of this sensitivity.[93] Paradoxically, lymphocytes are highly sensitive to radiation despite primarily residing in interphase while circulating and in various tissues. Unlike most other cell types, even minimal DNA damage in

lymphocytes readily triggers apoptosis.[23] It is hypothesized that lymphocytes are intrinsically "primed" for apoptosis, maintaining a basal state closer to the apoptotic threshold than other cell types. Apoptosis processes are used widely in various contexts of lymphocyte regulation and development.[94] Therefore, it suggested that the molecular mechanisms are in place to predispose irradiated lymphocytes towards apoptosis, without having to attempt entering the cell cycle or sustain extensive biomolecular damage. Although this phenomenon is widely observed, there remains a dearth of literature specifically addressing the molecular mechanisms underlying the heightened radiosensitivity of lymphocytes in the context of radiation.

In Resnick-Silverman et al. the C-terminal domain (CTD) of p53 was shown to be essential for modulating apoptosis in radiosensitive tissues like the spleen and thymus.[24] In these tissues, p53's CTD enables strong activation of apoptotic genes, leading to heightened radiation sensitivity and cell death. By contrast, in the liver, the CTD recruits factors that suppress apoptosis, conferring radioresistance. When the CTD is truncated, this selective suppression is lost, making the liver respond to radiation more like the thymus and spleen, with increased apoptosis and sensitivity. Perhaps this represents one potential mechanism underlying the propensity of lymphocytes to undergo radiation-induced apoptosis.

While immune cells are generally more radiosensitive than other cell types, variation exists across immune cell subsets and organs. Paganetti performed an extensive literature review of in-vitro, animal and human studies to assemble consensus on this subject.[93] The review summarizes that B cells exhibit the greatest radiosensitivity, followed by T cells, with NK cells being the most resistant. Among T cells, helper T cells (CD4+) tend to be more radiosensitive than cytotoxic T cells (CD8+). Studies indicate that circulating lymphocytes are generally more vulnerable than lymphocytes residing in non-lymphoid organs, and tumour-infiltrating lymphocytes often display enhanced radioresistance. Following HDIR radiation, nucleated cells of the spleen recover much faster than the thymus and especially the mesenteric lymph node.[95]

Many differences in signalling pathways pre and post-radiation exposure contribute to this heterogeneity, emphasizing the complexity of immune cell radiosensitivity.[23,96] For example, the study by Heylmann et al. shows that non-stimulated lymphocytes are highly sensitive to ionizing radiation due

to elevated ATM pathway activity, which promotes apoptosis following DNA damage.[23] Upon CD3/CD28 stimulation, lymphocytes downregulate ATM and associated DNA repair pathways, resulting in enhanced radioresistance. This has critical implications: the high basal sensitivity of non-stimulated lymphocytes to radiation ensures rapid elimination of damaged cells, preventing the accumulation of mutations among circulating immune cells. However, in tumour environments, where lymphocytes are often activated and proliferating, this acquired radioresistance can help maintain immune responses despite local radiation exposure.

Beyond immunodepletion, radiation can induce inflammation, especially at moderate to high doses. This is especially apparent in localized high-dose radiotherapy. In response to the biomolecular stress, irradiated cells can release a variety of pro-inflammatory cytokines such as TNF-α, IL-1, IL-6, IL-8 and IL-17.[4,97,98] In addition, the accumulation of mitochondrial DNA and ROS in irradiated cells can activate inflammasomes, further promoting cytokine production.[99] If the cell is unable to repair the molecular damage, it will undergo programmed cell death. As Najafi et al. describe, “when IR induces widespread cell death, it can overwhelm the phagocytic system responsible for clearing dead cells. This leads to the accumulation of dead cells and their molecular components within irradiated tissues.”[100] Some of these released components, known as damage-associated molecular patterns (DAMPs), act as danger signals that trigger an inflammatory response from macrophages and dendritic cells. Radiation released DAMPs include ATP, HMGB1, DNA, nucleotides and calreticulin.[4,101] Therefore, irradiated cells can become immunogenic by releasing cytokines, ROS, and their cellular components.

Activated macrophages subsequently release additional cytokines, further amplifying the inflammatory signalling cascade.[4,102–104] Neutrophils and monocytes are actively recruited to the irradiated site and readily migrate into tissues. Importantly, radiation causes vascular changes that promote immune infiltration into damaged tissue. Indeed, radiation induces endothelial phenotypic changes of activation and dysfunction, including “an increase in the expression of the adhesion molecules vascular cell adhesion molecule 1, intercellular adhesion molecule 1, platelet endothelial cell adhesion molecule, and E- and P-selectins,” which mediate recruitment of circulating immune cells.[4] scRNA-seq of murine radiation-induced lung injury showed that vascular endothelial cells express

Cxcl16 to recruit Cd4+ Cxcr6+T cells to the site of radiation damage.[102] In a scRNA-seq study of radiation-induced intestinal damage, endothelial cells expressed high levels of ICAM-1, ICAM-2, Ccl5 and Cxcl12 contributing to the recruitment of monocytes and pro-inflammatory macrophages who in turn expressed VEGF to support endothelial expansion.[103] Therefore, "the vascular endothelium can be considered as a main control point of radiation-induced inflammatory and immune processes."[4]

When recruited leukocytes come into the irradiated tissue, they can exasperate the inflammation by producing more pro-inflammatory cytokines like TNF-α, IL-1, and IL-6.[4,102,103] This response is triggered by their activation from immunogenic signals in the irradiated tissue, coming from cytokines, DAMPs, ROS, contact with collagen fragments and fibronectin. The increased production of these molecules can cause extrinsic apoptosis and fibrosis[105] Radiation-induced inflammation resolves as macrophages clear apoptotic cells and DAMPs, switch to an anti-inflammatory phenotype, and produce cytokines like IL-10 and TGF-β to suppress further inflammation. Simultaneously, immune cells leave the tissue, ROS are neutralized, and endothelial cells return to a quiescent state, restoring tissue homeostasis.

Canonical descriptions of radiation-induced inflammation and hematopoietic syndrome are not comprehensive. Notably, local and total body irradiation can elicit different immune responses. Local high-dose radiation that does not target bones, leads to significant localized tissue reactions without causing hematopoietic syndrome. This process leaves a reservoir of lymphocytes and facilitates the renewal of neutrophils and monocytes, which participate in radiation-induced inflammatory responses. This aspect is central to cancer radiotherapy, where local HDIR not only causes cell death of radiosensitive tumour cells, but also induces inflammation and immune recruitment to the tumour.[4] This contrasts with HDIR in TBI contexts, which is characterized by pancytopenia from death of both peripheral and central mature and progenitor immune cells. Localized in vivo HDIR of mouse femurs at 15 Gy induced distinct hematologic and immunologic effects compared to TBI.[106] Specifically, it led to a reduction in total WBC count and lymphocyte proportion, while concurrently increasing RBC count and granulocyte proportion in the blood. Additionally, a profound depletion of cellularity was observed in the bone marrow, spleen, and thymus. The authors conclude that localized bone marrow irradiation induced systemic hematologic alterations consistent with hematopoietic syndrome, underscoring the broader

systemic impact of targeted radiation exposure. Therefore, it is important to consider radiation exposure patterns when evaluating immune and hematopoietic responses.

Interestingly, radiation has been shown to be anti-inflammatory in different contexts, particularly when lower dose radiation is applied to already inflamed tissues.[107] A single exposure of moderate radiation can reduce inflammatory cytokine and NO production by macrophages in inflamed joints.[4] It has been shown to reduce ROS production, increase anti-oxidant capacity and impair leukocyte adhesion to endothelial cells.[107] In human TNF-a transgenic mice with a polyarthritic phenotype, moderate dose TBI reduced paw swelling and increased grip strength.[108] Furthermore, when moderate radiation was given locally to the hind limb, irradiation reduced joint pro-inflammatory cytokines, reduced the proliferation of fibroblast-like synoviocytes and reduced the differentiation and bone-resorbing activity of osteoclast.[109] Furthermore, it promoted osteoblast mineralization, leading to an increase in bone-forming activity. Nakatsukasa et al. found fractionated radiation could attenuate collagen induced arthritis in a mouse model, while upregulating Tregs, and suppressing IL-6 and IL-17.[110] Therefore, radiotherapy is hailed as being an anti-inflammatory treatment modality for inflammatory diseases. In human studies, LDRT is claimed to reduce inflammation in patients with arthritis and chronic joint inflammation. [111,112] In COVID-19-related lung inflammation, LDRT has been observed to reduce inflammatory biomarkers, though with mixed results.[113–116] Note that while frequently called “low-dose radiotherapy” most studies use absorbed doses in significant excess of the NCRP’s definition of low-dose radiation. LDRT fractionated doses typically range from 0.1 to 1 Gy per session, which is below conventional radiation therapy doses, but much greater than occupational and diagnostic exposures. The total cumulative dose in clinical LDRT often remains under 6 Gy for inflammatory diseases. While LDRT advocates argue that low doses stimulate hormetic mechanisms, critics highlight that even low doses could contribute to cancer risk, as shown in long-term studies of low-dose radiation exposure. While some studies in arthritis and osteoarthritis reported pain relief, randomized sham-controlled trials have failed to push the treatment to approval. This challenges claims of LDRT’s efficacy in inflammatory conditions. Larger controlled trials and biomarker studies are necessary to confirm LDRT’s efficacy and safety in non-cancer applications.

In summary, IR can induce potent immune perturbations. Despite this understanding, the impact of LDIR on the immune system remains inadequately explored. At the cellular level, significant knowledge gaps persist regarding which immune cell populations are most affected by LDIR and the specific organs where these effects are most pronounced. Understanding how immune cell composition is influenced by selective apoptosis in radiosensitive populations or the selective expansion of LDIR-stimulated immune cells is crucial yet remains poorly understood. Key pathways, such as DDR and oxidative stress, may be activated even at low doses, potentially leading to phenotypic changes in immune cells. The degree to which these processes modulate immune phenotype in LDIR exposure is unclear. Furthermore, given the minimal cell stress and tissue damage, it is unclear whether low-dose radiation exposure may still trigger inflammation. Additionally, non-targeted effects are likely involved in LDIR immune perturbation, but their exact roles are not well-defined. Furthermore, the cytokine and chemokine milieu following LDIR exposure is not yet fully characterized, leaving critical gaps in our understanding of the immune-modulatory landscape in response to LDIR. Further research is essential to clarify these complex interactions and their implications for immune system function.

Significant questions have emerged regarding the health effects of LDIR on the immune system. Today, it is increasingly recognized that the immune system plays a central role not only in traditionally immune-related conditions like allergies but also in a broad spectrum of diseases, including cancer, cardiovascular diseases, and neurological disorders. Chronic occupational exposure to LDIR may lead to persistent inflammation, which, in turn, could contribute to the development of various diseases. This underlying mechanism may help explain the observed positive ERR for both cancerous and non-cancerous diseases associated with occupational LDIR exposure. Conversely, LDIR is also being investigated for its therapeutic potential due to hormetic effects, where low doses may stimulate protective anti-inflammatory and anti-cancer responses. This duality in the effects of LDIR highlights the need for comprehensive studies to fully understand its impact on human health and its potential applications in medical treatment.

1.5.1 In-vivo Studies of Low-Dose Radiation & The Immune System

At the in-vivo low dose TBI exposure level, studies have investigated immune system changes following radiation exposure. These studies are pivotal for addressing key knowledge gaps, offering insights into how LDIR influences immune responses within their complex biological context. By analyzing immune cell population size changes, phenotypes, cytokine production, and inflammatory markers across various radiation exposures, such research helps establish a foundational understanding of the processes activated at lower doses. This knowledge is essential for predicting potential health impacts and exploring therapeutic applications of LDIR.

Li et al. explored the impacts of moderate acute gamma radiation doses on murine immune cells across peripheral blood, spleen, thymus, and bone marrow.[117] At 3-5 Gy, TBI significantly decreased circulating lymphocytes, monocytes, and neutrophils for extended periods. Lower doses (1Gy and 0.5 Gy) also caused declines in lymphocytes and neutrophils, though recovery was more swift. Red blood cell counts remained stable following 0.5 and 1 Gy exposures, while higher doses led to reductions in RBC levels. Though no significant cell death occurred in the spleen or thymus, bone marrow progenitor clonogenicity was suppressed. Serum cytokine analysis also revealed that 0.5 Gy TBI elevated various cytokines, notably IL-2, IL-3, and IL-5. Meanwhile, pro-inflammatory cytokines IL-1 and TNF-α increased only following 1 Gy exposure or higher. This study demonstrated that moderate doses of TBI have milder effects on the immune system compared to high doses, causing only temporary more modest peripheral immune fluctuations with no significant cell death in immune organs. However, they could implicate bone marrow progenitor suppression and cytokine production following 0.5 Gy exposure.

Relevant to this thesis is the investigation of the effects of low-dose TBI exposures ranging 100 mGy and below. Shimura et al. conducted a study where mice were exposed to TBI at acute doses ranging from 0.1 Gy-5 Gy.[60] Their hematology analysis showed that even at 0.1 Gy, there was a reduction in total white blood cells and lymphocytes just one day after exposure. Other cell types, such as monocytes, granulocytes, platelets, and red blood cells, remained unchanged. This suggests that peripheral immune cells are particularly sensitive to acute exposure at the top end of the low-dose range.

Maccullum et al. also exposed mice to acute low-dose TBI, with exposures ranging between 0.01 Gy and 0.1 Gy. [59] Their findings revealed that even a low dose of 0.01 Gy prompted detectable p53

induction in the spleen and liver, with levels rising as doses increased. This suggests an extremely sensitive mechanism in mammalian cells for detecting and responding to ionizing radiation, challenging the necessity for a threshold to trigger such responses. Similarly, Shimura et al. could find upregulation of Nrf2 in PBMCs of mice exposed to acute TBI as low as 0.1 Gy, indicating that oxidative stress responses are involved in immune cell responses to low-dose radiation.[60]

In the study by Bogdandi et al., mice were exposed to acute low-dose (0.01 Gy, 0.05 Gy, and 0.1 Gy), moderate-dose (0.5 Gy), and high-dose (2 Gy) total body gamma radiation.[117] This study presents evidence of immune cell-specific radiation sensitivity. Specifically, using the TUNEL assay, they showed that HDIR exposure significantly increased apoptosis, with B cells being the most sensitive. Contrastingly, NK cells and DCs showed no significant changes in apoptosis following HDIR, suggesting potential radio-resistance. Furthermore, they measured less TUNEL staining among NK cells and DCs following LDIR compared to unirradiated controls. Their analysis of the spleen revealed that HDIR exposure caused a marked reduction in all immune cell populations, persisting for up to 7 days. At 0.1 Gy and below, most cell populations experienced significant reductions in cell numbers at least at one time point within 7 days post exposure, with a general downward trend even when changes weren't significant. At 7 days post 0.1 Gy exposure, total splenocytes were reduced by around 35%. Exposure to 0.01 Gy led to more minor changes, with total splenocytes being reduced by around 10% on days 3 and 7. Finally, cytokine profiling via RT-PCR showed notable increases in GM-CSF, IL-5, IL-12, GDF15, IL-10, and IFN-γ following HDIR exposure. In contrast, cytokine modulation at doses ≤0.1 Gy was minimal and described as "less unequivocal." Overall, the results highlight that low-dose TBI can perturb splenocytes, causing reductions in various immune cell populations.

Puukila et al. analyzed transcriptional responses of rats exposed to acute TBI ranging from 2 mGy to 4 Gy.[118] As expected, 4 Gy exposure caused an increase of apoptosis, cell cycle checkpoint and repair genes in the spleen. This included major upregulation of Bax, Bad, Bcl-xl, Tnfrsf1a, Cdk1, Ccnb1, Rad51, Ku70 and Xrcc1. Interestingly, 20 mGy exposure resulted in reduced Tnfsrf1a and Pycard and increased Bcl2 compared to sham controls. The authors concluded that this provides evidence for a

reduction in apoptosis caused by 20 mGy exposure specifically, corresponding with their previous studies showing reduced apoptosis in the spleens of rats receiving 20 mGy TBI.[119]

Most studies analyze the effects of radiation on the immune system immediately following the irradiation period. However, the effects that persist long after the exposure remain unclear. Importantly, the LSS showed that the impacts of the atomic bomb exposure on the immune systems of survivors can last decades.[120]Jangiam et al. investigated the late effects of acute, low-dose whole-body gamma irradiation. [121] Specifically, they analyzed bone marrow, lung, and testis tissues of mice six months post-exposure to doses of 0.05, 0.1, or 1 Gy. The study found that at the lowest dose of 0.05 Gy, there were no significant changes across all metrics compared to controls, with the exception of an increase in IL-10 in all tissues. They suggest this increase indicates a possible anti-inflammatory or protective response at low doses. In contrast, exposure to 0.1 Gy resulted in marked increases in inflammatory markers, including activated NF-κB, TNF-α, IL-1β, and IL-6, across all tissues, indicative of chronic inflammation 6 months following exposure. Additionally, there was a significant reduction in global 5-hydroxymethylcytosine (5hmC) levels, suggesting epigenetic alterations as a late effect of this dose. These findings underscore that even relatively low doses, such as 0.1 Gy, can induce long-term inflammatory responses and epigenetic changes.

In another in-vivo study by Candeias et al., the long-term effects of acute LDIR (0.1 Gy) on the TCR repertoire were analyzed.[122] Using high-throughput sequencing, they found that low-dose radiation led to pronounced and persistent “aging-like” effects on TCR diversity, detectable within a month and lasting at least six months. These effects included reduced TCR diversity, increased clonal expansion of certain T-cell subsets, and a shift in TCR V gene usage, indicative of accelerated immune aging. Furthermore, low-dose radiation impaired the function of HSCs, as demonstrated by transplant experiments in immunodeficient mice, where HSCs from irradiated donors exhibited diminished capacity to regenerate a diverse T-cell repertoire. This study underscores the potential health risks of low-dose radiation, implicating potential acceleration of immune aging, leaving individuals more susceptible to age-related immune deficiencies.

In Liu et al., mice were exposed to either a single dose (0.01-1 Gy) or long-term fractionated irradiation (10 times for a total dose of 0.2, 0.5, or 1 Gy over six weeks).[123] Single-dose exposure ranging up to 0.5 Gy had no effect on hematology metrics measured 24 hours post-exposure. In the spleen, doses as low as 0.01 Gy caused a reduction in the proportion of dendritic cells and macrophages, whereas splenic NK cells were unaffected. Furthermore, thymocyte populations were unaffected by single-dose LDIR. In contrast, 2 days after fractionated low-dose radiation, significant initial suppression of dendritic cells, NK cells and macrophages was measured. Like single-dose exposure, fractionated radiation had limited impact on the proportion of thymocyte populations. By days 7 and 14, most immune cell populations stabilized or partially recovered, showing an early immune suppression phase with gradual adaptation over time, contrasting with the milder effects observed after single-dose exposure. Using western-blot analysis, the authors measured ROS-related protein expression in the spleen and thymus across conditions. Single-dose irradiation did not result in significant changes in ROS-related protein expression. In contrast, fractionated exposure caused levels of antioxidant proteins such as Nrf2 and HO-1 to be initially reduced before later increasing, suggesting a temporal upregulation to counter oxidative stress over time.

Song et al. also investigated the effects of single-dose TBI versus fractionated low-dose TBI on murine immune systems.[124] Total absorbed doses of 0.1, 1, or 10 cGy were administered in either a single acute exposure or divided into three fractionated doses. Both single and fractionated 10cGy exposures led to a decrease in neutrophils, erythrocytes, and platelets. In the spleen, both single and fractionated exposures caused slight but statistically significant shifts in immune cell proportions. Single-dose exposure increased IFN-γ and IL-12, while fractionated exposure promoted IL-4 and IL-10. Western blot analyses revealed distinct differences in redox responsive protein expression, with single-dose exposure notably increasing levels of Nrf2, HO-1, and iNOS. Interestingly, the 10 cGy single exposure showed a weaker ROS-related protein response compared to the 0.1 and 1 cGy doses, which elicited more robust changes across these proteins. In summary, Liu and Song et al. highlight the immune-modulating differences between single and fractionated exposures, as well as the potential for very low doses, down to 0.1 cGy, to significantly increase ROS-related protein levels in splenocytes.

There exists limited studies investigating the effects of chronic LDIR exposure on the immune system. Shin et al. investigated the effects of chronic LDIR exposure in mice, applying a low-dose-rate of 0.7 mGy/h for 11.9 days to reach a cumulative dose of 0.2 Gy.[125] A high-dose group received 3.95 mGy/h for 21 days, totaling 2 Gy. The authors reported no significant changes in hematological metrics, including WBC, RBC, and platelet counts, at either dose rate. Additionally, they found no differences in splenocyte population proportions, even with a cumulative 2 Gy dose, contrasting with findings from Bogdandi et al., where 2 Gy delivered acutely caused substantial shifts in splenocyte populations.[126] Using an antibody-based membrane assay, the authors analyzed serum cytokine levels after 0.2 Gy exposure, comparing them to unirradiated controls. Their analysis revealed that "the sera from these mice exhibited elevated levels of IL-3, IL-4, leptin, MCP-1, MCP-5, MIP-1α, thrombopoietin, and VEGF along with slight reduction of IL-12p70, IL-13, IL-17, and IFN-γ."[125] The changes in cytokine levels were relatively small, with absolute differences under 0.5. This study highlights that chronic low-dose exposure causes no perturbations in immune cell populations shortly after exposure. However, the authors underscore that these subtle alterations in the peripheral cytokine milieu at 0.2 Gy suggest LDIR is not biologically inert and may induce subtle shifts in immune cell phenotypes.

In a study by Courtade et al., mice were irradiated with chronic very low-dose radiation. In this unique study, the mice received cumulative 20 cGy whole-body gamma irradiation over 24 months.[127] On a per-day basis, this rate is approximately 0.0274 mGy/day**.** Mice were euthanized at various time points throughout the study, and the spleen and thymus were analyzed. The results showed that this chronic low-dose exposure did not significantly alter the total counts of splenocytes or thymocytes, although a small, temporary and statistically significant increase in splenocyte and thymocyte counts were observed at 12 and 18 months, respectively. T-cell populations in both the spleen and thymus showed no notable changes, indicating that cellular immunity was not strongly affected by this dose rate. Immunoglobulin levels, however, showed a dose-dependent decline over time. Specifically, IgG1, IgG2a, and IgG2b levels decreased significantly at 12, 18, and 24 months, although B-cell numbers in the spleen remained stable. Overall, the study found that continuous very low-dose irradiation did not

stimulate or markedly suppress cellular immunity but did lead to a subtle reduction in specific immunoglobulins.

Guo et al. exposed C57BL/6 to 2, 10, 50, or 250 mGy γ-irradiation daily for 30 days until cumulative doses of 60, 300, 1500, and 7500 mGy were received, respectively.[128] Irradiation to a minimum of 1500 mGy caused a reduction in CD34+ bone marrow cells, while only 300mGy were needed to cause reduction in proportion of c-Kit+ population. Those c-Kit+ cells had elevated ROS, and DNA damage as indicated by quantification of 53BP1 foci. While the lower dose exposures did not statistically reduce the number of cells in the bone marrow, PCR array showed that they still exhibited changes in gene expression. While the majority of modulated genes were shared across exposure conditions, the authors did identify a handful of dose-specific differentially expressed genes, such as the upregulation of Nr0b2 and Hspb8 in mice exposed to a cumulative 60 mGy. This study demonstrated the sensitivity and dose-dependency of radiation's effect on the bone marrow of mice exposed to daily γ-irradiation.

In a recent study by Yanai et al., mice received 20mGy of whole-body gamma irradiation each day until a cumulative exposure of 1-8 Gy.[129] The treatment caused a decrease in peripheral white blood cell counts, with the reduction becoming greater with radiation dose received and remained low up to 210 days post-irradiation. The experiment showed no change to peripheral red blood cells or platelets. The authors also assessed the impact of low-dose radiation on hematopoietic stem and progenitor cells by injecting irradiated bone marrow or spleen cells into lethally irradiated mice and counting femur colonies at 7 (day-7 CFU-S) or 12 days (day-12 CFU-S) post-transplant. Results showed a dose-dependent decline in both day-7 and day-12 CFU-S, as well as day-7 macrophage lineage colonies, indicating radiation-induced damage to both short-term progenitors and primitive long-term hematopoietic stem cells. Notably, these stem cell populations did not recover compared to unirradiated controls during the post-irradiation follow-up period. Together, these results suggest that continuous low-dose rate radiation reaching cumulative high absorbed doses can reduce bone marrow stem cell counts and peripheral white blood cells.

There exists a need to investigate whether the minimal perturbations seen following LDIR exposure lead to any functional consequences. In one study, when mice were exposed to fractionated radiation

resulting in cumulative exposure of 20 cGy, macrophages exhibited increased nitric oxide production and phagocytic activity.[130] Specifically, Pandey et al. collected peritoneal exudate cells post in-vivo irradiation and incubated them with heat-killed *E. coli* to measure phagocytic activity. They found macrophages from irradiated mice engaged in more phagocytosis than cells from unirradiated mice. Increased NO production was measured by stimulating adherent splenocytes and measuring nitrite using Griess reagent.

Studies have assessed the effects of LDIR on anti-cancer immunity by performing low-dose TBI and tumour transplantation. For example, a study chronically exposing mice to γ-rays at dose-rates of 0.05, 1 or 20 mGy per day for 400 days found that low-dose radiation exposure caused no changes in tumour translatability compared to controls.[131] Only those mice exposed to the highest dose rate radiation experienced increased tumour translatability, potentially via radiation-induced immunosuppression. In Cheda et al., whole body 0.1Gy irradiation prior to sarcoma injection limited tumour metastasis in an NK cell dependent mechanism.[132] In Song et al., whole body single dose 10cGy or fractionated radiation to cumulative dose of 10 cGy radiation was protective against tumour growth and metastatic potential against several tumour types.[133] Clinical trials for LDR in cancer therapy have shown interesting results in enhancing immune responses and supporting immunotherapies.[134] However, LDR in this context is not yet approved due to a lack of large-scale, conclusive data on patient outcomes, and it remains controversial, as critics question the long-term safety and consistency of its effects across different cancers.

While controversial, LDIR has also been explored as an anti-inflammatory modality in the low-dose range. For example, hypercholesterolemic ApoE-deficient mice were exposed to low-dose TBI and had their heart sections analyzed.[135] This study found decreases in ICAM-1 and Thy 1 expression, indicating an anti-inflammatory effect by impairing leukocyte attachment. Therefore, LDIR exposure may contribute to reduced inflammation when tissues are chronically inflamed, however more studies are needed in the low dose range to explore that possibility.

As suspected, these studies suggest that whole-body LDIR exposure, whether delivered acutely or chronically results in mild immune perturbations in comparison to HDIR exposures. They provide

compelling evidence in contrary to a general low-dose hypersensitivity of the immune system, as most measurements at the cellular and molecular level are mild in magnitude. Observations revealing the existence of DDR and antioxidant responses within the low-dose range suggest that cells have an exceptionally low threshold for radiation detection, supporting the hypothesis that DDR activation might be relevant at low doses. By examining immune cell populations across multiple organs, these studies demonstrate a variety of transient fluctuations in immune cell populations. Differences in dose, dose-rate and fractionation likely contribute to the heterogeneity in immune cell sensitivity and fluctuation across studies. Furthermore, findings of subtle but persistent shifts in cytokine levels without overt cell loss or stimulation, indicate that cytokine modulation may be a key mechanism by which LDIR shapes immunity. Interestingly, despite these minor changes, LDIR may sufficiently modulate the immune system to realize differences in anti-cancer immunity. With significant variations in study design, strains, exposure conditions, and findings, together these studies highlight that low-dose radiation can lead to nuanced changes in the immune system.

1.5.1 Epidemiolocal Observations of Ionizing Radiation Mediated Immune Perturbation

The LSS study interrogated the immune systems of atomic bomb survivors up to 60 years following their exposure. Astonishingly, these studies found residual immune injury persisting amongst the survivors many years following the exposure. These findings included a significant dose-dependent reduction in CD4+ and CD8+ T cells, and a dose-dependent increase of B cells.[136,137] Unfortunately, this study did not subset any statistical analysis in the low dose range to clearly demonstrate the effects of LDIR on those measurements. In an earlier study, Kusunoki et al. showed that atomic bomb survivors exposed to LDIR (between 1-9 cCy or 10-49 cGy) had no significant differences in the numbers of peripheral CD19+, CD4+, CD8+ or CD5+ cells, no matter the age at exposure or age attained.[138] Functionally, there was a significant but minor decrease in IL-2 production by CD2+ cells isolated from highly irradiated survivors.[139] Survivors had a significant trend of increasing levels of inflammatory markers, including TNF-α, IFN-γ, IL-10, ESR, and certain immunoglobulins (IgA, IgM, and total Ig) with cumulative radiation dose.[120] However, the statistics reported do not suggest that each of these markers

is significantly upregulated specifically at low doses. Instead, the significance lies in the observed dose-dependent increase across the full range of radiation exposure. In conclusion, the LSS does not show specific effects of low-dose radiation on the immune system but highlights lasting dose-dependent changes attributable to atomic bomb exposure.[140]

A study by Gyuleva et al. investigated the effects of protracted low-dose occupational exposure in employees at a nuclear power plant in Bulgaria.[141] The study followed employees over their entire length of service, ranging around 20-30 years. The cohort was divided into groups based on cumulative exposure (n=19-32 per group), with the lowest exposed group having exposures beneath 25mSv, attaining an average 11.8 mSv cumulative exposure. The largest group had an average 324.6mSv cumulative exposure. The analysis revealed no statistically significant differences between the control group and the low-dose groups (0-25 mSv and 25-100 mSv) in terms of total T cell population proportions, and levels of immunoglobulin and cytokines. Similarly, when Rees et al. compared power plant workers cumulatively exposed to >200mGy vs <27.5mGy, they found no significant differences in the proportions of T cells and B cells.[142]

Godekmerdan et al. analyzed the peripheral blood of 50 radiology workers exposed to LDIR compared to age-matched controls. They found lower CD4+ T cells and lower IgG, IgA, IgM and C3 and C4 amongst radiology workers.[143] Another study of 47 radiology workers showed increased CD19+ cell counts but decreased proportions of B1 (CD5+CD19+) and memory B cells (CD27+CD19+).[144] These reductions were more pronounced in workers with over 15 years of exposure, indicating that prolonged LLIR exposure may impair humoral immunity.

Studies on populations in high background radiation areas such as Ramsar, Iran, and Yangjiang, China, have demonstrated significant alterations in immune parameters compared to control groups from regions with normal background radiation levels.[107] In Ramsar, researchers collected blood samples from 100 individuals, divided into an exposed group (from high-radiation areas) and a control group (from areas with normal radiation levels).[145] Lymphocytes were cultured with PHA mitogen to stimulate cytokine release which was measured by ELISA. The results indicated that residents from high-radiation areas showed significantly lower levels of IL-2 and IFN-γ production and higher levels of

IL-4 and IL-10 production, signalling a shift towards a less inflammatory immune profile. Residents of Yangjian showed increases in peripheral CD8+ T cells, as well as increases in cytokines including IFN-γ, IL-1a, MCP-1, sIL-6R, EGFR, CRP, VEGF, and IL-10.[146]

Interestingly, a transcriptomic study of PBMCs in people living in the Kerala coast of India has been performed.[147] Their study cohort included 36 individuals exposed to a wide range of background radiation doses, ranging from under 1 mGy to 45 mGy per year. They receive this radiation from the presence of radioactive elements like thorium in monazite sands. They found a dose-dependent increase in the expression of genes related to the DDR pathway. Specifically, people exposed to >5mGy per year showed an over representation of genes involved in DNA repair, cell cycle regulation, mRNA processing, protein transport, histone modifications, apoptosis, and immune response.

Altogether, the body of evidence including in-vivo and epidemiological studies indicates that low-dose ionizing radiation can result in subtle but significant alterations to the immune system, which may persist long-term. While some studies suggest minimal effects at very low doses, there is clear evidence of dose-dependent changes in immune parameters as exposure levels increase. In summary, the ICRP claims that LDIR exposure has “immunomodulatory effects”, with accumulating studies showing varying outcomes.

1.5 Challenges and Directions of Low-Dose Radiation Research

Research on the effects of low-dose radiation is essential for understanding its potential health impacts and guiding protective measures. However, this field faces numerous challenges, both in terms of research infrastructure and the intrinsic complexities of studying low-dose effects. This section briefly discusses the primary challenges and knowledge gaps associated with low-dose radiation research and highlights the future directions proposed to address these challenges. Special emphasis is made on knowledge gaps specific to the field of low-dose radiation immunology.

Unfortunately, the molecular and cellular effects of low-dose radiation are intrinsically difficult to study. There is ample evidence showing that these responses are subtle, making them difficult to detect and quantify. Many experiments may lack the sensitivity and sample size necessary to capture these

subtle perturbations. Furthermore, research has shown great variability in LDIR responses. Effects vary across absorbed doses, dose-rates and radiation type. Moreover, the response to low-dose radiation also varies across cell types, organs, genotypes, ages, and organisms, contributing to inconsistencies in findings. This diversity complicates the ability to generalize findings and requires a broad spectrum of studies to account for these variations. Compounding the inherent variability and subtleness of LDIR responses means that large sample sizes need to be combined with high resolution analysis to make significant findings.

Another hurdle is a lack of infrastructure available to study low-dose-rate exposures in vivo, especially over the long term at low-dose-rates. Conducting such studies requires specialized facilities capable of housing mice in consistent low-dose radiation environments for extended periods, which are currently limited. Specialized irradiation facilities, such as those at the CNL or IES, are unique and not broadly available to researchers.

Epidemiological studies face unique challenges due to the nature of low-dose radiation exposure. The inherent subtle, low incidence, stochastic, and latent health effects of radiation exposure require long-term studies with large sample sizes to make meaningful conclusions. Health effects of low-dose radiation may take years or decades to manifest, requiring long-term studies to establish relationships. Separating the effects of low-dose radiation from other environmental and lifestyle factors is complex and requires meticulous study designs. The absence of specific radiation biomarkers further complicates the analysis.

In light of these challenges, understanding the effects of LDIR on the immune system remains a critical area of scientific inquiry. Despite efforts in both epidemiological and experimental studies, the field lacks a unified comprehension of the underlying mechanisms. While HDR is known to cause significant disruptions in immune homeostasis, it is not yet clear if LDIR induces similar yet subtler changes or entirely different effects. Identifying the thresholds for these responses and evaluating their physiological significance is imperative. Furthermore, it is essential to differentiate between transient and persistent immune alterations following LDIR exposure. Current literature often highlights immune perturbations without providing molecular insights, underscoring the necessity for in-depth investigation.

Without a thorough understanding of these effects, the role of the immune system in contributing to the observed ERRs for cancer and other diseases remains uncertain.

Evidence from epidemiological and experimental studies suggests that immune cells exhibit varying sensitivities to LDIR, yet significant discrepancies exist across research findings. This results in an incomplete understanding of which specific immune cell types or states are most susceptible to radiation-induced immunomodulation. Identifying the cell types or conditions that confer increased vulnerability to LDIR remains a crucial research gap that needs to be addressed, with important implications for optimizing radiotherapy strategies.

In 2022, the US National Academy of Sciences (NAS) laid out several key priorities to address critical gaps in the understanding of LDIR effects[40]. One of the central recommendations was to establish more facilities capable of delivering precise, low-dose, and low-dose-rate exposures for long-term in vivo studies. Moreover, they advocate for enhanced coordination and collaboration across research institutes to ensure broader access to specialized irradiation facilities and address the current infrastructure limitations that hinder long-term, controlled LDIR studies.

The NAS places particular emphasis on the need for more in vivo studies, arguing that "cells function within a specific biological context and are strongly controlled by the signals they receive," which highlights the complexity of biological responses to radiation.[40] They stress the importance of in-vivo work due to the nature of cellular communication including bystander and abscopal responses to radiation. The report concludes that "to fully understand the effects of LDIR, it is imperative to study these interactions in vivo as much as possible." [40]

They recommended future research identify biomarkers that link cellular radiation responses to adverse health outcomes as a high priority. They suggest the identification of “Diagnostic biomarkers [that] identify adverse outcomes… preferentially induced by low-dose and low-dose-rate radiation” and “biomarkers of response may identify cellular and molecular features or biological processes that change in response to low-dose and low-dose-rate radiation exposures." [40]

The NAS also highlights the transformative potential of emerging technologies such as single-cell RNA sequencing, CRISPR-based genetic manipulation, and advanced imaging techniques, which allow

for more precise mapping of the cellular and molecular processes influenced by LDIR. [40] They strongly encourage the comprehensive use of omics technologies to better understand the nuanced biological effects of low-dose exposures. Additionally, they stress that modern advances in computational power, will be crucial for analyzing the large-scale data produced by epidemiological and biological studies, ultimately enabling more detailed and accurate assessments of LDIR's effects.

2 Study Objectives

The objective of this study was to characterize the effects of sustained LDIR on the immune system. Specifically, we sought to uncover and describe the mechanisms by which different immune cell populations respond to sustained whole-body radiation exposure. This research was conducted in collaboration with CNL, leveraging their state-of-the-art facilities that enable prolonged exposure to low-dose-rate radiation in an in-vivo model.[148]

In this study, mice were exposed to continuous low dose rate cobalt-60 gamma rays for one week in-vivo, reaching cumulative low absorbed doses of 10 mGy or 100 mGy. For our purposes, a murine model facilitated a controlled experiment, with genetic consistency, and the ability to study immune cells from various organs. The total body dose of 100 mGy was chosen because it represents the upper limit of "low dose" radiation in the literature. By setting this dose as the highest level of exposure, we aimed to investigate potentially, the most intense response within the low-dose range. On the other hand, 10 mGy represents a cumulative dose experienced occupationally.

To achieve a comprehensive system-wide understanding, we analyzed immune cells isolated from both central and peripheral immune organs. This thorough approach targeted the capture of a wide spectrum of cell responses to irradiation and attempted to connect changes in the bone marrow and thymus to the blood and spleen. Our analysis utilized a combination of advanced techniques: hematology to assess systemic blood parameters, flow cytometry to quantify and profile various immune cell populations, bulk RNA sequencing to measure gene expression changes across the entire immune cell population, and single-cell RNA sequencing to provide unsupervised and transcriptome wide insights at single-cell resolution. To the best of our knowledge, this study represents a unique experimental model and is the first to leverage scRNA-seq to study immune responses to whole-body low-dose radiation exposure.

Our hypothesis was that chronic low-dose radiation exposure would induce subtle changes to immune system homeostasis. We anticipated identifying cell-type-specific responses to radiation, as experiments have demonstrated that different types of immune cells can exhibit distinct reactions to the

LDIR exposure. Furthermore, we expected transcriptomic experiments to reveal in detail the molecular mechanisms underlying immune cell responses to LDIR exposure, potentially generating novel low-dose radiation response gene-sets of biomarkers for future research. Furthermore, we predicted to characterize dose-dependent responses of immune cells to radiation, potentially identifying thresholds for cell responses. Murine studies utilizing whole body exposures around and below 100 mGy have shown at most subtle cellular and molecular responses. Combining comprehensive, sensitive and high-resolution methodologies in our approach, we anticipated revealing novel insights which may have been missed by previous studies. By identifying these changes, we hoped to contribute to the broader understanding of how exposure to low dose radiation can perturb immune homeostasis.

3 Methodology

3.1 Mice Irradiation and Organ Dissociation

Eighteen-week-old female C57BL/6 mice (Jackson Laboratories) were housed and irradiated at the CNL (Chalk River, Ontario, Canada). The entire facility, including the irradiation hall and the conventional animal room where control mice were housed, is Specific Pathogen Free. The mice were fed PicoLab Rodent 20 5K75 chow and provided water in bottles. Housing conditions were maintained at a temperature of 20-26°C, humidity of 20-80%, with a 12-hour light/dark cycle. Three mice per cage were housed in Animal Care Systems Optimice cages with BlockParty bedding, and during acclimatization, the cages were individually ventilated on an Optimice rack system. During irradiation in the Gamma Beam Facility, the cages were placed on wooden racks, open to the room air, with Biofresh™ Performance Bedding. Enrichment materials included an enviropack, nestlet, wooden block, and hut, with food enrichment of Cheerios provided after ear punching and cage changes.

Whole-body γ-irradiation was administered using a Nordion Gammabeam 150C irradiator equipped with a Cobalt-60 source. The irradiation was continuous for 7 days in the pathogen-free irradiation hall of the CNL. Treatment groups were positioned at varying distances from the irradiator to achieve different dose rate exposures. Mice receiving a cumulative dose of 10 mGy (n=6) were exposed to an average dose rate of 0.0614 mGy/hr. Mice receiving a cumulative dose of 100 mGy (n=6) were exposed to an average dose rate of 0.625 mGy/hr. The positioning ensured the beam targeted the mid-level of each cage, centered between the two cages. Dosimetry was performed using an Exradin A8 ion chamber and a Supermax electrometer. Control mice (n=6) were housed separately in a conventional animal room.

Following irradiation, mice were euthanized and dissected immediately to collect spleen, bone marrow, thymus, and blood samples via cardiac puncture. Blood samples were immediately analyzed using the Zoetis Vetscan MS5 hematology analyzer. The remaining organs were transported on ice for around 2.5 hours to the University of Ottawa (Ottawa, Ontario, Canada) for further analysis. All animal

procedures were approved by the CNL Animal Care Committee and adhered to Canadian Council on Animal Care standards.

3.2 Cell Isolation

Spleens were mechanically disrupted by pressing through a 70 µm cell strainer (Bio Basic Canada Inc.) using a syringe plunger. The disrupted tissue was suspended in RPMI medium supplemented with 2% fetal bovine serum (FBS) (Gibco™, Canada) and kept on ice. The suspension was centrifuged at 1200 rpm for 10 minutes at 4°C. The pellet was resuspended in 1 mL of red blood cell (RBC) lysis buffer (Roche) to lyse erythrocytes. Post-lysis, cells were washed with RPMI containing 2% FBS and filtered through a nylon mesh to remove debris. Thymus samples underwent the same mechanical disruption and subsequent processing steps as spleens, with the omission of red blood cell lysis.

Bone marrow cells were obtained by excising femurs, cleaning them of excess tissue, and placing them in cold PBS. Femurs were dried with a kimwipe, removing remaining connective tissue. The ends of the femurs were removed, and marrow was flushed out with a 27 g needle and 1 mL of FBS into a microcentrifuge tube. The marrow was collected by repeated flushing and scraping with the needle to ensure complete extraction, and the femurs were discarded when they appeared pale/white. Bone marrow was kept on ice. Cells were then centrifuged at 1200 rpm for 10 minutes at 4°C, resuspended in RBC lysis buffer, washed with RPMI containing 2% FBS and filtered through nylon mesh.

3.3 Flow Cytometry

Cell staining was conducted under cold conditions and protected from light to preserve cell integrity and prevent fluorophore photobleaching. Single-cell suspensions (1E6 cells) were aliquoted into a 96-well V-bottom plate and washed in staining buffer (PBS supplemented with 2% HI-FBS). Cells were incubated at 4°C for 10 minutes in α-CD16/32 (clone 2.4G2 from Bioexpress) to block non-specific

binding. Cells were then stained with a cocktail of fluorophore-conjugated monoclonal antibodies in staining buffer and incubated at 4°C for 25 minutes. Post-staining, cells were washed with staining buffer and fixed with 2% paraformaldehyde (PFA) for 10 minutes at 4°C. Cells were then washed and resuspended in staining buffer for acquisition. Flow cytometry was performed using an Attune NxT flow cytometer (Attune, ThermoFisher) and analyzed with Kaluza (Beckman Coulter). Antibodies used included: anti-TCRb (H57-597), anti-CD8 (53-6.7), anti-CD49b (DX5), anti-CD11b (M1/70), anti-NKG2D (CX5) from eBioscience™; anti-CD19 (1D3), anti-CD4 (RM4-5), anti-F4/80 (T45-2342), anti-NK1.1 (PK136), anti-Ki-67 (B56), anti-CD69 (H1-2F3), anti-Ly6C (AL-21), anti-Gr1 from BD Biosciences™; anti-CD43 (1B11) from BioLegend™; and Live/Dead Fixable Yellow Dead Cell Stain from Invitrogen™.

3.4 Bulk RNA-Sequencing and Bioinformatics

RNA was extracted from isolated splenocytes using Trizol (Thermofisher). RNA integrity was ensured with a minimum RIN cut-off of 6.5. Poly-A enriched stranded cDNA libraries were generated and subjected to 100 bp paired-end sequencing on a NovaSeq6000 at Genome Quebec (Montreal, Canada). Samples were sequenced to a minimum depth of 23E6 reads. FASTQ files were pseudo-aligned to the mouse transcriptome assembly (mm10) using Kallisto (v.0.46.1). Gene-level quantification was performed with Tximport (v1.32.0). Normalization, differential expression, and principal component analysis were conducted using DESeq2 (v1.44.0). Differentially expressed genes were identified using an adjusted p-value threshold of <0.05. Gene ontology overrepresentation analysis was performed using PANTHER. Gene set enrichment analysis (GSEA) was performed using fgsea (v1.30). Heatmaps were generated from variance-stabilized data. Lists of radiation-responsive genes were sourced from the Gene Ontology database, specifically from GO:0009314, GO:0071478, and GO:0010212.

3.5 Single Cell RNA-Sequencing and Bioinformatics

Cell viability was assessed prior to library preparation using fixable live-dead staining and flow cytometry. Single-cell RNA-seq libraries were prepared using the 10X Genomics Chromium 3’ v3.1

protocol at the Ottawa Hospital Research Institute. Libraries targeted 10,000 cells per sample. Raw sequencing reads were processed with the 10X Genomics cellranger pipeline (v7.0.0), aligning reads to the GRCm38 mouse genome and generating feature barcode matrices.

Downstream analysis was conducted primarily with Seurat (v5.1.0). scDblFinder (v1.18.0) was employed to identify doublets. Filtering removed predicted doublets, cells with high proportion of mitochondrial reads and cells with low transcript and feature counts. Specifically, in the spleen dataset, cells were filtered to include only those with 300–6000 detected genes, 2000–20000 RNA counts, ≤10% mitochondrial content, and identified as singlets. In the bone marrow, cells were filtered to retain those with ≥350 detected genes, ≥1000 RNA counts, ≤6% mitochondrial content, and classified as singlets. Genes expressed in <1% of cells were excluded. Cell cycle scores were computed with Seurat's CellCycleScoring function. Data normalization and technical factor regression (mitochondrial reads percentage, UMI count, cell cycle scores) were performed with scTransform. In the spleen, cell cycle was regressed directly using G2M and S scores, whereas in the bone marrow, regression was performed using the difference between the G2M and S phase scores to preserve the gene expression variation that will separate non-dividing and dividing cells (recommended by Seurat authors for bone marrow). Principal component analysis (PCA) was conducted and 23 and 25 PCs input into unsupervised Louvain clustering and Uniform Manifold Approximation and Projection (UMAP) for spleen and bone marrow datasets respectively.

Unbiased cell annotations were derived using SingleR (v2.6.0) with microarray data from the ImmGen database (accessed via Celldex (v1.14.0)). Cluster markers were calculated using FindAllMarkers function on the untreated dataset. The function was set to return only positive markers (only.pos=TRUE), and genes were considered markers if they were expressed in at least 30% of cells within a cluster (min.pct=0.3). Differential gene expression analysis was computed using the FindMarkers function to compare cells exposed to 10 mGy or 100 mGy with untreated cells within each cluster. The analysis considered genes expressed in at least 30% of cells in that cluster (min.pct=0.3). GSEA was performed on ranked gene lists for each cluster using the fgsea package (v1.30). Genes

were ranked by their average log fold change for 10 mGy or 100 mGy vs. untreated cells. Two pathway sets—MsigDB Hallmark and GO Biological Processes were used for enrichment analysis (accessed from Mouse MsigDB collections). The GSEA was run with a minimum gene set size of 20 and a maximum of 500, using 1000 permutations for statistical significance testing. Results were computed separately for each cluster and pathway set.

3.6 Plots and Statistics

Plots were generated using Kaluza (Beckman Coulter), ggplot2 (v3.5.1), ComplexHeatMap (v2.20.0), Seurat (v5.1.0), cowplot (v1.1.3), and ggVenDiagram (v1.5.2). Hematology and flow cytometry statistical analyses were conducted with the Rstatix (v0.7.2) package. Bulk RNA-sequencing and single-cell RNA sequencing statistical analyses were performed using DESeq2 (v1.44.0) and Seurat (v5.1.0), respectively. Figure 1 was generated using biorender.com.

4 Results

In our experimental model, 18-week-old female C57BL/6 mice were housed for 7 days in front of a ^{60}Co gamma beam source in the CNL Gamma Beam Irradiation Facility **(Figure 1)**. The cages were centered in front of the gamma-beam and staged at a distance from the source that enabled continuous exposures of around 0.06 mGy/hr (n=6) and 0.6 mGy/hr (n=6), resulting in cumulative absorbed doses of 10 mGy and 100 mGy, respectively. An untreated (UT) control (n=6) was housed separately, receiving no radiation treatment. Immediately following the radiation exposure period, the mice were euthanized, blood samples were acquired, and immune cells were isolated from the spleen, thymus and bone marrow for further study.

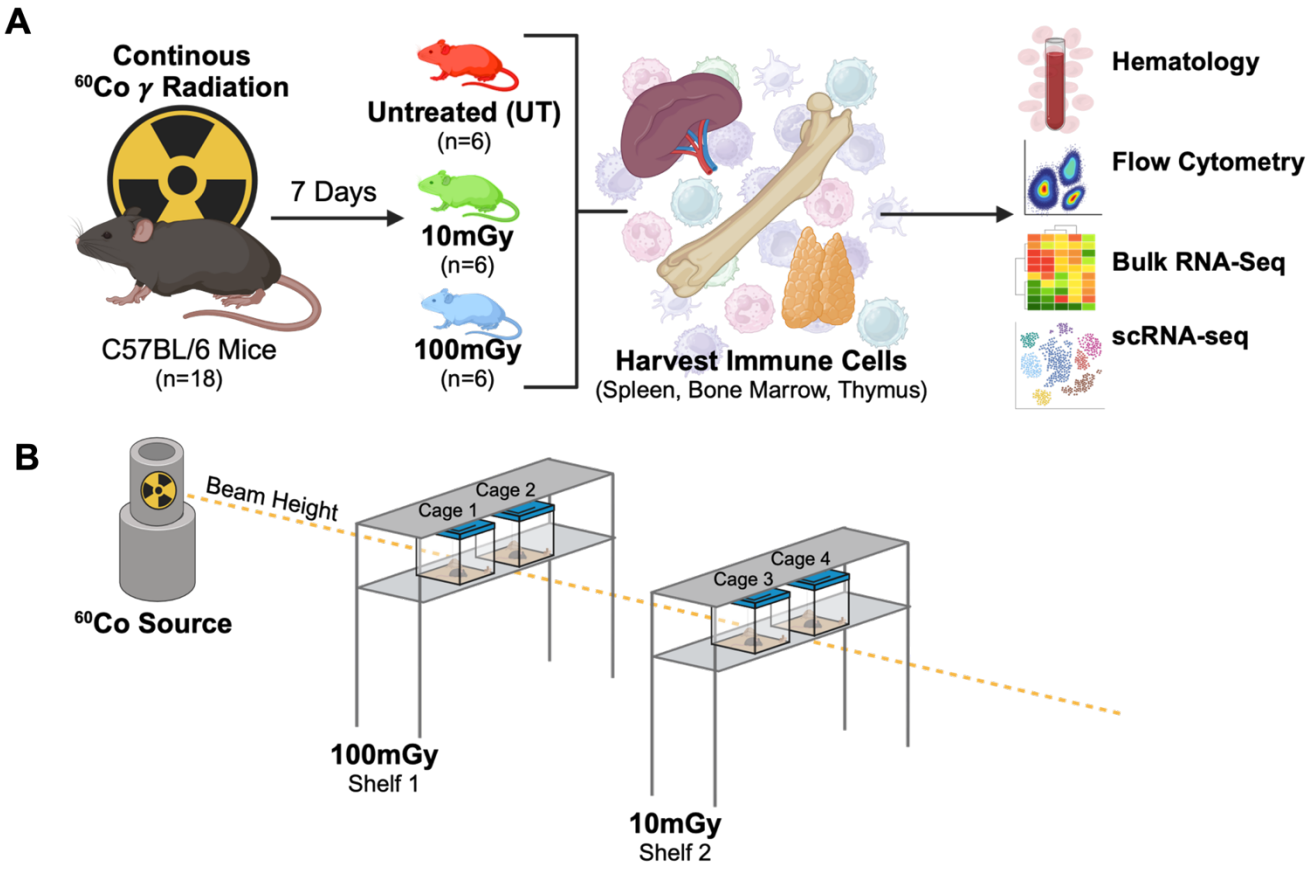

Figure 1. Radiation Exposure and Sample Collection. (A) 18-week-old female C57BL/6 mice were continuously exposed to whole-body ^{60}Co gamma radiation for 7 days in-vivo, at dose rates of 0.06 mGy/h or 0.6 mGy/h, to achieve cumulative doses of 10 mGy (n=6) or 100 mGy (n=6), respectively. An untreated control (n=6) was not irradiated. Immediately following the chronic radiation treatment, blood samples were acquired and immune cells were isolated from the spleen, bone marrow and thymus for further analysis. **(B)** Exposures were completed using a self-shielded ^{60}Co irradiator. Mice cages were placed on shelves in front of the irradiator at distances facilitating the targeted dose rate. The radiation beam was centered between the cages, at the height of the cage.

4.1 Hematological Stability in Mice Following Chronic Low-Dose Radiation Exposure

To assess changes in blood cells, which often reflect radiation-induced damage, a complete blood analysis was conducted. Blood samples were acquired via cardiac puncture and analyzed with an automated hematology machine. Comparing across treatment conditions, no statistically significant differences were measured in the number of white blood cells (WBC), red blood cells (RBC) or concentration of hemoglobin (HGB) **(Figure 2A-C)**. Furthermore, there were no significant differences in the proportion of lymphocytes (%LYM) or monocytes (%MON) (**Figure 2D & E)**.

A statistically significant increase was observed in both the mean count and proportion of neutrophils (%NEU) when comparing untreated samples to those exposed to 10 mGy of radiation **(Figure 2F & Figure S1C).** Specifically, the mean proportion of circulating neutrophils increased from 3.71±1.73 to

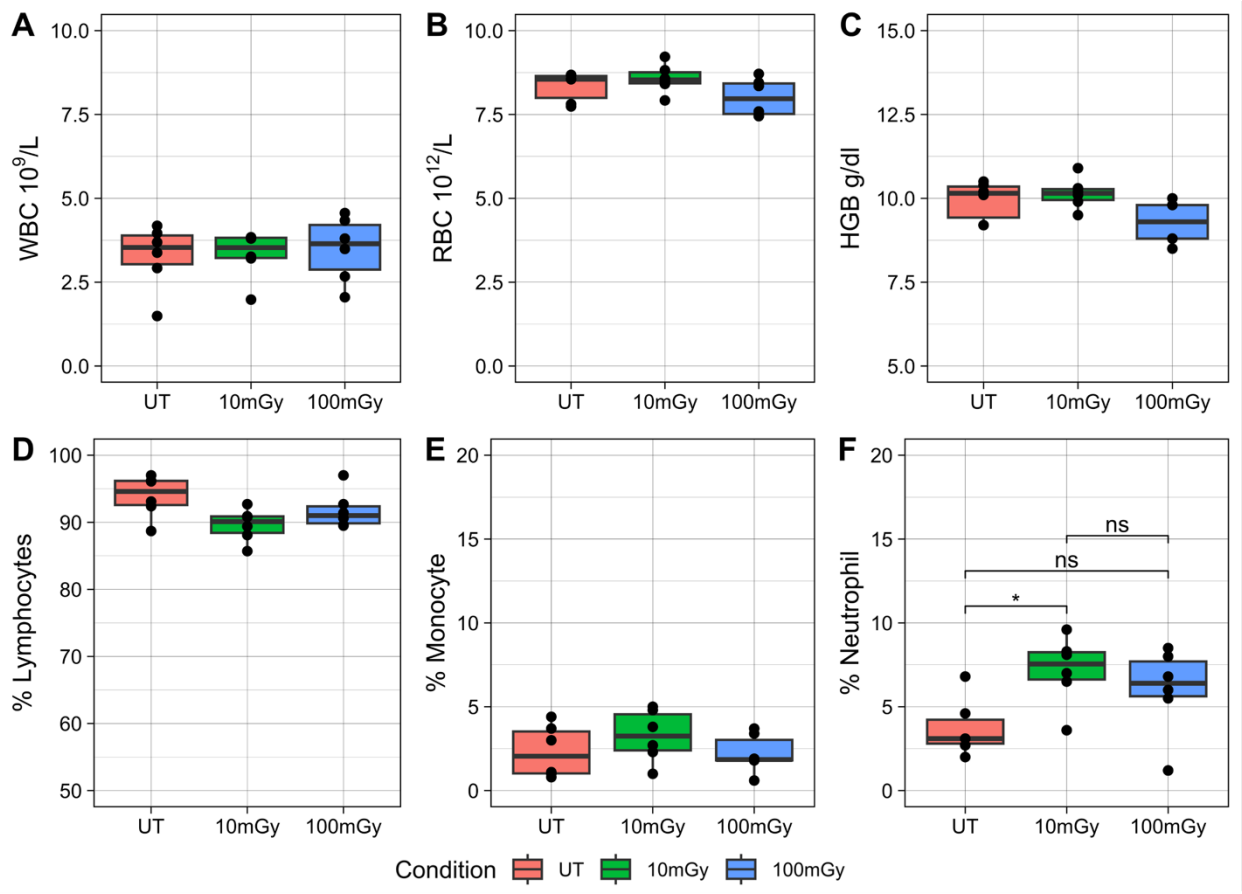

Figure 2. Post-Radiation Hematology Analysis. Following the chronic radiation treatment, blood samples were collected and analyzed using an automatic hematology analyzer. The results indicate no significant variations in (A) white blood cell (WBC) (B) red blood cell (RBC) counts or (C) hemoglobin (HGB). Additionally, the proportions of (D) lymphocytes and (E) monocytes were not statistically affected. There was a significant increase in the (F) proportion of neutrophils when comparing untreated (UT) and 10mGy conditions. Kruskal-Wallis test was used to compare means with post-hoc Dunn's tests. Red colour represents untreated, green represents 10 mGy and blue represents 100 mGy.

7.18± 2.06 (adjusted p-value 0.041)**.** While statistically insignificant, the trend also exists between untreated and 100 mGy as well.

Across a variety of other blood metrics, including hematocrit (HCT) and platelets (PLT), no meaningful differences were measured when comparing untreated samples to those of either treatment condition **(Figure S1)**. However, a minor but statistically significant difference in the mean corpuscular hemoglobin (MCH) from 11.9±0.1pg to 11.6±0.2pg between untreated (UT) and 100 mGy conditions was measured (adjusted p-value 0.026) **(Figure S1F).** In summary, the chronic radiation exposure largely caused no major perturbations in hematology metrics at either absorbed dose, suggesting a lack of systemic changes to immune system homeostasis.

4.2 Stability of Splenic, Thymic, and Bone Marrow Cell Populations following Low-Dose Radiation as Assessed by Flow Cytometry

Next, the spleen, thymus, and bone marrow were analyzed using flow cytometry to investigate the impact of radiation exposure on cell populations in these immune organs. Given that ionizing radiation can induce cell death, sample viability was assessed post-isolation using a fixable viability stain. The viability of splenocytes and thymocytes was consistently high, with most conditions showing a mean viability above 90% **(Figure S2)**. In contrast, bone marrow samples exhibited lower viability, ranging from 65-76%, potentially due to differences in sample shipping or handling. Across all exposure conditions, no significant differences in sample viability were observed, indicating that the radiation treatment did not affect the proportion of live cells in these organs.

The spleen, a crucial secondary lymphoid organ, facilitates interactions between diverse immune cell populations to orchestrate immune responses. The abundance of immune phenomena occurring in the spleen makes it an exceptionally valuable site for studying immune cell responses to various stimuli. The spleen is also particularly sensitive to radiation due to its high lymphocyte content, making it a valuable site for investigating cellular responses under such conditions.

Upon analysis, radiation exposure exerted no major effect on the proportion of immune cell subsets in the spleen **(Figure 3A)**. Among live CD45+ cells, the proportions of CD11b+, CD11c+, TCRb+, and

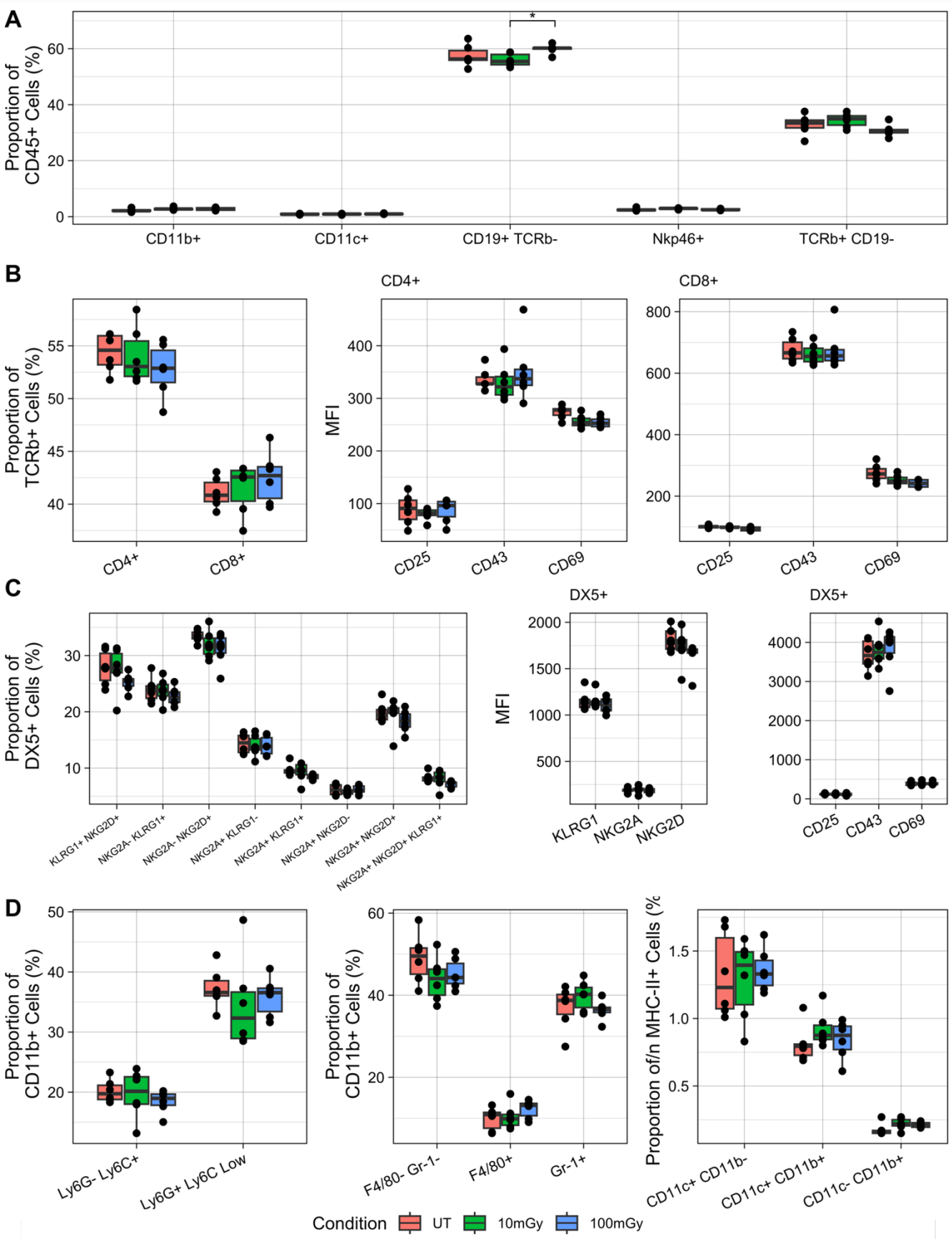
A
Proportion of CD45+ Cells (%)
CD11b+
CD11c+
CD19+ TCRb-
Nkp46+
TCRb+ CD19-
B
Proportion of TCRb+ Cells (%)
CD4+
CD8+
MFI
CD25
CD43
CD69
C
Proportion of DX5+ Cells (%)
KLRG1+ NKG2D+
NKG2A- KLRG1+
NKG2A- NKG2D+
NKG2A+ KLRG1-
NKG2A+ KLRG1+
NKG2A+ NKG2D-
NKG2A+ NKG2D+
NKG2A+ NKG2D+ KLRG1+
KLRG1
NKG2A
NKG2D
D
Proportion of CD11b+ Cells (%)
Ly6G- Ly6C+
Ly6G+ Ly6C Low
F4/80- Gr-1-
F4/80+
Gr-1+
Proportion of/n MHC-II+ Cells (%
CD11c+ CD11b-
CD11c+ CD11b+
CD11c- CD11b+
Condition
UT
10mGy
100mGy

Figure 3. Post-Radiation Analysis of Splenocytes. Following irradiation, immune cells were isolated from the spleen and surface-stained for flow cytometry analysis. The experiment revealed no statistically significant differences in the (A) proportion of cells expressing various immune subset markers, except for a significant but minor increase in the proportion of CD19+ cells. (B) No statistically significant changes were observed in the proportion of CD4+ and CD8+ T cell populations (gated on TCRb+), and the median fluorescence intensity (MFI) of their CD25, CD43, and CD69 expression remained unchanged. (C) There were no statistically significant differences observed in the proportion of NK cells (identified by gating on DX5+) expressing different combinations of NKG2A, KLRG1, and NKG2D markers, nor in the levels of expression of these markers. Furthermore, there were no significant differences in the expression level of CD25, CD43, and CD69 on NK cells. (D) No statistically significant differences were observed in the proportion of various CD11b+ subsets, including F4/80+, Gr1+, Ly6C+, and Ly6G+ cells. (E) Furthermore, there were no statistically significant differences in the proportion of CD11b+ or CD11c+ MHC-II+ cells. Statistical analysis was performed using Kruskal-Wallis test to compare means, followed by post-hoc Dunn's tests.

NKp46+ populations showed no significant differences across conditions. Although no significant changes were detected in the proportion of CD19+ cells when comparing untreated samples to treated conditions, a minor but statistically significant difference was observed between the 10 mGy and 100 mGy conditions (adjusted p-value = 0.039). However, this 3.7% difference in the mean proportions of CD19+ cells is not expected to be biologically significant. Within the T cell compartment (TCRb+), no differences in the proportion of CD4+ or CD8+ T cells were measured **(Figure 3B)**. There were no significant differences in the proportion of NK cell (DX5+) expressing any combination of NKG2A, KLRG1 and NKG2D, and no significant differences in the median expression level of these markers **(Figure 3C).** NK cells also showed no significant variation in the expression of CD25, CD43, and CD69 across conditions. Analysis of the CD11b+ compartment showed no significant alterations in the proportions of Ly6C+ or Ly6G+ $Ly6C^{Low}$ cells, nor in the proportions of F4/80+ and Gr-1+ cells **(Figure 3D)**. Finally, no differences in the small populations of CD11b+ and CD11c+ cells expressing MHC-II in the spleen were measured. Overall, flow cytometry analysis of splenocytes failed to detect any perturbations caused by radiation exposure.

As the site of T cell maturation, the thymus represents an important organ for investigating perturbations to T cell homeostasis. Comparing the proportions of CD3+ and TCRb+ cells in the thymus, no significant differences were measured across all treatment conditions **(Figure 4A).** Next, the proportion of T cells occupying major developmental stages was quantified. Most thymocytes were found in the double positive stage, with a mean proportion of over 85% across conditions **(Figure 4B).** No significant differences in the proportion of thymocytes occupying each developmental stage were measured. As a marker of T cell activation following interaction with MHC, CD69 represents an indicator of T cell stimulation during thymus selection events. No significant effect of radiation exposure on the

proportion of thymocytes expressing CD69 was observed **(Figure 4C).** Overall, these results highlight that T cell development in the thymus was unchanged by the radiation exposures.

Importantly, the bone marrow was also assessed for changes in response to radiation exposure. As the site of hematopoiesis, changes to bone marrow homeostasis can have far-reaching effects on the immune system. In fact, many of the immune related consequences of ARS are the result of massive cell death of bone marrow progenitors, causing changes to systemic blood parameters and susceptibility to infection. In this analysis, no significant differences in the proportion of CD45+ cells in the bone marrow were measured **(Figure 5A).** Furthermore, there were no significant differences in the proportion of both CD4+ and CD8+ T cells **(Figure 5B).** Next, we assessed NK cell development in the bone marrow by quantifying the proportion of DX5+ cells occupying a four-stage program identified by surface markers CD11b and CD27 **(Figure 5C)**[149]**.** Most NK cells in the bone marrow occupied the earliest developmental stages. No significant differences were measured when comparing the proportion of cells from each maturation stage across radiation conditions. Next, no significant differences were found in the proportion of cells expressing CD11b and Gr-1 **(Figure 5D).** Finally, the analysis focused on cells expressing stem cell markers C-Kit and Sca-1. It should be noted that our flow antibody panel did not include a lineage marker cocktail, which is often included to exclude all other immune cell lineages from the stem cell gates. No significant differences were observed in the proportion of C-Kit+ Sca-1+ double positive population, which includes hematopoietic stem cells and the common lymphoid progenitor populations **(Figure 5E**). Furthermore, there were no differences in the proportion of cells occupying the C-Kit+ single positive gate. Dividing the C-Kit+ single positive population by CD34 expression, there was a significant reduction in the proportion of CD34+ cells in both 10 mGy and 100 mGy conditions **(Figure 5F)**. The C-Kit+ CD34+ population includes the common myeloid progenitor and granulocyte-monocyte progenitor cells, suggesting that this population could be slightly reduced following radiation exposure. Altogether, flow cytometry analysis of the bone marrow revealed minimal changes to immune cell populations.

In summary, flow cytometry results indicate that chronic radiation exposure did not significantly alter the proportions of various immune cell subsets in the spleen, thymus, or bone marrow, suggesting a lack of major immunological perturbations in these organs.

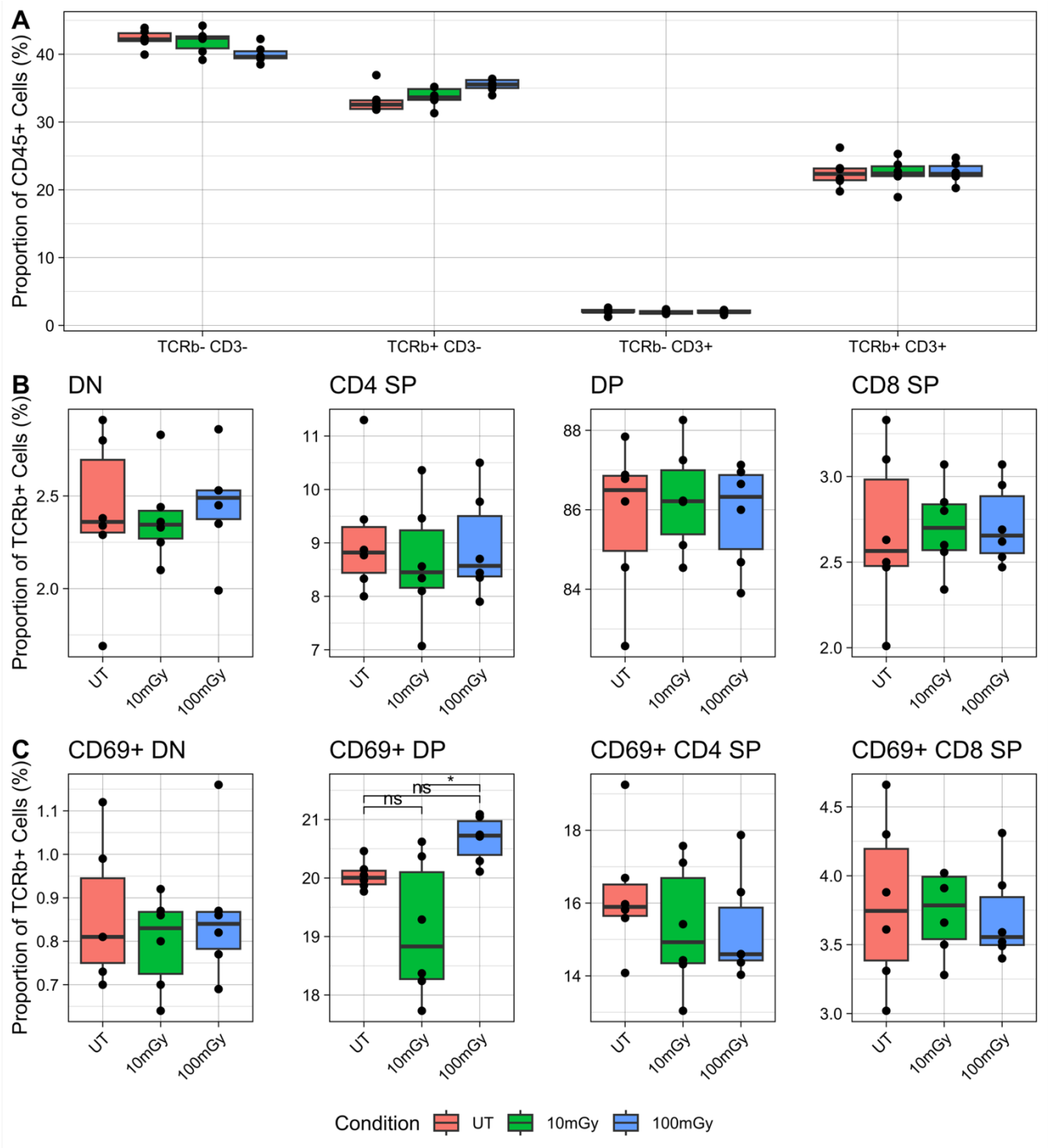

Figure 4. Post-Radiation Analysis of Thymocytes. Immediately following irradiation, immune cells were isolated from the thymus and stained for flow cytometry. The experiment revealed no significant differences in the proportion of **(A)** CD3+ and TCRb+ cells. **(B)** Furthermore, no differences were found in the proportion of thymocytes occupying different T cell maturation stages: CD4/CD8 double negative (DN), double positive (DP) and single positive (SP) (input gate TCRb+). **(C)** CD69 expression was found primarily on DP and SP cells and was not significantly altered by radiation condition. Kruskal-Wallis test was used to compare means with post-hoc Dunn's tests.

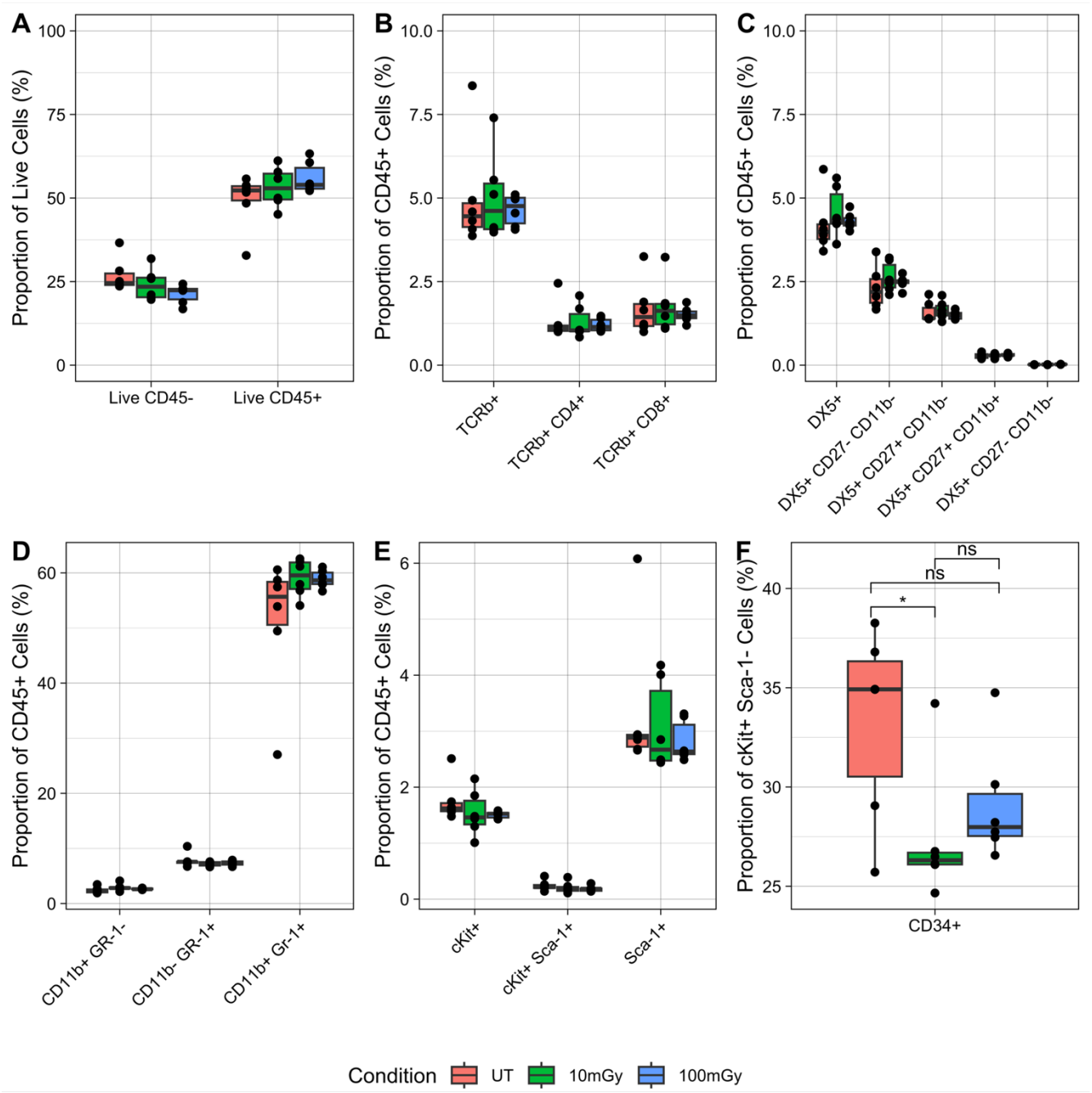

Figure 5. Post-Radiation Analysis of Bone Marrow. Immediately following irradiation, bone marrow cells were isolated from the femur and surface stained for flow cytometry. The experiment revealed no significant differences in the **(A)** proportion of CD45+ cells. Furthermore, no significant differences were found in the proportion of **(B)** different T cell populations, **(C)** NK cell populations, **(D)** myeloid and granulocyte populations, or **(E)** stem cell populations. However, there is a difference in the proportion of **(F)** CD34+ cKit+ Sca-1- cells. Kruskal-Wallis test was used with post-hoc Dunn's tests.

3.3 Minimal Bulk Transcriptomic Response of Splenocytes Exposed to Chronic Low-Dose Radiation Exposure

Our flow cytometry analysis revealed no significant impact of low-dose radiation on immune cell populations. Consequently, we employed bulk RNA-sequencing to explore transcriptome-wide changes, aiming to detect subtle shifts in gene expression that might not be reflected in limited dimensionality of flow cytometry. Principal component analysis (PCA) **(Figure 6)** was employed to visualize the variation between sample transcriptomes. The PCA revealed two principal components, accounting for 19% and 35% of the total variance, respectively. Interestingly, treatment replicates displayed a random distribution across the two axes, with no discernible organization by radiation treatment. This observation suggests that most variation in gene expression measured across samples is not attributable to radiation exposure. Rather, it is likely a result of inherent variability in gene expression and experimental noise.

Next, to investigate genes involved in radiation response, we performed differential expression analysis comparing untreated samples with those from mice exposed to either 10 mGy or 100 mGy doses **(Figure 7A & B)**. These analyses identified a limited number of significantly differentially

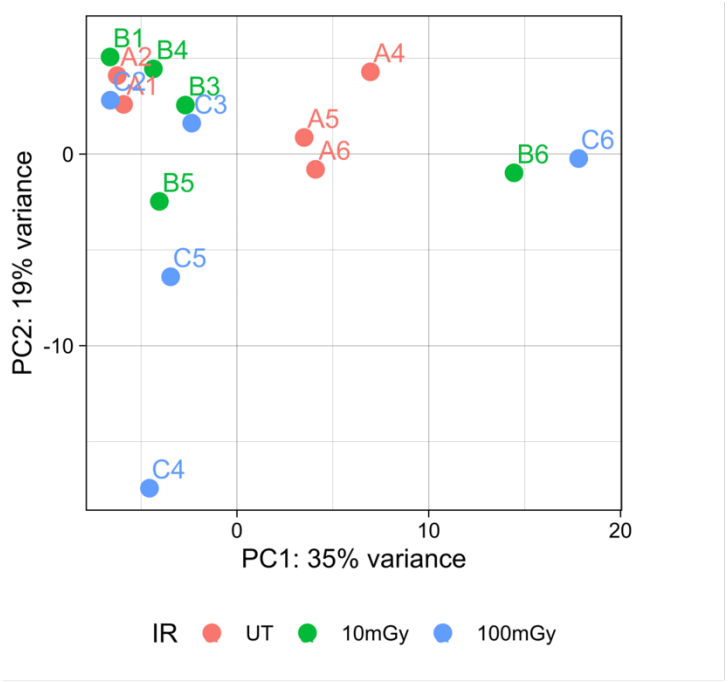

Figure 6. Principal Component Analysis of Bulk RNA-Sequencing Data from Splenocytes. Principal component analysis (PCA) was employed to visualize the variation in transcriptomes across samples. Treatment replicates were randomly distributed across the PCA plot, with no discernible organization by radiation treatment.

expressed genes (DEGs) (adjusted p-value < 0.05). We found 24 DEGs when comparing UT with 10 mGy and 92 DEGs when comparing UT with 100 mGy. It is noteworthy that most DEGs exhibited small changes in magnitude. Specifically, only 4 and 24 DEGs had an absolute log2-fold change above a cut-off of 0.5 when comparing UT to 10 mGy and 100 mGy, respectively **(Figure 7C)**. The median log2 fold changes were 0.46 and 0.47 comparing UT to 10 mGy and 100 mGy, respectively. These 28 genes represent candidate genes potentially involved in immune cell responses to LDIR exposure. Among these DEGs, seven were consistently differentially expressed in both comparisons **(Figure 7D).** A secondary analysis was conducted to compare untreated samples with all radiation-exposed samples combined (10 mGy and 100 mGy together) **(Figure S6A)**. This broader comparison identified 57 significant DEGs, many of which overlapped with those identified in the pair-wise comparisons **(Figure S6B).**

To dissect functional roles of these subtly modulated genes, all significant differentially expressed genes (adjusted p-value < 0.05) were inputted into a Gene Ontology Enrichment analysis. These tests yielded no significant results (data not shown), indicating that the genes were likely not related to any biological process cataloged in the GO database. Additionally, a gene set enrichment analysis (GSEA) was performed using a list of all genes ranked by their fold change when comparing untreated and treated samples, regardless of their significance **(Figure S7)**. When comparing UT vs 100 mGy using the MsigDB hallmark collection and GO Biological Processes collection, 5 gene sets were significantly enriched (adjust p-value < 0.05). However, when comparing the log fold change of all genes involved in these pathways between 100 mGy and UT conditions, none had log2 fold changes greater than 0.2. This diminutive magnitude of changes undermines the likelihood of any substantial biological relevance within these pathways. There were no enriched pathways when performing GSEA on genes ranked by differential expression comparing UT vs 10 mGy conditions.

Finally, a targeted examination of genes implicated in responses to ionizing radiation, particularly those related to DNA damage response, cell cycle regulation and antioxidant defences, was conducted. This focused investigation revealed that, bar the exception of Egr1 and Ccnb1, none of these historically

pertinent genes were significantly differentially expressed when comparing untreated samples with either radiation treatment group **(Figure 8)**. Egr1 was significantly upregulated when comparing UT

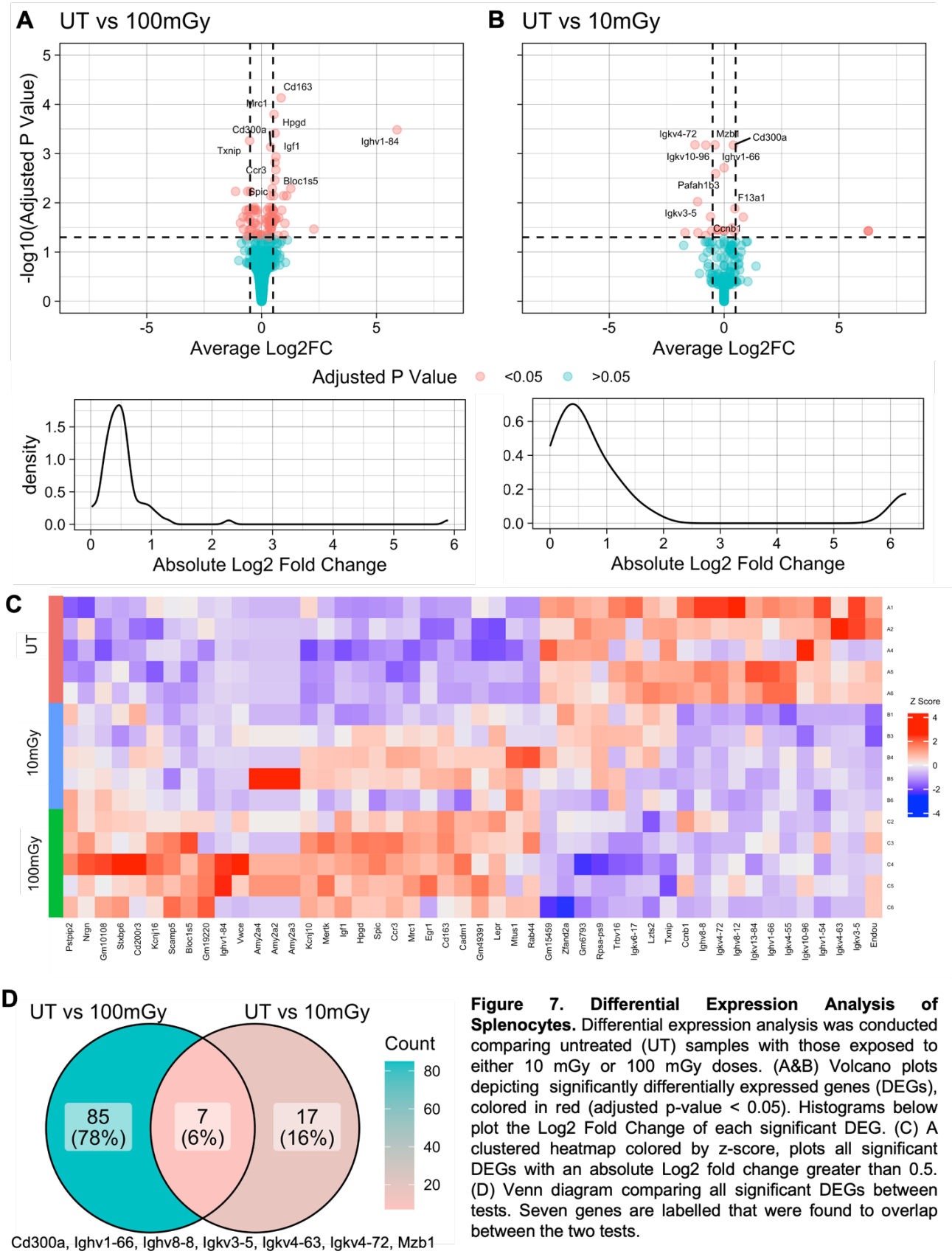

Figure 7. Differential Expression Analysis of Splenocytes. Differential expression analysis was conducted comparing untreated (UT) samples with those exposed to either 10 mGy or 100 mGy doses. (A&B) Volcano plots depicting significantly differentially expressed genes (DEGs), colored in red (adjusted p-value < 0.05). Histograms below plot the Log2 Fold Change of each significant DEG. (C) A clustered heatmap colored by z-score, plots all significant DEGs with an absolute Log2 fold change greater than 0.5. (D) Venn diagram comparing all significant DEGs between tests. Seven genes are labelled that were found to overlap between the two tests.

samples to either 10 or 100 mGy. Ccnb1 was significantly downmodulated only when comparing UT with 10 mGy samples. This indicates an absence of canonical radiation responses, such as DDR or antioxidant pathways following exposure to either 100 mGy or 10 mGy chronic LDR.

In summary, the RNA-seq analysis of splenocytes subjected to low-dose radiation exposure suggests that the bulk transcriptomic landscape remains largely unaltered, exhibiting limited perturbations in gene expression. Moreover, no significant enrichment in well-defined biological pathways was observed, collectively indicating a minimal transcriptomic response to the low-dose radiation conditions studied. A short list of candidate genes which may be involved in response to LDIR exposure was assembled.

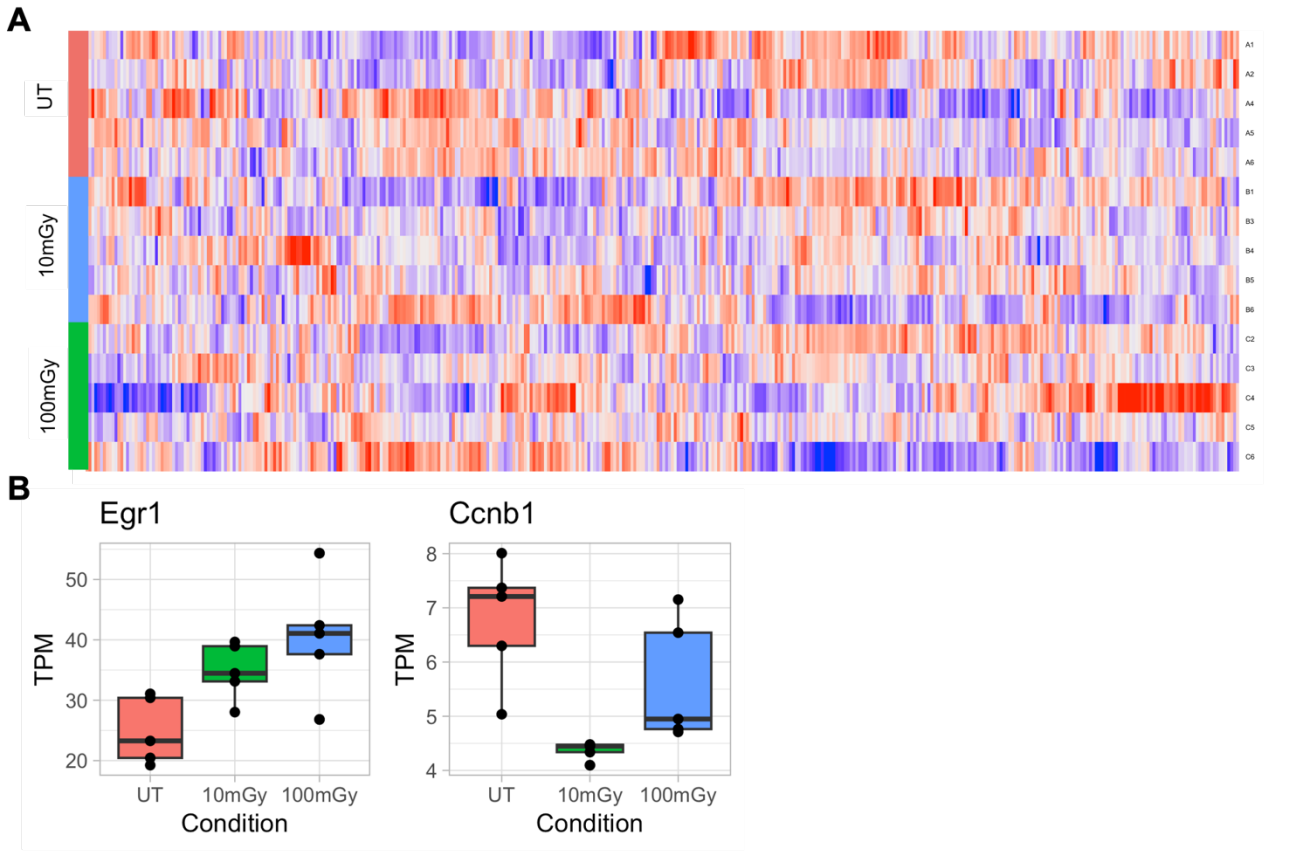

Figure 8. Analyzing Expression of Known Radiation Response Genes. List of genes implicated in the response to ionizing radiation was obtained from the Gene Ontology database. (A) A clustered heatmap plotting the z-score of the radiation pathway genes demonstrates minimal discernible organization of their expression across treatment replicates. (B) Expression of Egr1 and Ccnb1 across conditions in transcript per million (TPM). Significant differential expression of Egr1 was found when comparing UT with either 10 mGy or 100 mGy conditions (adjusted p-value < 0.05). Ccnb1 was only significantly modulated when comparing UT with 10 mGy.

3.4 Limited Impact of Low-Dose Radiation at Single-Cell Resolution in Bone Marrow and Spleen

3.4.1 Upstream Quality Control and Processing

Despite the limited changes observed in our bulk RNA-seq analysis, it is crucial to employ scRNA-seq to further investigate the cellular responses to low-dose radiation in our model. Bulk RNA-seq averages gene expression across heterogeneous cell populations, potentially masking cell-type-specific or rare transcriptional changes. In contrast, scRNA-seq provides the resolution to explore transcriptomic heterogeneity at the single-cell level, allowing us to identify subtle, yet biologically relevant, responses within distinct immune cell populations. Therefore, spleen and bone marrow samples were processed into single-cell suspensions and pooled into combined samples for scRNA-seq analysis using the 10x genomics experimental pipeline.

Both untreated and treated datasets revealed comparable quality control metrics **(Figure 9).** The distribution of the number of features (genes) detected per cell and the number of unique molecular identifiers (UMI) or unique mRNA transcripts detected per cell are comparable across samples **(Figure 9 A,B,G,H)**. The proportion of reads mapping to the mitochondrial genome were both comparable and very low across samples **(Figure 9 C & I)**. Having low mitochondrial read fractions is important because this metric is indicative of cell viability, with dying cells having compromised cell membranes losing their cytoplasmic RNA but retaining mitochondrial RNA[150]. As expected, each dataset shows a positive correlation between the number of UMI and a number of features detected. This is expected, as more UMIs corresponds to more transcripts being captured and sequenced, resulting in more of detected genes **(Figure 9D & J)**. Furthermore, cells with a higher mitochondrial read fraction tend to have a lower number of detected genes as expected due to the loss of cytoplasmic RNA **(Figure 9 E & K)**. Finally, predictions using a doublet prediction algorithm identified 2841 doublets in the spleen dataset and 1918 in the bone marrow dataset **(Figure 9 F&L)**.[151] The datasets were filtered to remove doublets and cells with low feature counts and UMI abundances or high mitochondrial read fractions. After quality control, over 95% of cells in each dataset had a log10GenesPerUMI ratio above 0.8, indicating high transcriptomic complexity. This suggests that most cells retained for analysis captured a diverse range

of gene expression, ensuring high-quality data for downstream analyses while minimizing technical artifacts from low-complexity cells. The filtered datasets contained 27,170 cells for the spleen and 18,916 cells for the bone marrow. Genes expressed in less than 1% of cells were excluded.

Following data normalization using SCTransform, dimensionality reduction was performed using principal component analysis and unsupervised Louvain clustering.[152] Notably, minimal batch effects were observed in the dimensionality reduction, with extensive overlap between samples from both untreated and treated conditions within each cluster **(Figure 10A, E).** Furthermore, Uniform Manifold Approximation and Projection (UMAP) plots demonstrated limited separation based on transcript or gene abundance **(Figure 10B,C,F,G)**. With cell cycle stage regression, major clusters in the spleen showed no strong separation by cell cycle **(Figure 10D)**. In the bone marrow, cell cycle regression was performed by regressing out the difference between the G2M and S phase scores to preserve the gene expression variation that will separate non-dividing and dividing cells (recommended by Seurat authors).[153] The resulting clusters are biased towards a particular cell cycle stage **(Figure 10H)**. Overall, the generated clusters likely represent groups of phenotypically similar cells rather than cells with similar quality control metrics.

3.4.2 Cell Type Annotation and Markers

Spleen

To annotate the clusters, each individual cell was labelled based on reference data from the ImmGen database.[154] The ImmGen dataset referenced contains microarray profiles of various sorted immune cell populations. Using SingleR, each cluster was compared to that database and assigned a label based on similarity in gene expression.[154] Subsequently, the proportions of predicted labels within each cluster were analyzed and a "majority rules approach" was applied to interpret a title for each cluster. Furthermore, cluster markers were computed by calculating the differential expression of each cluster against all other clusters. Combining predicted cell type annotations and interpretation of cell type markers led to the assignment of a label for each cluster.

The unsupervised Louvain clustering resolution was set to generate 22 splenocyte clusters **(Figure 11A & B)**. The spleen is primarily composed of B cell populations, with notable clusters including

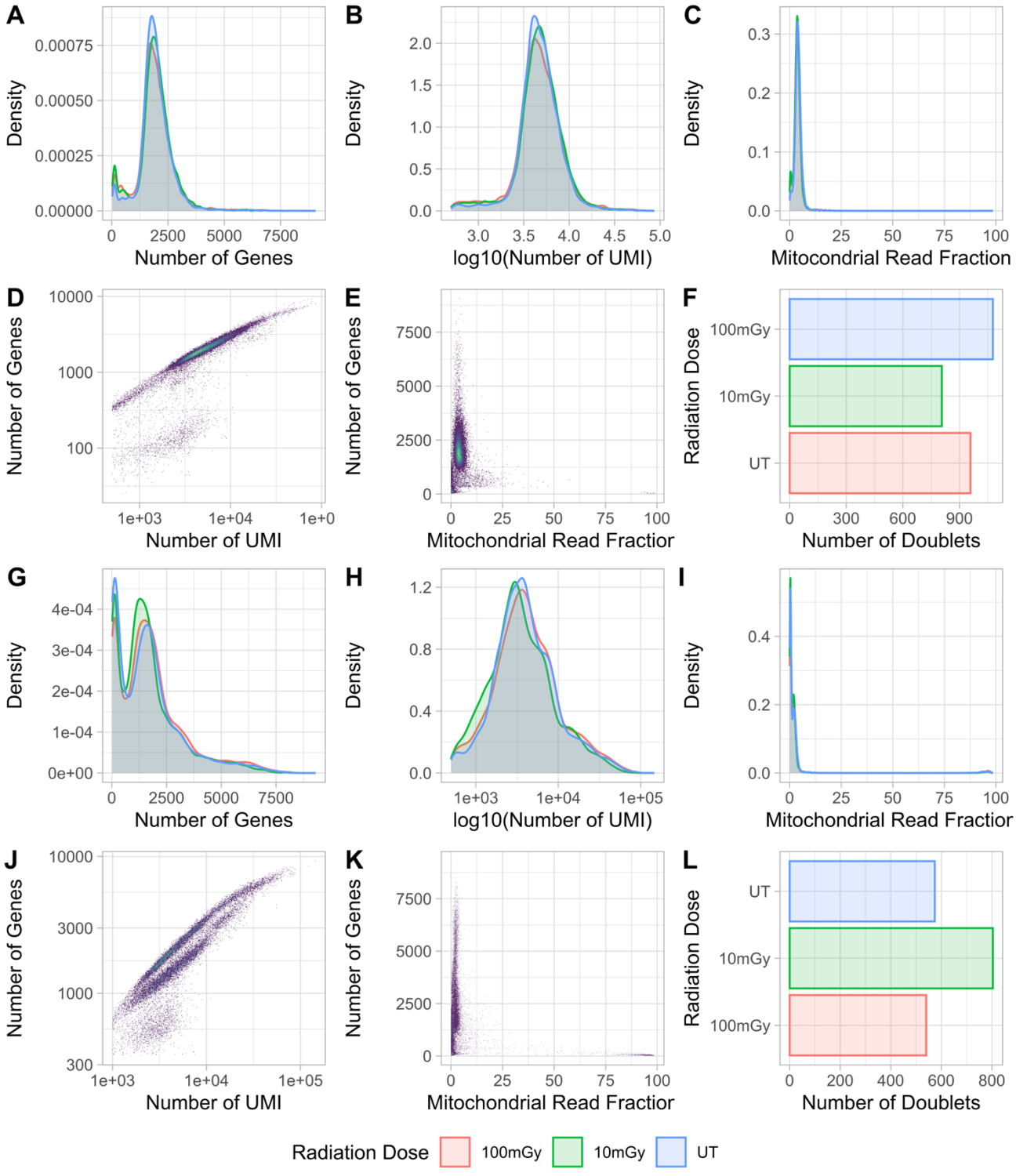

Figure 9. Quality Control of scRNA-seq data sets. (A, G) Distribution of the number of detected genes per cell across conditions. (B, H) Distribution of the number of UMIs (Unique Molecular Identifiers) per cell, log-transformed. (C, I) Distribution of mitochondrial read fractions (%), an indicator of cell quality and stress. (D, J) Scatter plot showing the correlation between the number of UMIs and the number of genes detected per cell. (E, K) Scatter plot showing the relationship between the number of genes detected and mitochondrial read fraction. (F, L) Bar plots showing the number of detected doublets per condition. The colors represent different radiation doses: untreated control (UT, blue), 10mGy (green), and 100mGy (red).

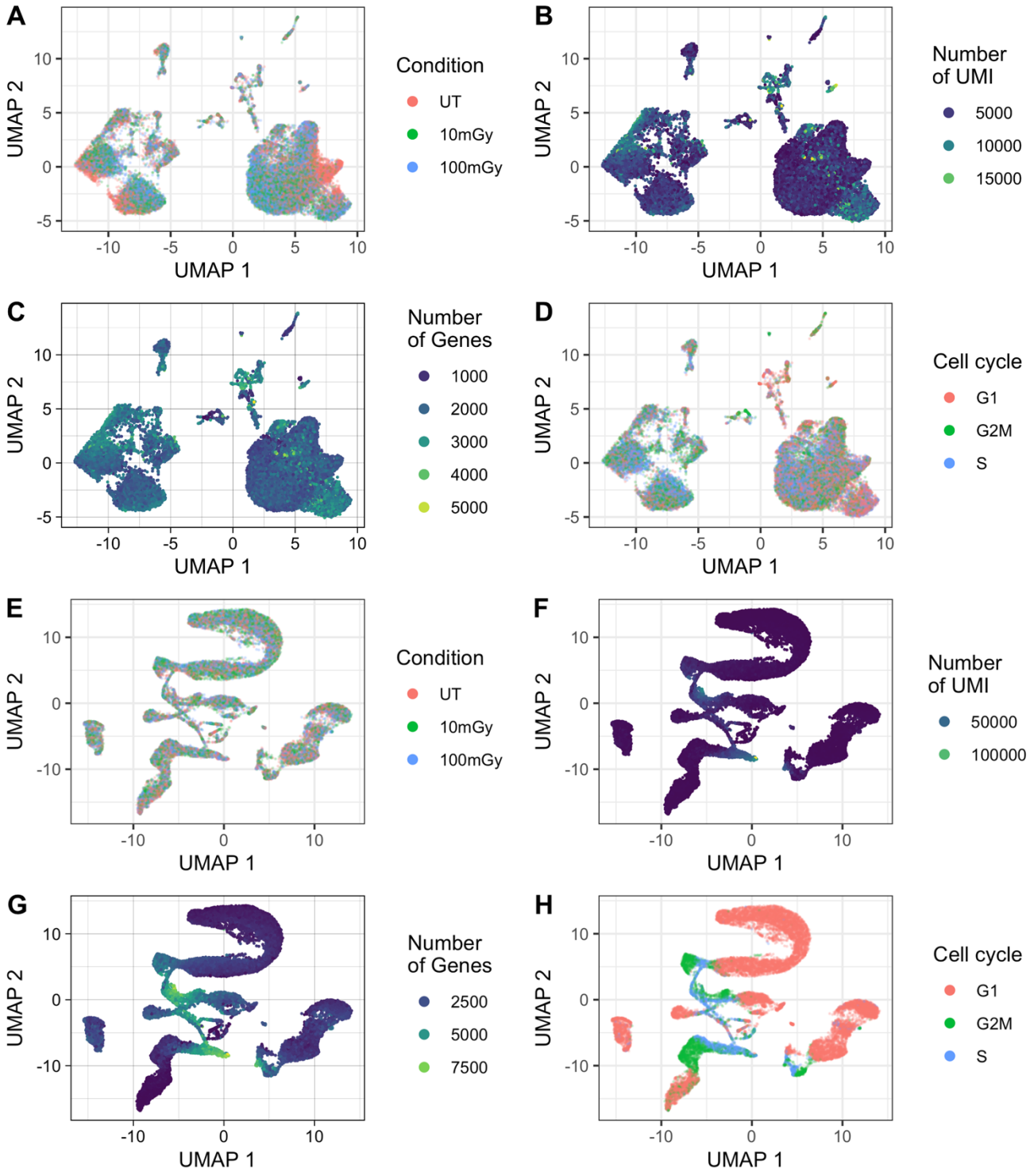

Figure 10. UMAP visualization of quality control metrics. Top two rows (A–D): Spleen; Bottom two rows (E–H): Bone marrow. (A, E) UMAP plots colored by experimental conditions: untreated control (UT, blue), 10 mGy (green), and 100 mGy (red), highlighting minimal batch effects. (B, F) UMAP plots colored by the number of UMIs per cell, with darker colors indicating higher UMI counts. (C, G) UMAP plots showing the number of detected genes per cell, with darker colors representing more genes detected. (D, H) UMAP plots showing cell cycle phase classification (G1, G2M, and S phases), highlighting differences in cell cycle states across the dataset.

follicular B cells (clusters 0, 1, 7), marginal zone B cells (clusters 5 and 12), transitional B cells (cluster 3), germinal center B cells (cluster 12), and B1a cells (clusters 10 and 19). To further explore the distinctive markers of each B cell cluster, we performed differential expression analysis of each B cell cluster against the other B cell clusters using data from the control treatment **(Figure 11D).**

The spleen also contains a significant number of T cell populations **(Figure 11 A & B)**, including CD4 T cells (clusters 2 and 6), CD8 T cells (clusters 4, 8, and 15), and NKT cells (cluster 17). Cluster 2 and cluster 4 were predicted to represent naïve CD4 and CD8 T cells, respectively. In contrast, clusters 6 and 8 were enriched for memory T cells, characterized by the expression of activation and memory markers such as CD122 and CD44 (data not shown). Notably, cluster 6 also contains a population of regulatory T cells (Tregs), distinguished by the co-expression of CD25 and Foxp3. Furthermore, within cluster 8, we identified a smaller subset of gamma-delta T cells, which sets this cluster apart from the other CD8 T cell populations. Differential expression was also performed specifically to compare each T cell cluster against the remaining T cell clusters to find more detailed markers (**Figure 11C).**

Beyond T and B cell populations, the spleen dataset contains clusters representing several other immune cell types **(Figure 11B)**. For instance, cluster 9, annotated as NK cells, aligns with the known splenic composition. This cluster is marked by strong expression of Ncr1, Klra4, Gzma, and Klr8, all of which are classic NK cell markers. Granulocytes were also found in the spleen, with clusters 14 and 21 showing markers Clec4d and Csf3r. Interestingly, cluster 20, though small, contains cells annotated as basophils and mast cells. This cluster is distinguished by the expression of basophil-specific markers like Ccl9 and Ifitm1. Cluster 11 was predicted to contain dendritic cells and exhibited heterogeneity in the expression of the calculated markers. Macrophages and monocytes are predicted to be present in clusters 13 and 18. Cluster 13 is represented by markers Plcb1, Zfyve9 and Plcb1. Cluster 18 appears to represent a mixed population of macrophages and B cells clustering together, as indicated by the presence of a group of cells expressing Ms4a1 (data not shown). Lastly, cluster 16 contains a population of cells expressing hemoglobin genes, likely representing erythroid-lineage cells due to high expression of Alas2 and hemoglobin family genes. Although red pulp macrophages can express erythroid-like genes, cluster 16 lacks typical macrophage markers like F4/80, further supporting their erythroid identity.

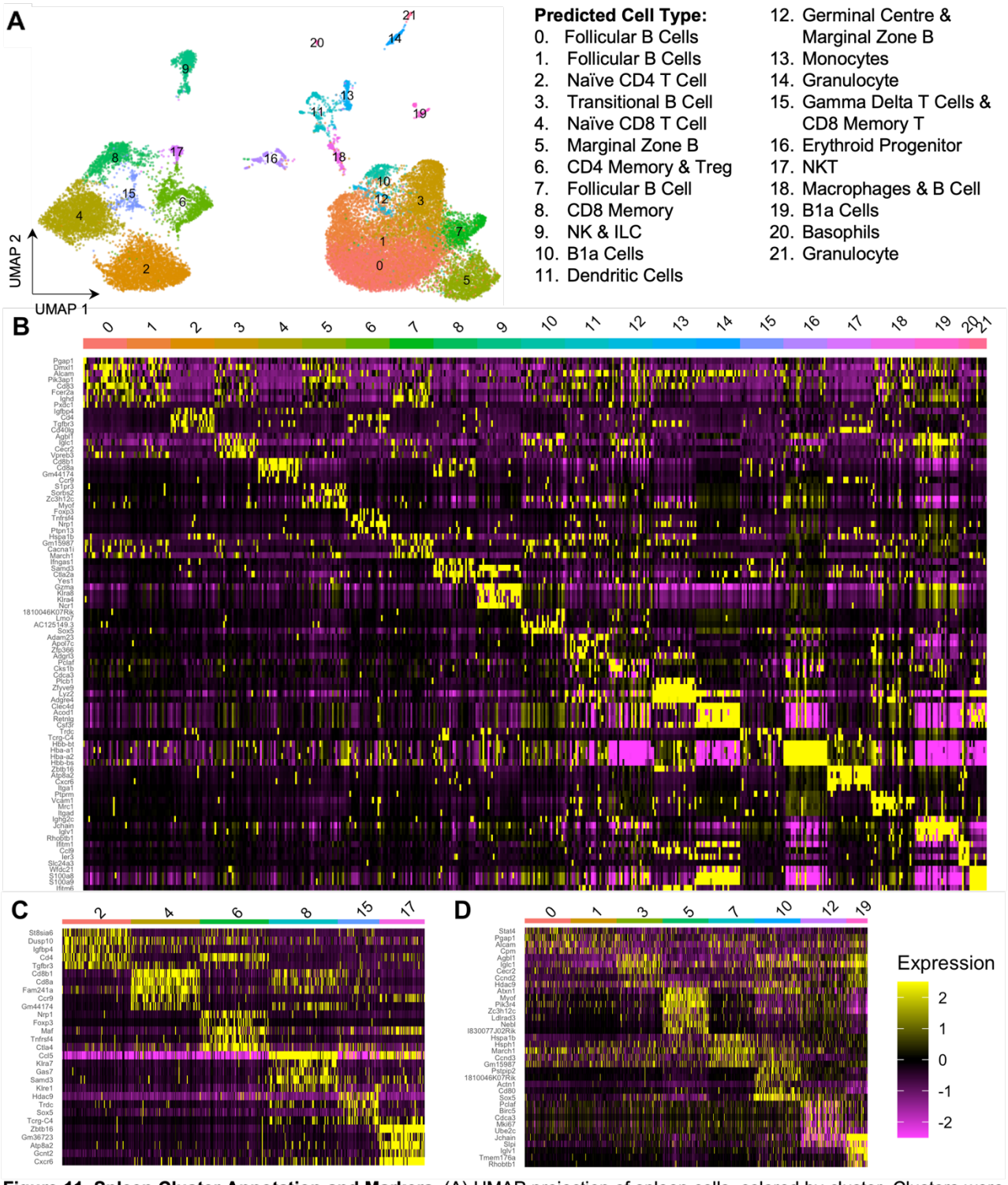

Figure 11. Spleen Cluster Annotation and Markers. (A) UMAP projection of spleen cells, colored by cluster. Clusters were annotated using SingleR with reference to murine immune cell microarray profiles from the ImmGen database. The numbers correspond to the predicted cell types listed in the legend. (B) Heatmap displaying the top 4 marker genes for each cluster, calculated from untreated sample data. The data were down-sampled for visualization purposes. (C) Heatmap highlighting the top marker genes differentiating T cell clusters, using data from untreated samples. (D) Heatmap showing top marker genes distinguishing B cell clusters, also calculated from untreated data. Gene expression values are scaled, with yellow indicating higher expression and purple indicating lower expression.

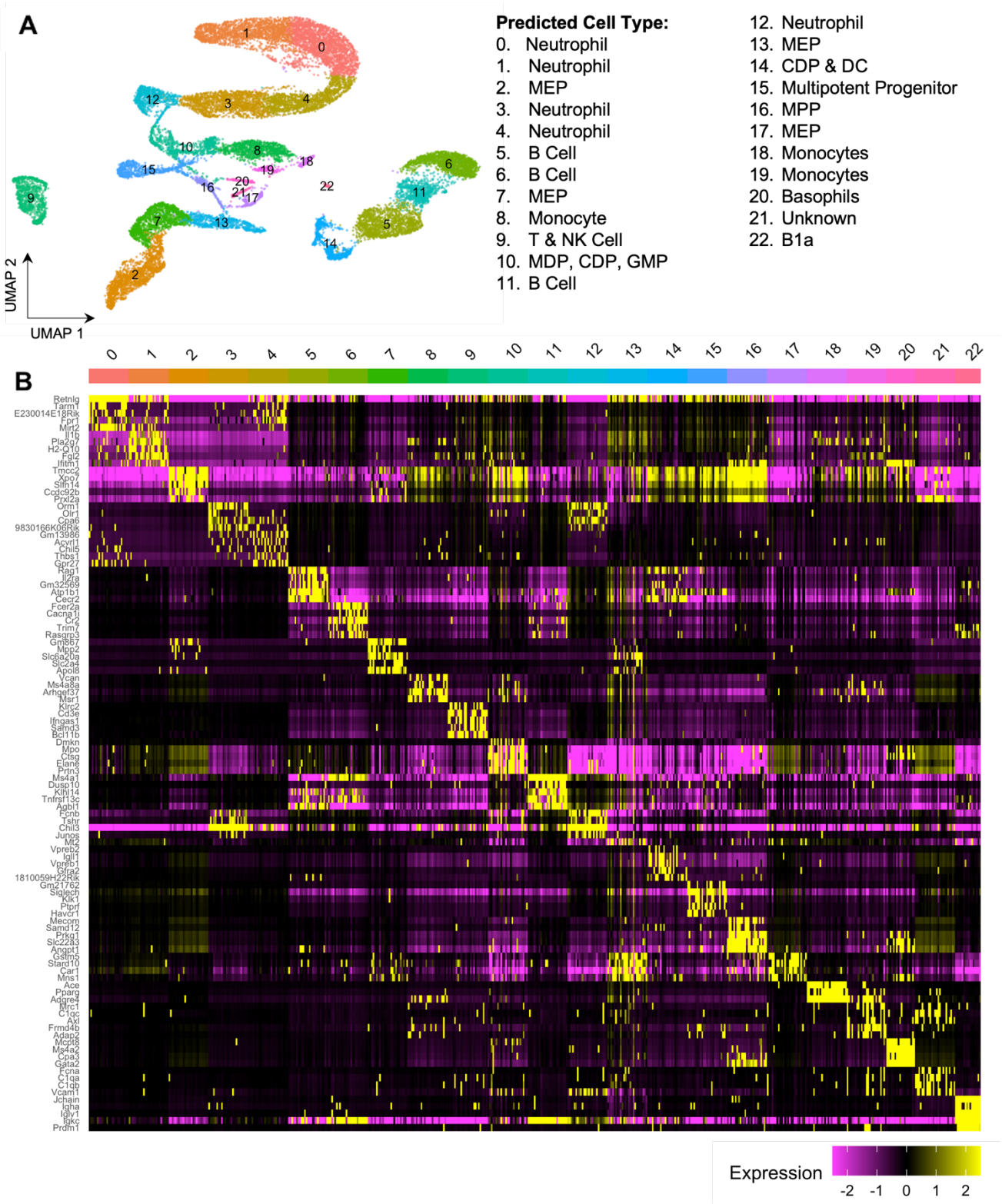

Figure 12. Bone Marrow Cluster Annotation. Unbiased annotation of cells were assigned using SingleR and sorted murine immune cell microarray profiles from the ImmGen database. For each cluster, the proportion of cells assigned to each label was calculated. Using a ”majority rules” approach, labels were interpreted for each cluster. (A) UMAP colored by cluster, with clusters labelled in legend. (B) Heatmap organized by cluster plotting the top 4 marker genes for each cluster. Markers calculated using untreated sample data comparing each cluster against all other clusters. Data was down sampled to 300 cells per cluster.

Bone Marrow

As anticipated, bone marrow clusters displayed elongated shapes, reflecting ongoing cell differentiation processes **(Figure 12A)**. Using Louvain clustering, 23 distinct bone marrow cell clusters were identified. These clusters encompassed a range of cell types, including stem cells and progenitors, various stages of neutrophil and B cell differentiation, as well as myeloid, T cell, and NK cell populations **(Figure 12A & B).**

Given the role of the bone marrow as the site of hematopoiesis, multiple populations of stem cells and progenitors were expected **(Figure 12A)**. Cluster 10 contained various progenitor populations, including monocyte-dendritic cell progenitors (MDP), common dendritic cell progenitors (CDP), and granulocyte-macrophage progenitors (GMP). Cluster 15 was enriched for multipotent progenitors (MPP). Cluster 14 also contained many CDP cells. Cd34 and Kit expression were highly expressed in cells of both cluster 10 and cluster 16 (data not shown).

Neutrophil production, a key function of the bone marrow, involves a series of differentiation stages. Granulocyte-monocyte progenitors (GMP) give rise to committed neutrophil progenitors (G1), followed by pre-neutrophils (G2), immature neutrophils (G3), and mature neutrophils (G4 and G5a-c). Early-stage neutrophil precursors were found in cluster 12, representing the G1/G2 stages and expressing markers such as Fcnb and Tuba1b **(Figure 12B)**. Mid-stage neutrophils, marked by Mmp8, were located in cluster 3 and portions of cluster 4 (G3/G4). The most mature neutrophils, marked by genes such as Il1b, Fgl2, Pla2g7, Gngt2, and Gm2a, were predominant in clusters 0 and 1, reflecting the later stages of neutrophil maturation (G4/G5).

B cell development in the bone marrow follows a progression from hematopoietic stem cells to pro-B, pre-B, and immature B cells. Once fully matured, B cells expressing functional B cell receptors leave the bone marrow for further maturation in peripheral lymphoid tissues. Cluster 14 contained the earliest committed B cell precursors, including pro-B cells and some pre-B cells, marked by early B cell precursor markers such as Vpreb2 **(Figure 12B)**. Pre-B cells in clusters 5 and 11 continued their development. Cluster 5 was marked by Rag1, IL2Rα and cluster 11 was marked by Ms4a1, and Dusp10. The latest stage of B cell differentiation was found in cluster 6, likely representing immature B cells ready to leave

the bone marrow. Cluster 6 was represented by markers Fcer2a and Cr2. Cluster 22, distinct from the main B cell developmental trajectory, was annotated as B1a cells.

MEP cells (Megakaryocyte-Erythroid Progenitors) are a type of progenitor cell in the bone marrow committed to the production of both megakaryocytes (which give rise to platelets) and erythrocytes. Clusters 12,3,4,0 and 1 represent erythroid progenitors predicted as MEPs. Other notable clusters included various monocyte populations (clusters 8, 18, and 19), NK and T cells (cluster 9), and basophils (cluster 20) **(Figure 12A).** Finally, cluster 21 represented an unidentified population that did not express canonical cell type markers. This cluster was characterized by the expression of hemoglobin genes, as well as Tent5c, Bpgm, Mkrn1, and Alas2, suggesting a distinct, possibly erythroid-related, cell population.

3.4.3 Cell Composition

By comparing the proportion of each cell cluster across radiation conditions, it is clear that the radiation exposure did not exert dramatic effects on cellular composition within either organ. In the spleen, most clusters were present in similar proportions in the untreated dataset and both treated datasets, except cluster 7 **(Figure 13A & B)**. This cluster represented around 10% of cells in the untreated sample and only around 3% in both 10 mGy and 100 mGy datasets. Upon further investigation, Cluster 7 was annotated as a group of follicular B cells expressing heat shock protein markers Hspa1a/b+, Hsph1+ **(Figure 11B).** Bulk RNA-seq data revealed that one spleen sample uniquely expressed high levels of these heat shock genes **(Figure S8)**, indicating that the presence of this cluster is likely driven by an outlier sample. In scRNA-seq, where data from multiple replicates are pooled, these outlier B cells were clustered alongside other follicular B cells, but their distinct expression of heat shock proteins caused them to form a separate cluster. Thus, the reduction in the proportion of cluster 7 in the radiation-treated datasets likely reflects the absence of these outlier cells rather than a radiation-sensitive population of B cells. These findings suggest that cluster 7 represents an artifact of the clustering process, influenced by an outlier sample, rather than a biologically meaningful response

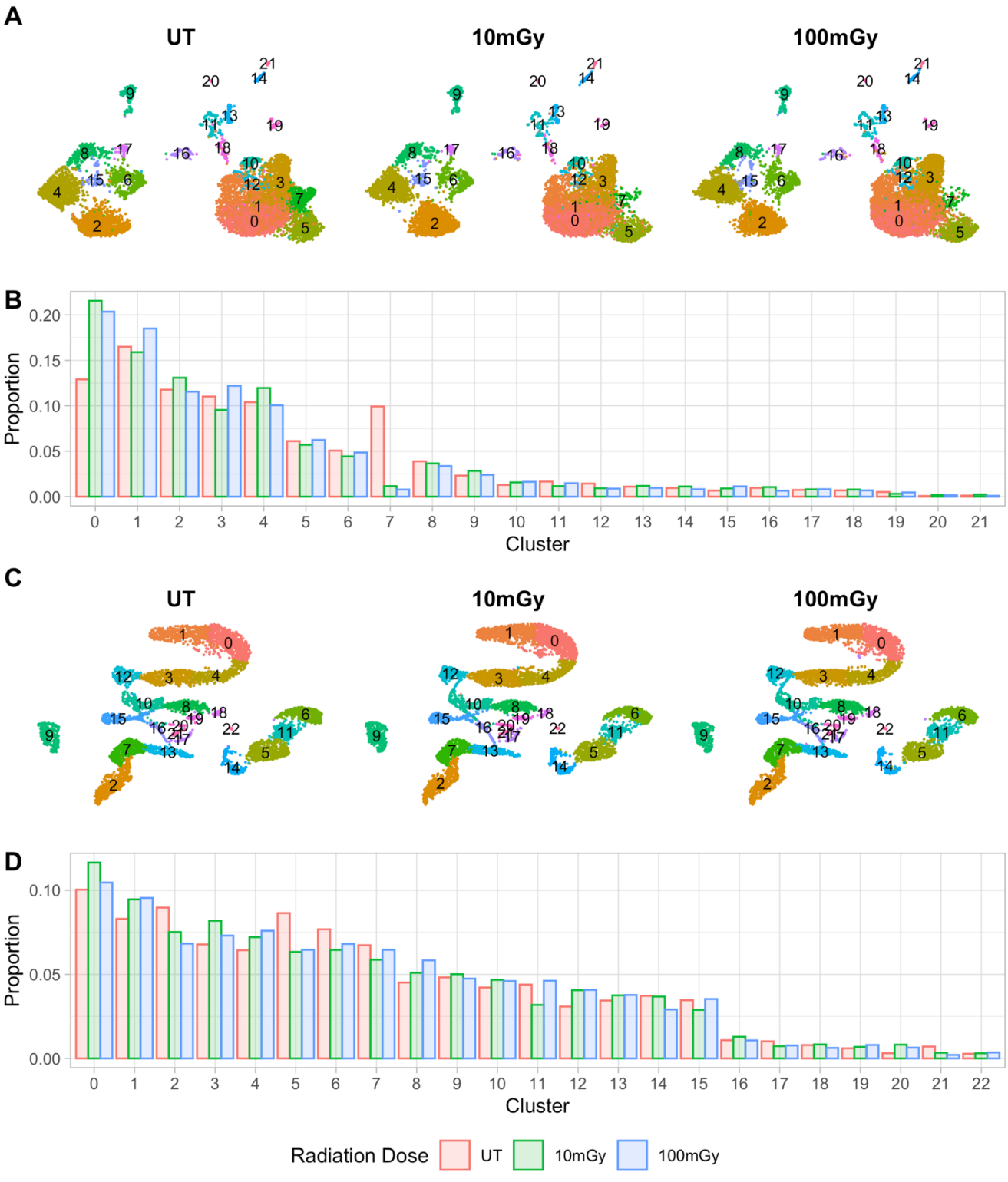

Figure 13. Changes In Cell Compartmentalization Following LDR Exposure. A&B correspond to the spleen dataset, while C&D correspond to the bone marrow. (A, C) UMAP projections of spleen and bone marrow cells, colored by cluster and split by radiation condition (100 mGy, 10 mGy, and untreated control). These UMAPs show minimal variance in cellular compartmentalization across radiation conditions. (B, D) Proportions of cells in each cluster were calculated by dividing the number of cells within each cluster by the total number of cells in the sample. Cluster proportions similarly exhibit minimal differences across radiation conditions.

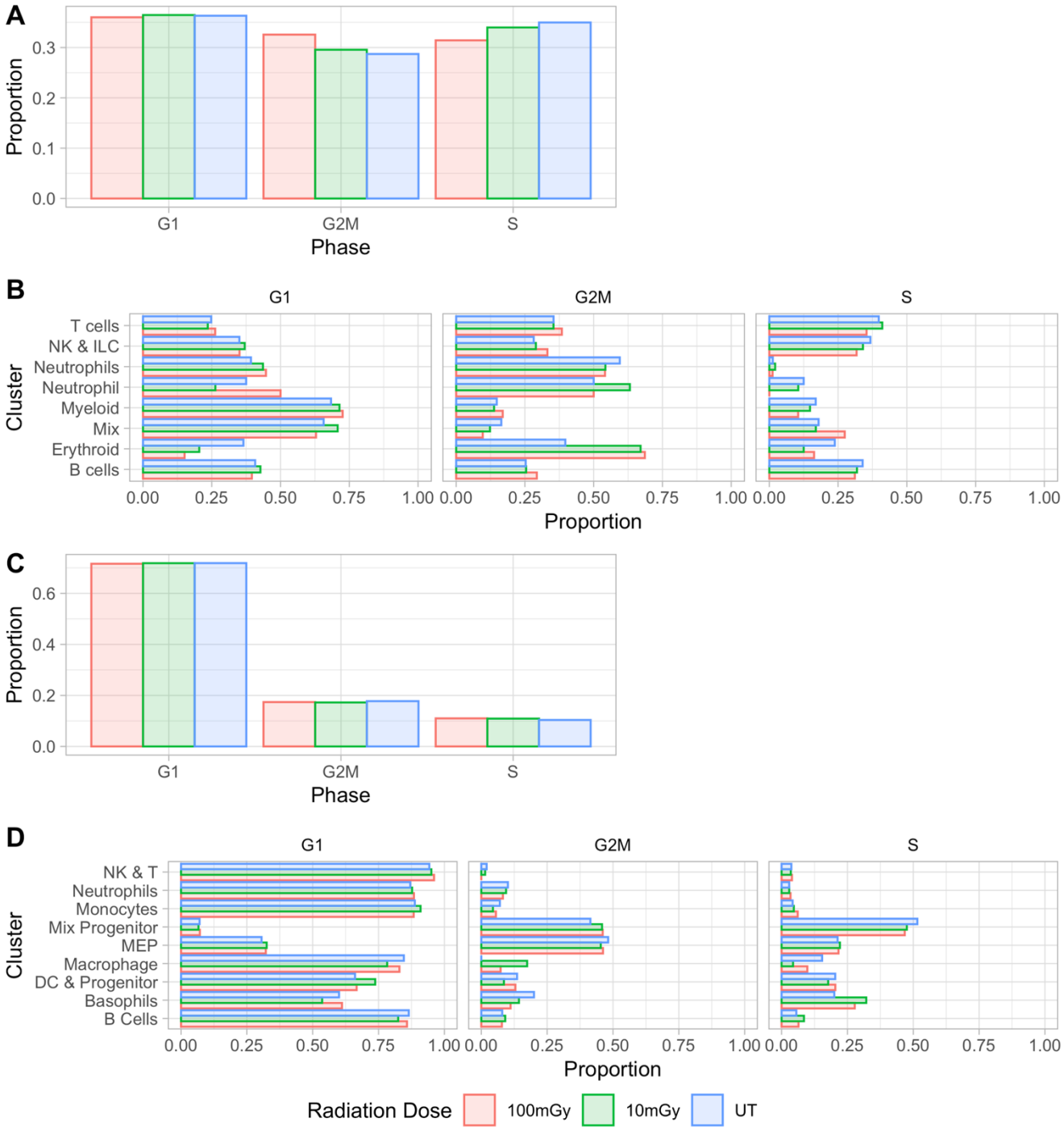

Figure 14: Cell cycle stage distribution across radiation conditions. The top row (A,B) shows the spleen dataset, while the bottom row (C,D) presents the bone marrow dataset. (A, C) Bar plots showing the proportion of cells in each cell cycle phase (G1, G2M, and S) across the three conditions: 100 mGy (red), 10 mGy (green), and untreated control (blue). These proportions indicate minimal variance in cell cycle distribution across conditions. (B, D) Cell-type specific distribution of cells in each cell cycle phase (G1, G2M, and S) across radiation conditions, for spleen (B) and bone marrow (D). These plots highlight little effect of radiation dose of cells.

to radiation exposure. The outlier sample with elevated heat shock protein expression may be attributed to variation in sample handling, such as differences in processing time or temperature. In the bone marrow, no clusters demonstrated a change in proportion greater than a few percent (**Figure 13C&D)**. Therefore, the sustained radiation exposure had no discernable effect on the composition of the spleen and bone marrow at single-cell resolution.

Cells at different stages of the cell cycle can exhibit varying sensitivity to radiation-induced apoptosis. To explore this, we performed cell cycle scoring based on the expression of stage-specific marker genes, allowing us to assign each cell to a particular cell cycle stage. Across both spleen and bone marrow samples, we observed no major differences in the overall proportion of cells in each cell cycle stage between untreated and radiation-exposed groups **(Figure 14 A & C).** When examined at the level of cell types, the distribution of cells across cell cycle stages also showed minimal variation, indicating that radiation treatment did not significantly alter cell cycle dynamics within either organ **(Figure 14 B & D)**. Thus, the composition of both the spleen and bone marrow, in terms of cell cycle distribution, remained largely unaffected by radiation exposure.

3.4.3 Differential Expression Analysis

Spleen

Although radiation did not induce observable changes in cell composition, we hypothesized that cell phenotypes might still be impacted in a dose-dependent or cell-type-specific manner. To test this, we conducted differential gene expression analysis comparing untreated samples to those exposed to 10 mGy and 100 mGy doses of radiation across various clusters. In the spleen, we identified 410 and 447 significant DEGs (adjusted p-value < 0.05) when comparing UT to 100 mGy and 10 mGy conditions, respectively. However, the magnitude of gene expression changes was relatively modest, with only 104 and 96 genes passing an absolute log2 fold change cutoff of ±0.5 in mRNA abundance **(Figure 15A & B)**. Of these, 39 DEGs were common to both radiation doses, suggesting some overlap in the transcriptional response to different radiation exposures. Importantly, no single cluster exhibited a disproportionately higher number of DEGs, indicating an overall lack of heightened sensitivity to

radiation across specific cell populations. Furthermore, some clusters had no differentially expressed genes.

An examination of the most significantly differentially expressed genes revealed frequent downregulation of ribosomal protein genes (Rps and Rpl) across multiple clusters under both 10 mGy and 100 mGy conditions **(Figure 15 C & D)**. These genes encode ribosomal proteins that constitute the large and small subunits of the ribosome, which are essential for protein synthesis. The consistent downmodulation of these genes suggests a potential reduction in ribosomal function and, by extension, protein synthesis, as a key component of the cellular response to radiation exposure. Additionally, the Ubb gene, encoding ubiquitin B, a small protein critical for tagging damaged proteins for degradation, was downregulated across nearly all clusters. This may indicate a broader reduction in protein turnover in response to radiation. HexB, a gene encoding the beta subunit of hexosaminidase, was also upregulated across several clusters.

One of the primary objectives of the scRNA-seq analysis was to evaluate the extent of heterogeneity or homogeneity in the transcriptional response to radiation exposure across different cell populations. In **Figure S9**, we visualized the top significant DEGs and mapped their expression across various clusters. These plots reveal that some genes exhibit a nearly uniform response to radiation across multiple clusters, such as the ribosomal genes discussed earlier. This suggests that certain cellular processes, such as protein synthesis, may be broadly affected by radiation in a manner that transcends specific cell types, indicating a common stress response. However, the figure also highlights substantial heterogeneity in the radiation response, with certain clusters displaying unique transcriptional modulation. For instance, cluster 16 shows distinct expression changes in a small group of genes that are not broadly modulated in other clusters. This suggests that certain cell types may exhibit specialized responses to radiation that are not shared across the broader population. Interestingly, we observe that some genes, including Cxcr4, Nr4a3, Txnip, and Gapdh, are upregulated in a select group of clusters predominantly composed of lymphocytes. While this selective modulation could reflect genuine cell type-specific responses to radiation, it is important to consider an alternative explanation: the greater number of cells in these clusters may afford higher statistical power to detect DEGs. This suggests the possibility

that these genes are more uniformly modulated across clusters than the data indicates, but insufficient cell numbers in some clusters may limit our ability to detect these changes.

For each cell cluster, differential gene expression was analyzed, and genes were ranked by log fold change. These ranked gene lists were input into GSEA using the Hallmark and GO reference databases. GSEA results were filtered for significance (adjusted p-value < 0.05) and ranked by normalized enrichment scores (NES) for visualization of biological processes potentially affected by radiation **(Figure 15E)**. Below, I discuss significant gene sets by analyzing the driving genes that were both significantly and adequately differentially expressed (above an absolute log2 fold change cut-off of 0.3).

Several clusters demonstrated a significant downregulation of pathways associated with ribosomal biogenesis and protein translation (**Figure 15E)**. A closer inspection of the driving genes revealed that this effect was primarily due to the downregulation of various ribosomal protein genes, consistently observed across clusters. These included genes encoding for both large and small ribosomal subunits, potentially implicating a broad suppression of ribosomal assembly following radiation exposure **(Table S1)**. This downregulation could indicate an overall reduction in protein synthesis capacity, potentially reflecting a stress-induced translational arrest in response to radiation-induced damage.

Multiple clusters were enriched for the TNF-α signalling via NF-κB gene set **(Figure 15E)**. Genes contributing to this term included Nfkb1, Nr4a3, Egr1, Kdm6b, Zfp36, Egr3, and Irs2 **(Table S1)**. Interestingly, while key mediators of TNF-α signalling were not differentially expressed, many of these genes are downstream targets of NF-κB activation, suggesting that the enrichment reflects the broader transcriptional response to NF-κB activation rather than the core components of TNF-α signalling itself.

Several clusters showed significant downregulation of oxidative phosphorylation gene sets **(Figure 15E)**. Upon examining the genes implicated in these terms, many clusters exhibited reduced expression of subunits of the ATP synthase enzyme complex, including Atp5k, Atp5j2, and Atp5e **(Table S1)**. In addition, subunits of NADH oxidoreductase (Ndufa3, Ndufa1) and cytochrome c oxidase (Cox5b, Cox6c, Cox7b, Cox7c) were also downregulated. These findings suggest a potential impairment in mitochondrial energy production, which may reflect metabolic stress or mitochondrial dysfunction induced by radiation exposure.

Interestingly, some clusters exhibited significant upregulation of gene sets related to the UV response **(Figure 15E)**. This could implicate the activation of pathways involved in the cellular response to DNA damage or oxidative stress. Key genes driving this enrichment included Nfkb1, Akt3, Smad7, and Prkce **(Table S1)**. Notably canonical DDR genes, such as Trp53, did not show significant differential expression. The absence of strong DDR or oxidative stress gene activation may suggest that the UV response enrichment reflects broader stress-response signalling rather than direct activation of classical radiation pathways.

Finally, differentially expressed genes from the bulk-RNA sequencing were compared to those of scRNA-seq to look for common signatures across experimental modalities. The comparison of bulk-RNA sequencing and scRNA-seq revealed that Egr1, Txnip, and Pde3b were differentially expressed across both modalities, with specific patterns in different clusters. Txnip was downregulated across multiple clusters, including clusters 1, 2, 3, 4, 5, and 6, indicating broad suppression in response to radiation exposure. Egr1 was upregulated in clusters 0, 1, and 5, potentially mediating radiation response in these populations. Finally, Pde3b was upregulated in cluster 3. Despite the conservation of a few genes like Egr1, Txnip, and Pde3b, most genes identified as differentially expressed in bulk RNA-seq were not significantly differentially expressed at the single-cell level in scRNA-seq. This is an important finding, as genes widely differentially expressed across multiple clusters in scRNA-seq, such as HexB, Ubb, and ribosomal proteins, were not conserved across the two modalities. This lack of overlap raises the possibility that some genes identified in either bulk RNA-seq or scRNA-seq may represent noise and technical variation, rather than true, conserved signals.

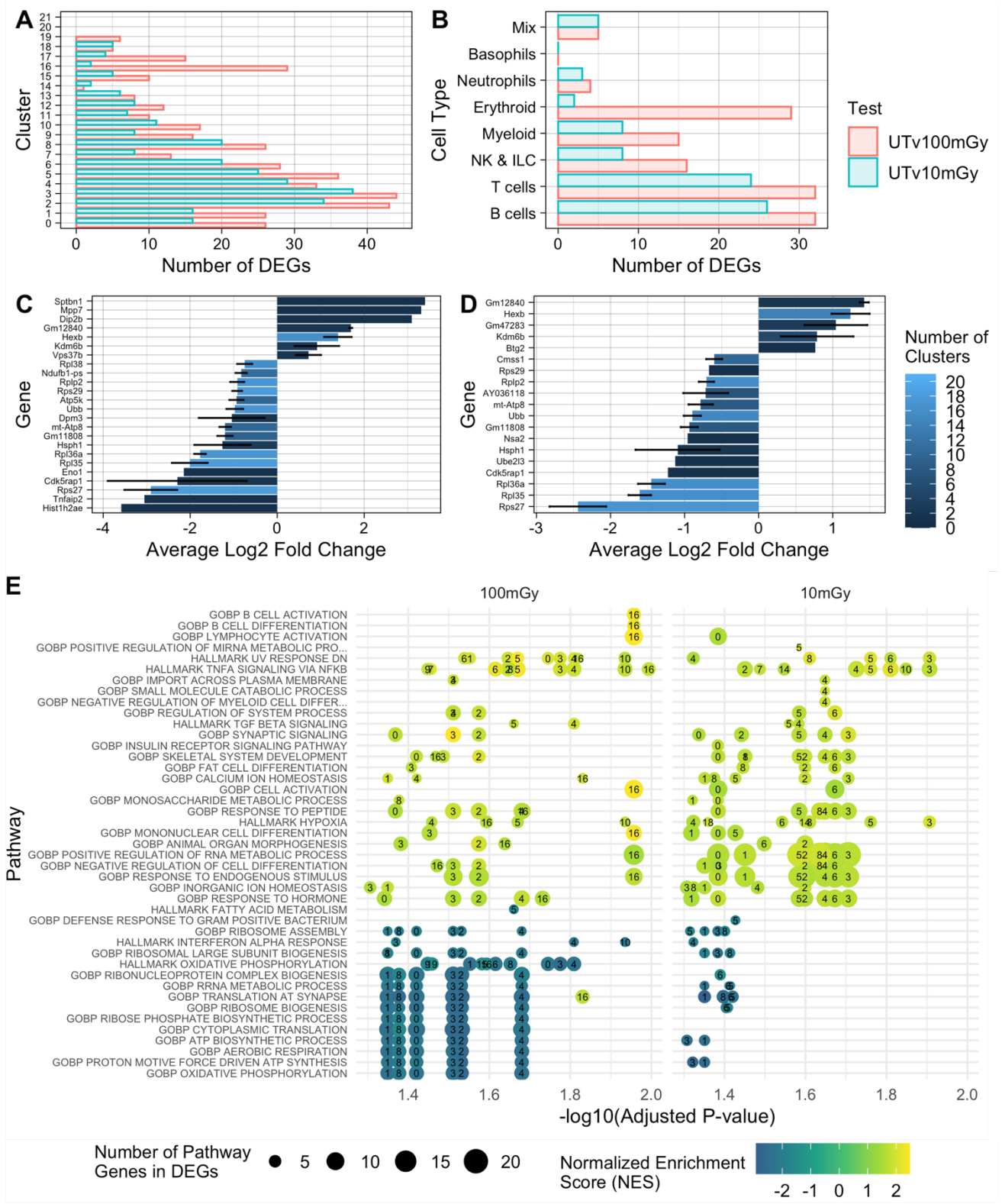

Figure 15. Differential Expression Analysis of Spleen. (A) Number of DEGs (abs log2 fold change > 0.5) for each cell cluster. (B) Number of significant DEGs (abs log2 fold change > 0.5) grouped by cell type, comparing 100 mGy and 10 mGy vs UT. (C, D) Plot top DEGs (selected top 3 per cluster) in 100 mGy and 10 mGy vs UT, with color indicating the number of clusters in which genes are differentially expressed. (E) (E) GSEA of DEGs ranked by log2 fold change, with bubble size representing the number of genes in each pathway found in the DEG list and color indicating normalized enrichment score (NES).

Bone Marrow

In the bone marrow, the number of DEGs was lower compared to the spleen dataset **(Figure 16A & B)**. Interestingly, more DEGs identified when comparing UT cells to those exposed to 10 mGy than to 100 mGy. Specifically, 279 DEGs were detected when comparing UT to 10 mGy, while only 137 DEGs were found when comparing UT to 100 mGy. As observed in the spleen, the magnitude of gene expression changes was modest, with most genes not surpassing a log2 fold change cutoff of ±0.5. Only 104 and 31 genes passed this threshold when comparing UT to 10 mGy and 100 mGy, respectively, underscoring the relatively subtle transcriptional changes induced by radiation exposure.

Most DEGs exhibited heterogeneous expression patterns, with changes confined to a single cluster **(Figure S10)**. However, a small subset of genes showed more uniform modulation across multiple clusters. This subset included several of the same genes observed in the spleen, such as ribosomal protein genes (Rps and Rpl) and HexB. Additionally, other notable genes consistently modulated across clusters included Cmss1, Lars2, Cdk8, Gapdh, and Hbb-bs. The imbalance in the number of DEGs between the 10 mGy and 100 mGy conditions resulted in few common DEGs between these comparisons.

GSEA in the bone marrow revealed a limited number of significant pathways, further reflecting the modest nature of the transcriptional response to radiation in this tissue **(Figure 16E)**. Pathways involved included RNA and protein biosynthesis, metabolic processes, MYC target pathways, ribosomal and translational processes, and cytoplasmic translation. Similar to the spleen, these pathways suggest that radiation exposure may influence protein synthesis. Furthermore, the scarcity of enriched pathways contrasts with the more pronounced alterations observed in the spleen, suggesting tissue-specific differences in the response to low-dose radiation.

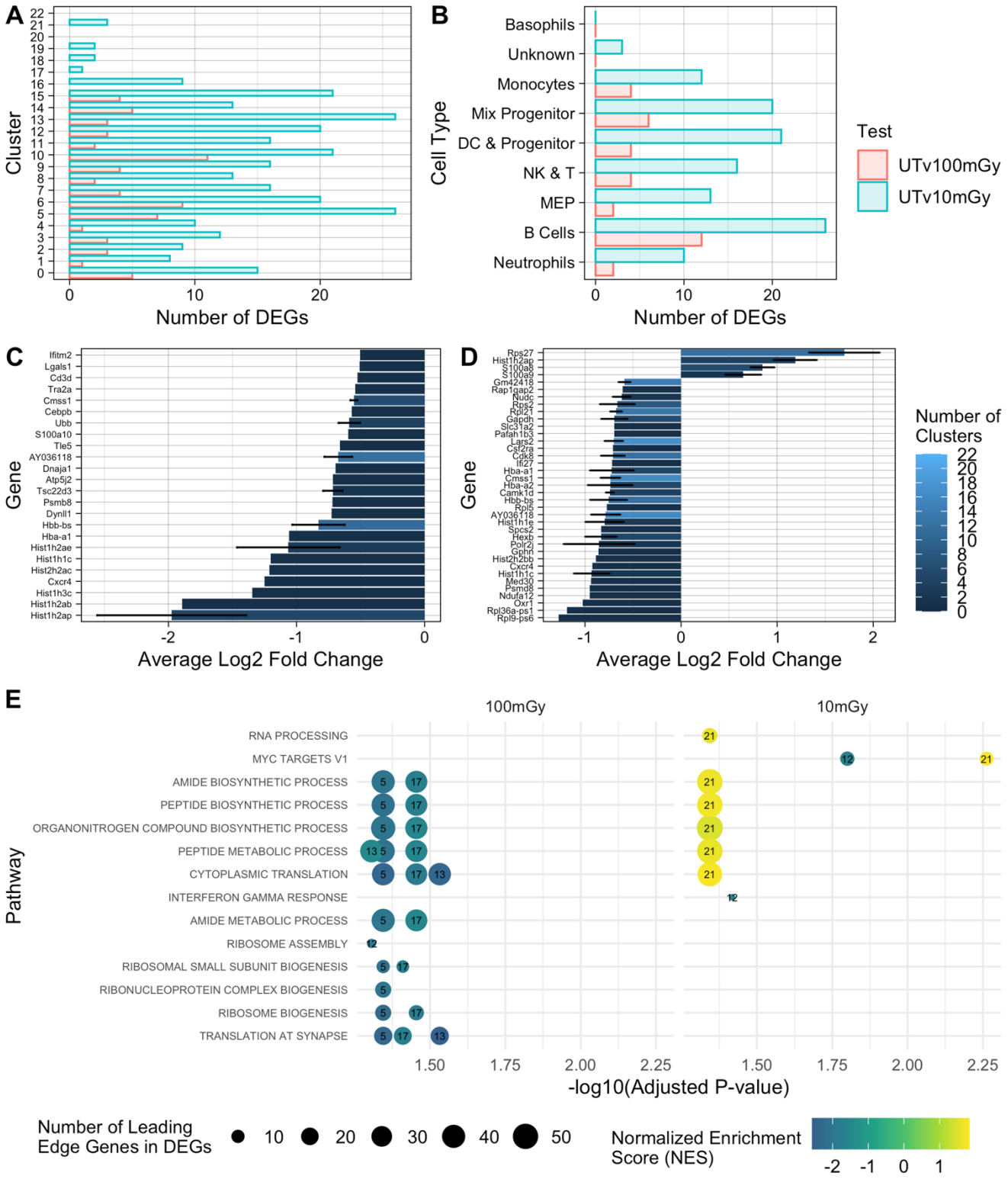

Figure 16. Differential Expression Analysis of Bone Marrow. (A) Bar plot showing the number of DEGs (abs log2 fold change > 0.5) for each cell cluster. **(B)** Number of significant DEGs (abs log2 fold change > 0.5) grouped by cell type, comparing 100 mGy and 10 mGy vs UT. (C, D) Plot top DEGs (selected top 3 per cluster) in 100 mGy and 10 mGy vs UT, with color indicating the number of clusters in which genes are differentially expressed. (E) (E) GSEA of DEGs ranked by log2 fold change, with bubble size representing the number of genes in each pathway found in the DEG list and color indicating normalized enrichment score (NES).

5 Discussion

LDIR exposures are common among the world's population in various occupational, medical and natural environments. However, there is still an incomplete understanding of what cellular responses and immune system reactions may be triggered by these exposures. Observations across epidemiological and experimental studies demonstrate that low-dose radiation can be immunomodulatory, affecting the proportion and phenotype of immune cells across various organs. Changes to the immune system from radiation exposure have also been shown to be both transient and persistent, even lasting many years. In some studies, no effects of LDIR exposure on the immune system can be measured. The precise effects and underlying mechanisms of radiation immune responses remain a critical question. While the dramatic response to high-dose radiation exposure seen in ARS is well understood to be the result of massive levels of cell death, the molecular mechanisms driving cellular responses in the low-dose range are likely to be driven by mechanisms outside of dramatic cell death that have yet to be adequately described.

Here we aimed to perform a controlled study elucidating the effects of LDIR exposure on the immune system, searching for changes to various immune cell populations in response to sustained TBI. Using several experimental methodologies across various organs, we aimed to comprehensively describe immune cell responses to low-dose radiation exposure. Our results indicate that cells of the mature female C57BL/6 mice immune system are largely unchanged following chronic low dose gamma radiation exposure. Overall, immune homeostasis appears to be maintained following exposure in our model.

5.1 Minimal Hematological Perturbations Following Low-dose Radiation

Our hematology analysis revealed a limited impact of protracted LDIR exposure on blood composition **(Figure 2)**. Most metrics analyzed were unaffected by LDIR, including WBC and lymphocyte counts, which represent the most radiation-sensitive peripheral cell populations. However, we observed a statistically significant doubling in the proportion of circulating neutrophils in the 10 mGy

condition compared to the untreated control. This increase could suggest a potential LDIR-induced activation of neutrophils. However, we found no increase in neutrophil output from the bone marrow, with scRNA-seq clusters representing neutrophil differentiation unchanged by LDIR exposure. Furthermore, no changes to granulocytes were identified in the spleen or bone marrow when flow cytometry results were evaluated. Therefore, the increase in neutrophil proportion was isolated only to the hematological analysis. Given the short lifespan of neutrophils, one would expect that for an increase in circulating neutrophils, there should be a concurrent increase in bone marrow neutrophil output. In other studies employing infection models of C57BL/6 mice, blood neutrophil proportion can increase by multiple to several fold as the bone marrow engages in emergency granulopoiesis.[155,156] Thus, the increased neutrophils measured in this study represent a subtle upregulation compared to an immune response to infection. The absence of significant changes in other hematological parameters, the lack of change in neutrophil proportion in other organs, and the small magnitude of change suggest that this neutrophil response is at most limited or perhaps even artifactual.

We also measured a slight but statistically significant decrease in MCH from 11.9±0.1pg to 11.6±0.2pg when comparing UT and 100 mGy samples (adjusted p-value 0.026) **(Figure S1)**. MCH is calculated by dividing the amount of hemoglobin in a given blood volume by the number of RBCs. Various sources show that the mean MCH of C57BL6 mice is around 14-15pg. According to Charles River, female C57BL/6 mice aged 8-10 weeks old have a mean MCH of 15pg (95% CI 13-16.8). Jackson Labs claim that at the age of 26 weeks, the mean MCH is 14±0.8pg. The mean MCH, MCV and hemoglobin of all the mice from this study sit considerably lower than those averages. The variation could be due to several factors, such as hydration status, nutritional status, and time of day. The decrease of around 0.3pg (decrease of 2.52%) observed in response to radiation is statistically significant but of insufficient magnitude to be biologically relevant. Since the range of MCH measured in healthy conditions can vary, this minor decrease measured falls within a range of natural variation. Furthermore, we would not expect such a small change to impact broad hemoglobin or red blood cell status. Indeed, the change in MCH was measured alongside an absence of change in HGB, MCV or RBC count, further demonstrating its irrelevance. In comparison, in a study feeding male mice low or

high-iron diets, MCH decreased or increased by around 2pg (change of around 11%), a much greater change magnitude.[157]

Other experimental studies have analyzed changes in blood metrics following low-dose radiation exposure, most of which also highlight minimal perturbations. One study involved C57BL/6 mice chronically exposed to either 200 mGy or 2 Gy at low dose rates of 0.7 mGy/hr or 3.95 mGy/hr, respectively. These mice showed no changes in white and red blood cell counts.[125] Similarly, Balb/c mice exposed to a single acute exposure at doses between 10 and 500mGy also presented no changes in peripheral blood metrics.[123] In another study, fractionated exposures resulting in a cumulative absorbed dose of 100 mGy could reduce monocytes, neutrophils and erythrocytes.[124] This highlights that while single acute or chronic exposures may not significantly impact blood parameters, fractionated exposures, even at low doses, can lead to detectable changes in certain blood metrics. In summary, our findings align with other mouse studies, indicating that low-dose radiation exhibits minimal impact on blood parameters. This consistency across studies provides strong evidence that low-dose radiation exposure does not significantly alter peripheral blood composition.

5.2 Limited Immune Cell Perturbations in Radiosensitive Organs Following Sustained Low-dose Radiation Exposure

Radiosensitive organs, including the spleen, thymus, and bone marrow, are critical sites for investigating the impact of radiation on immune cell populations due to their high concentrations of diverse immune cells and essential role in immune function. High-dose radiation exposure leads to profound immunological disturbances in these organs. However, the effects of LDIR remain poorly understood, underscoring a crucial gap that demands comprehensive exploration.

In our study, flow cytometric analysis was conducted to analyze immune cell populations across various organs from mice exposed to LDIR. The spleen showed no significant changes in immune cell subsets due to radiation exposure **(Figure 3)**. In the thymus, T cell populations and developmental stages were unaffected by radiation **(Figure 4).** Furthermore, the bone marrow revealed no significant shifts in the proportion of most immune cell populations **(Figure 5)**. Overall, chronic radiation exposure

did not significantly alter the proportions of various immune cell subsets in these organs as measured via flow cytometry, suggesting no major immunological disturbances. These assays demonstrate that despite the known sensitivity of these tissues to radiation, even cumulative doses up to 100 mGy can not significantly alter the immune cell composition in these organs.

In low-dose TBI animal studies, the spleen, bone marrow and thymus have been previously examined. In Shin et al., female C57BL/6 mice exposed to chronic TBI resulting in 0.2 or 2 Gy exposure over 12 and 21 days, respectively, showed no changes in the proportion of splenic T, NK or B cells.[125] However, Bogandi et al. showed that acute TBI of female C57BL/6 mice to 10 and 100 mGy caused an overall reduction in splenocytes 3 and 7 days post exposure.[126] Furthermore, they showed reductions in the proportion of various T cell populations, NK cells and B cells. Liu et al. showed that a single exposure of 10 mGy could decrease the proportion of monocytes and DCs but not NK cells amongst splenocytes 24 hours post exposure.[123] Additionally, they found no changes in proportion of different thymocyte populations following TBI ranging 10 mGy to 500 mGy.

Therefore, while high-dose radiation exposure results in well-characterized deleterious effects on these radiosensitive organs, low-dose exposure presents a nuanced landscape of variable immunological responses depending on exposure conditions. Our study contributes to broader knowledge by highlighting the potentially limited effects of sustained low-dose rate LDIR exposure, underscoring the necessity for further research into the specific conditions and cellular dynamics that govern these outcomes.

5.3 Uncovering Minimal Transcriptomic Responses to Low-dose Radiation Exposure through Bulk & Single-Cell RNA Sequencing

Given the absence of significant findings from our flow cytometry analyses, we turned to transcriptomics for a more detailed examination of immune cell responses to LDIR exposure. While flow cytometry is a powerful tool for quantifying broad cell populations, it lacks the resolution required to detect subtle phenotypic differences. In contrast, transcriptomics provides a comprehensive, unbiased view of gene expression changes across the entire transcriptome, allowing for the discovery of novel

responses that flow cytometry cannot detect. scRNA-seq in particular, is ideal for identifying subsets of radiation-sensitive immune cells that might be masked within the bulk population. This high-resolution technique allows us to explore the transcriptomes of individual cells, enabling the detection of even rare cell populations and subtle transcriptional alterations caused by LDIR exposure. By integrating both bulk and single-cell transcriptomics into our study, we aimed to uncover more detailed and potentially significant insights into the molecular mechanisms governing immune responses in LDIR-exposed mice.

Our bulk transcriptomic analysis revealed minimal changes in gene expression following low-dose radiation exposure. Importantly, PCA demonstrated that most the variance in gene expression across splenocyte samples was independent of radiation treatment **(Figure 6).** We identified 116 significant differentially expressed genes (adjusted p-value < 0.05) when comparing UT and irradiated samples, but only 50 exhibited an absolute log2 fold change greater than 0.5. Therefore, the magnitude of change in gene expression was generally low **(Figure 7)**. Furthermore, Gene Ontology Enrichment found no significant biological processes linked to the differentially expressed genes. While five pathways showed enrichment in the GSEA analysis comparing 100 mGy to untreated samples, the small log2 fold changes in the involved genes indicate limited biological significance. Additionally, no pathways were enriched using GSEA to compare the10 mGy against untreated samples.

Similar to flow cytometry, our scRNA-seq analysis revealed minimal effects of chronic low-dose radiation exposure on the proportion of cell clusters in both spleen and bone marrow, suggesting that there were no major expansions or contractions in specific immune cell populations **(Figure 13)**. Furthermore, separating cell populations by cell cycle stage showed no effect **(Figure 14)**. Therefore, at single-cell resolution with unsupervised clustering, radiation did not impact composition of either organ. Differential expression analysis across both organs indicated that low-dose radiation led to minor transcriptional changes, with most DEGs exhibiting small fold changes. A large proportion of the DEGs did not surpass a log2 fold change threshold of ±0.5, further reinforcing the subtlety of the transcriptional response.

One of the most notable findings was the consistent downregulation of ribosomal protein genes (Rps and Rpl) in both the spleen and bone marrow. This downregulation suggests a common cellular

response to radiation exposure, possibly involving suppression of ribosomal biogenesis and protein synthesis. Such a response may represent a protective mechanism by which cells reduce their translational activity to conserve energy and mitigate the risk of producing misfolded or damaged proteins under stressful conditions, such as radiation exposure. This downregulation of ribosomal proteins occurred alongside the downregulation of Ubb, a crucial component of the ubiquitin-proteasome system, which is responsible for marking damaged proteins for degradation. The reduced expression of Ubb may indicate a decreased capacity to target damaged proteins for degradation, potentially reflecting a broader cellular stress response. Together, these findings hint that low-dose radiation exposure could impair both protein synthesis and degradation pathways, indicating a potential vulnerability in the cell's ability to maintain proteostasis under chronic LDIR conditions.

We also observed significant downregulation of key subunits involved in oxidative phosphorylation in the spleen, suggesting potential disruptions in mitochondrial energy production. Key proteins included subunits of the ATP synthase enzyme complex, subunits of NADH oxidoreductase and cytochrome c oxidase. This indicates that LDIR exposure may alter the cellular metabolic state in the spleen, potentially shifting to alternative metabolic pathways as a compensatory response to radiation-induced stress.

Despite the statistical significance of these findings, several factors suggest that the observed gene expression changes may not represent biologically meaningful effects. First, the magnitude of changes across DEGs were modest, with a large proportion exhibiting log2 fold changes below commonly accepted thresholds for biological relevance. Second, the lack of uniform modulation of gene expression within known pathways raises doubts about the impact of these changes. GSEA pathways predicted to be affected showed only a handful of involved genes, most with miniscule log2 fold changes, indicating a limited influence on those biological processes.

One compelling argument against the robustness of these results is the lack of conservation between bulk RNA-seq and scRNA-seq. Even genes that were uniformly modulated across multiple large clusters in scRNA-seq showed no corresponding differential expression in bulk RNA-seq, despite expectations that such genes would be consistently differentially expressed at the population-level.

Therefore, the changes we observed may represent technical noise or stochastic fluctuations in gene expression rather than true biological signals. Alternatively, it is possible that discrepancies between the two technologies could account for genes being differentially expressed in one dataset but not the other. Bulk RNA-seq and scRNA-seq differ fundamentally in their library preparation methods, sequencing depth, and sensitivity to lowly expressed genes.

On the other hand, the modest changes in gene expression are consistent with what one would expect given the weak nature of the low-dose radiation stimulus. Subtle transcriptional shifts may be a natural response to mild stress. Therefore, these small changes might still hold biological relevance. It is also possible that we are observing only a subset of the differentially expressed genes that exceed the sensitivity threshold of our assays, while other related genes might be modulated more subtly, remaining below detection limits. The identified changes, modest as they may be, could represent biomarkers or candidate signatures of chronic low-dose radiation exposure and should be explored in future studies to assess their potential role in monitoring or predicting radiation-induced effects.

To date, there have been limited transcriptomic studies utilizing in-vivo low-dose radiation models in the literature. Using RT-PCR, Puukila et al. analyzed splenic expression changes in important genes central to radiation response.[118] Their model involved exposure of rats to whole body radiation as low as 2 and 20mGy. In that low-dose range, the expression of genes involved in apoptosis, cell cycle regulation and DNA repair were unchanged compared to control. An exception was the significant decrease in Pcna and p27 following LDIR exposure.

Though less comparable, multiple studies have performed transcriptomics of ex-vivo irradiated cells. Luo et al. investigated a dataset containing irradiated human PBMCs and human cell lines.[158] Their analysis established a threshold of 0.1 Gy to distinguish between low-dose and high-dose radiation effects and identified pathways such as ubiquitin-mediated proteolysis, natural killer cell-mediated cytotoxicity, and Rap1 signalling as highly responsive to low-dose radiation. Cho et al. performed ex-vivo LDIR exposure of anti CD3/CD28 stimulated CD4+ T cells, analyzing their responses using RNA-seq.[159] Overall, they showed that 50mGy exposure of these cells upregulated genes related to mRNA translation, mitochondrial function, and cytokines IFN-γ, IL-4 and IL-5, while downregulating TGF-β1.

Fang et al. performed RNA-seq on PBMCs irradiated ex-vivo at 50 and 150 mGy.[160] They showed subtle upregulation of genes related to antigen processing.

Recently, scRNA-seq has been performed on bone marrow cells following murine TBI at 6 Gy.[91] The results indicated that the most radiosensitive populations were GPS, HPSCs and B cells, which all decreased in proportion following IR exposure. Genes related to apoptosis, inflammatory response, and ROS regulation were enriched in radiosensitive cells. Furthermore, in B cells specifically, mitochondrial genes were upregulated, potentially indicating higher levels of oxidative phosphorylation post-irradiation. Downregulated genes were involved in pro-survival pathways like NF-κB and AMPK. Despite the sensitivity of bone marrow populations following HDIR, no such transcriptional changes could be observed following 100 mGy cumulative exposure in our study.

In general, our minimal transcriptomic findings suggest that low-dose radiation may not elicit strong transcriptional responses across immune cell populations in either the spleen or bone marrow, consistent with the absence of phenotypic shifts. However, these subtle transcriptional changes, while not reflective of a strong radiation response, may still provide important clues about the molecular events that occur following LDIR exposure.

5.4 Insights from Multi-Modal Analysis

In our study, immune cells remained largely unperturbed across multiple organs and experimental modalities. At most, our findings point to extremely subtle gene expression changes in response to LDIR. A more parsimonious conclusion, however, is that the immune system was largely unaffected by the treatment. This aligns with the notion that the immune system is resilient to LDIR exposure, particularly when administered at low-dose-rates.

Previous studies discussed above have documented that exposure to 100 mGy and below can elicit biological changes. However, in our model, the cumulative doses of 10 and 100 mGy were delivered at a low-dose-rate. This means that the effects of radiation on cells were temporally spread out, potentially resulting in a limited response to radiation insult at the time of euthanasia and analysis. Furthermore, any cumulative radiation effects on the cellular environment might have remained below the threshold required to activate significant immune cell transcriptional variation across these organs. Supporting this

interpretation, Bogdandi et al. observed a reduction in total splenocyte count in C57BL/6 mice exposed to the same absorbed dose of 100 mGy of ^{60}Co radiation at a high dose rate, a finding that contrasts with our study.[126] Therefore, its compelling to argue that in contrast to low-dose exposures delivered at high dose rates, low-dose rate exposures do not manifest into any dramatic change to the immune system. Consistently, Shin et al. reported that C57BL/6 mice exposed to 200mGy at 0.7 mGy/hr for around 19 days or a substantial cumulative dose of 2 Gy radiation at a dose rate of 3.95 mGy/hr over 21 days exhibited no significant perturbations in weight, complete blood counts or immune populations in the spleen.[125] However, the same dose of 2 Gy given at a high dose rate by Bogdandi et al. caused dramatic fluctuations in splenic immune cell proportions.[126] Yanai et al. showed that C3H/HeN mice which received 20mGy a day (0.83 mGy/hr) had a radiation induced drop in peripheral white blood cells and bone marrow stem cells starting when reaching a cumulative 2.8 Gy exposure.[129] Importantly, reaching cumulative doses between 3-8 Gy caused much more dramatic impacts on blood counts and bone marrow stem cell populations. Together, evidence suggests that low-dose rate radiation is less perturbing to the immune system compared to the same dose given at a high-dose rate. Low-dose rate radiation given to a low cumulative dose is likely very minimally affective, while low-dose rate radiation given to higher cumulative doses may be sufficient to trigger systemic immune system responses, with variation depending on the radiation dose, quality and rate as well as the mouse strain, age, and sex.

It is interesting to note that the cumulative doses and dose rates used in our study are higher than those typically encountered by radiation workers. For instance the CNSC claims NEWs receive 1-2 mSv of ionizing radiation exposure per year in excess of background.[42] Furthermore, the million person study reported a mean cumulative NEW career dose of 52.6 mSv, and a maximum dose of 1.32 Sv with only around 15% of workers having career exposures in excess of 100 mSv.[44] Despite this, our results demonstrate that even at the upper threshold of what is considered a low dose (100 mGy) and low-dose rate, we found little to no evidence of immune perturbation. This conclusion is further reinforced by our use of highly sensitive and high-resolution techniques, analyzing multiple organs and cell populations. The similarities between irradiated and unirradiated controls support a dose threshold model, where immune system perturbations only manifest beyond a certain exposure condition. While our study did

not establish a dose-response curve to precisely define this threshold, the absence of discernible changes in immune homeostasis indicates that the exposure conditions in our study fall below it. This is not to suggest that biomolecular damage, such as DNA damage, follows a threshold model, as it is often characterized by a more linear dose-response relationship. Rather, our findings indicate that there may be a threshold level of biomolecular insult required to elicit more systemic changes, which can be more readily distinguished from control conditions. This distinction highlights the complexity of translating molecular damage into broader physiological effects.

In this study, female C57BL/6 mice, aged 18 weeks, were selected as the model organism. This strain was chosen due to its extensively characterized transcriptome and widespread use, enabling robust bioinformatic analyses and reliable comparisons with existing literature. The decision to use a single sex was based on the recognition that, at the feasible sample size, analyzing sex-based differences would lack sufficient power. Consequently, using one sex ensured consistency in the experimental outcomes. Additionally, 18-week-old mice were selected to focus on a mature immune system rather than one in developmental stages. The discrepancies between our findings and those of other studies may result from diverse experimental models used. Factors such as model organisms, strains, age, and varying radiation quality and quantity can significantly impact biological outcomes. Epidemiological and experimental evidence clearly show these variables are crucial in determining the radiation response, potentially explaining the variations observed in other research compared to ours.

A central hypothesis of this study was that by employing highly sensitive and high-resolution methodologies, we would detect dose-specific and cell-type-specific LDIR responses. However, our results did not provide strong evidence to support these expectations. In terms of dose-response, the bulk RNA-sequencing data revealed more significant DEGs at 100 mGy compared to 10 mGy, suggesting a potential dose relationship. Similarly, at the scRNA-seq level, the spleen exhibited slightly more DEGs at 100 mGy than at 10 mGy. However, in contrast, the bone marrow showed the opposite pattern, with fewer DEGs at 100 mGy than at 10 mGy. Regarding cell type-specific effects, flow cytometry and scRNA-seq did not reveal notable changes in cell proportions across various cell types and organs, implying that LDIR did not induce sufficient cellular stress to trigger cell death, proliferation,

or migration. At the transcriptional level, the responses of all cell types were largely unchanged following LDIR exposure. Although a few DEGs were specific to certain clusters, most were modulated across all clusters, and the genes identified did not appear to correspond to cell type-specific biological responses. Therefore, there was an absence of clear cell type-specific or dose-dependent effects.

5.5 Strengths, Limitations, & Future Directions

An important strength of our research is the employment of a unique in-vivo chronic LDIR model, facilitated through our collaboration with CNL. The pathogen-free gamma-radiation facility at CNL is distinguished for its ability to execute extensive in-vivo experiments at low dose rates over prolonged exposure periods. While the majority of radiation studies concentrate on high-dose-rate scenarios, our investigation is crucial for elucidating the distinct effects associated with lower dose rate exposures, which may significantly diverge from those observed at higher dose rates.

Furthermore, to the best of our knowledge, this study is the first to use scRNA-seq to examine cell responses to low dose ionizing radiation. This novel approach offers unprecedented resolution to our findings. The unbiased nature of single-cell transcriptomic analysis, combined with the integration of multiple methodologies to study several organs, enhances the robustness of our findings. The convergence of results from hematology, flow cytometry, and transcriptomics provides a consistent and comprehensive description of the lack of radiation response, thereby enhancing the credibility of our conclusions.

Despite the comprehensive nature of our analysis, our study has important limitations. The sample size was small, which may limit the statistical power to detect the subtle changes expected from LDIR exposure. Increasing the sample size in future studies would improve the robustness and reproducibility of the findings. Additionally, our study would have benefited from incorporating multiple experimental replicates for the scRNA-seq analysis. This would allow for a more thorough exploration of the heterogeneity between individual samples. The pooled nature of the samples means that certain single-cell gene expression changes measured could represent contributions of outliers that cannot be identified. Furthermore, incorporating measurements of DNA damage following radiation exposure,

such as γ-H2AX staining, would have provided more direct evidence of radiation-induced DNA damage, thereby contextualizing our findings.

Future studies on radiation immunology should focus on the impact of chronic low-dose radiation on immune parameters over more extended periods in mice. This approach would yield a comprehensive understanding of the long-term effects on the immune system. Using a mouse model similar to the IES study, which simulates conditions faced by nuclear industry workers, would be instrumental for informing radiation protection guidelines. Moreover, it is crucial for upcoming LDIR studies to distinguish between the acute and persistent effects of exposure on various immune-populated organs. Our study examined the effects immediately after exposure, yet the potential impacts at later stages remain uncertain.

Our study did not perform targeted follow-up studies on candidate genes identified in transcriptomic analyses to elucidate their role in radiation response. These targeted studies are essential for clarifying the specific functions and regulatory mechanisms of the genes flagged in our initial analysis. Future studies from our group will perform gene knock-out and over expression assays to directly observe the resultant impacts on cellular function and response to radiation. With the aim of identifying low-dose radiation sensitive gene promoters, our group has recently analyzed the promoter sequences of candidate genes identified in this study and cloned them into luciferase reporter constructs. Our group is currently generating cells harbouring these constructs which could potentially serve as radiation sensitive reporter cell lines.

Our study focused exclusively on 18-week-old female C57BL/6 mice, neglecting age and gender variability, which are known to affect radiation sensitivity. Consequently, our results may not apply to different ages, strains, or sexes of mice. This limitation underscores the need for future studies to explore the effects of sustained LDIR on a more diverse population. Specifically, it is important to test both young and adult mice of each sex to better understand how age and sex might influence radiation sensitivity.

Incorporating functional assays to directly assess immune responses across immune populations would further elucidate the potential impacts of low-dose radiation. For instance, conducting a controlled immune challenge study, such as introducing an infection in the context of sustained LDIR, would provide valuable insights not available through epidemiological studies.

Finally, unsupervised analysis of single-cell modalities should continue to be employed to uncover novel molecular signatures of radiation response. Single-cell transcriptomic approaches will help provide a detailed overview of the molecular processes underlying cellular responses across diverse cell types. This will address the challenge of heterogeneity in LDIR research. Additionally, identifying radiation biomarkers would be extremely valuable for future LDIR epidemiology. Such biomarkers could help researchers distinguish between radiation-induced health effects and background variations, thereby contributing to reducing the current uncertainties in epidemiological surveys at low dose exposures and contributing to the generation of radiation dose response models.

6 Conclusion

This study aimed to unveil the effects of LDIR on the immune system, with a detailed focus on molecular mechanisms and cellular responses to sustained whole-body γ-radiation. Utilizing a unique experimental model, female C57BL/6 mice were continuously exposed to low dose rate ^{60}Co γ-rays over seven days, accruing cumulative doses of 10 mGy and 100 mGy. This investigation sought to bridge critical gaps in our understanding of LDIR, with significant implications for public health, occupational safety, and medicine.

Our findings indicate that certain instances of low-dose rate ionizing radiation exposure do not significantly alter the murine immune system, particularly when cumulative doses reached remain in the low-dose range. Hematological analysis showed no major changes in blood composition, and flow cytometry revealed no significant differences in the proportion of immune cell subsets in the spleen, thymus, and bone marrow across radiation conditions. Additionally, bulk RNA-sequencing and unsupervised scRNA-sequencing analyses identified limited differentially expressed genes. No canonical signatures of radiation exposure, such as DDR and oxidative stress, were observed. These results suggest a broad preservation of immune cell homeostasis under these exposure conditions. This is significant given that the cumulative dose delivered reached the upper threshold of what the NAS considers low-dose radiation exposure. Several subtly modulated differentially expressed genes represent candidates for LDIR response and merit follow-up investigations.

These findings contribute to the broader understanding of radiation biology, demonstrating that the effects of LDIR on the murine immune system are limited, especially at very low dose rates. The results align with a threshold model of immune effects from radiation, suggesting that the doses applied in this study fall below an undefined threshold required to induce measurable disruptions in immune homeostasis. However, caution should be exercised in generalizing these findings beyond our specific experimental model, as radiation sensitivity can vary across different organisms and even among mouse strains. Different genetic backgrounds, age groups, and environmental conditions could potentially

influence the immune response to LDIR, necessitating further investigation to confirm these results in other models and contexts.

Disseminating these results will support the ongoing scientific effort to comprehend the biological effects of low-dose radiation exposure. This study's insights could inform guidelines for radiation safety, providing evidence that low dose rate radiation exposures may have minimal impact on the immune system. Such information is crucial for assessing the risks associated with chronic low-dose radiation in various contexts, including medical treatments, nuclear industry work, and other occupational exposures. Moreover, these findings could help to refine our understanding of the thresholds at which radiation becomes harmful, potentially leading to more accurate risk assessments and improved safety regulations. While our study provides a foundational perspective on the effects of LDIR on the immune system, continued research is necessary to fully elucidate the long-term implications and subtler biological effects of such exposure.

In conclusion, this study provides valuable insights into the resilience of the immune system to cumulative low dose radiation exposures delivered at low-dose rates. Future studies should aim to explore the effects of LDIR on the immune system at dose rates and durations which better mimic typical occupational exposures and should discriminate carefully between the acute and long-term effects of such exposure.

7 Contribution of Collaborators

Study was conceptualized and designed by Bryan Marr, Abrar Khan, Seung-Hwan Lee, Holly Laakso and Melinda Blimkie. Mice housing, irradiation, dissection, and hematology was performed by Melinda Blimkie and Holly Laakso at the Canadian Nuclear Laboratories. Cell isolation and flow cytometry was performed by Bryan Marr and Abrar Khan at the University of Ottawa. Bulk RNA-sequencing library preparation and sequencing was performed by Genome Quebec. Single-Cell RNA sequencing library preparation, sequencing and Cell Ranger analysis was performed by the Ottawa Hospital Research Institute Stem Core Labs. Data analysis and bioinformatics was performed by Bryan Marr at the University of Ottawa. Thesis was written by Bryan Marr and revised with Seung-Hwan Lee. The thesis project was supervised by Seung-Hwan Lee and Arvind Mer. Computation was enabled in part by support provided by Digital Research Alliance of Canada.

8 Disclosure

I would like to acknowledge the financial support provided by the CANDU Owners Group, whose support made this research possible. The funding organization had no role in the study design, data collection, analysis, interpretation of results, or in the decision to submit this thesis for academic purposes.

9 Statement on Artificial Intelligence

In writing this thesis, OpenAI's ChatGPT was used as a supplementary tool to aid in literature review and idea generation. The AI was utilized to clarify complex topics and assist in structuring the initial drafts of certain sections. Additionally, ChatGPT was employed to revise writing for correct grammar, conciseness, organization, and tone. All interpretations and final writings were reviewed and refined by the author to ensure originality and adherence to academic standards. ChatGPT was not used for experimental design, hypothesis generation, or the direct analysis of data. It was used to debug errors in bioinformatic code and to assist in generating code for figure creation and other specific instances within the bioinformatic analysis. All data analysis computations and calculations were conducted independently of AI.

10 Appendix: Engineering CAR NK Cells Overexpressing IL-2Rα

10.1 Project Background

Following the success of Chimeric Antigen Receptor (CAR) T-cell therapy, there is increasing interest in using NK cells as a platform for CAR-based therapy. CARs are synthetic proteins that direct immune cell cytotoxicity toward cells expressing a defined target antigen. The CAR's extracellular domain typically consists of a single-chain variable fragment, derived from the antigen-binding regions of an antibody's variable heavy and light chains, enabling highly specific recognition of surface tumour antigens. The intracellular domain contains signalling motifs derived from the T-cell receptor, often including CD3ζ, as well as co-stimulatory motifs such as 4-1BB or CD28. These extracellular and intracellular domains are connected by transmembrane and hinge regions, derived from immune receptors, which can be modified to fine-tune the receptor's response.[161] CAR expression is typically engineered ex vivo using lentiviral transduction to insert a CAR-encoding transgene into the immune cell genome. The resulting CAR-expressing cells function as "living drugs," capable of recognizing tumour cells defined by the target antigen and subsequently activating signalling pathways that lead to immune cell activation, proliferation, cytokine secretion, and cytotoxicity.

CAR-T cell therapy has proven revolutionary, capable of achieving durable remissions in patients facing relapsed and refractory hematological malignancies.[162–167] However, several limitations hinder its broader application. Most notably, T cells are alloreactive, restricting their use to autologous cell therapy. This presents a significant limitation, as autologous therapies are costly, highly variable, and require extended manufacturing times.[168,169] This constraint restricts accessibility and scalability, as manufacturing must occur in specialized centers and is inherently long due to patient-specific nature, potentially allowing disease progression in aggressive cases. Additionally, the process is prone to errors such as insufficient T-cell expansion, reduced viability, and contamination. Patient-derived T cells further introduce variability in quality and function, particularly in heavily pre-treated patients, complicating production and efficacy. Furthermore, CAR-T cells cannot discriminate between healthy and cancerous cells expressing the target antigen, leading to substantial off-target effects. For instance, CD19 CAR

therapy targets both CD19+ malignant and healthy B cells, resulting in B cell aplasia.[170] CAR-T cells also pose risks of dangerous side effects, including cytokine release syndrome (CRS) and immune effector cell-associated neurotoxicity syndrome (ICANS).[171,172] While side effects have become better managed with treatments such as IL-6 inhibitors and corticosteroids, they continue to remain a risk for patients.

In contrast, CAR Natural Killer (NK) cell therapy presents potential advantages while addressing the limitations of CAR-T cell therapy. Crucially, NK cells have been proven safe for allogeneic use, meaning they can be derived from cell lines, healthy donors or bio-manufactured from induced pluripotent stem cells, which opens the door to the development of standardized, "off-the-shelf" CAR NK cell products. This eliminates the need for autologous manufacturing, allowing quicker, more scalable treatments that can be administered in multiple doses. Furthermore, NK cells possess specific innate tumour-recognizing abilities that operate without the need for antigen presentation. This inherent specificity may limit off-target killing of healthy cells, while providing alternate routes of cancer killing cytotoxicity.[173,174] This natural cytotoxicity, combined with the specificity provided by CAR-directed targeting, makes CAR NK cells an increasingly attractive approach for cancer therapy. Unlike CAR-T cells, NK cell therapy has not shown side effects of CRS and neurotoxicity, enhancing their safety.

At the time of writing this thesis, there are around 40 clinical trials of various CAR-NK cell therapy applications listed on the clinicaltrials.gov database. One of the first clinical trials exploring CAR NK cell therapy utilized irradiated NK92 cells and showed limited clinical efficacy.[175] Since then, clinical trials have explored use of cord-blood derived, peripheral blood derived and iPSC derived CAR NK cells. Limited data has been published in peer reviewed journals from these trials thus far. Most promisingly, in a single-arm trial, the Rezvani group at MD Anderson demonstrated that CAR NK cells targeting CD19+ hematologic malignancies could achieve significant tumour reduction with minimal adverse effects.[176] Specifically, relapsed refractory B cell malignancies showed a 1-year progression-free survival rate of 32% and an overall response rate of 48.6%. This suggests that CAR NK cells could provide a safer, more readily available alternative to CAR-T therapy.

Interleukin-2 (IL-2) is a cytokine central to activating NK cells and is commonly administered following adoptive transfer to support NK cell activity in a patient. It also plays an important role in activating NK cells during immune responses. Unstimulated NK cells express only a low affinity heterodimeric IL-2 receptor composed of the IL-2/15Rβ (CD122) and γc chains (CD132). Once activated, NK cells gain the expression of IL-2Rα (CD25), promoting the formation of a heterotrimeric IL-2Rα$\beta\gamma$ with dramatically increased affinity for IL-2.[177–180] The strengthened responsiveness to IL-2 enhances NK cell cytotoxicity and stimulates proliferation. In the clinic, high-dose IL-2 injections cannot be used to activate NK cells since they have been proven toxic by causing cytokine storm, excessive inflammation, capillary leak syndrome, and organ dysfunction.[181,182] Low dose IL-2 injections are well tolerated and have been used extensively in combination with cellular immunotherapies, including NK cell therapy. However, it has been shown that immunosuppressive regulatory T cells (Tregs) use their high-affinity IL-2Rα expression to sequester the injected IL-2, leading to Treg expansion and immunosuppression during low dose IL-2 therapy.[183,184]

As it stands, NK cell therapies still face limitations, including challenges in engineering, inadequate persistence, expansion, and tumour clearance. Amelioration of NK cell activity is being challenged on many fronts. For example, clinical trials have investigated the use of cytokine-induced memory-like (CIML) phenotypes in NK cells via stimulation with IL-21, IL-18, and IL-15.[185–188] This CIML phenotype improves IL-2 responsiveness through CD25, increases persistence, and enhances cytotoxicity. Modifications of CAR constructs to optimize NK cell activity has also been explored, focusing on incorporation on NK cell signalling domains and inclusion of cytokines like interleukin-15 (IL-15).[176] Playing a crucial role in NK homeostasis and activation, IL-15 is a key target for improving NK cell-based therapies. It's incorporation in CAR constructs has enhanced NK cell persistence and anti-tumour activity. Additionally, advances in genetic engineering, such as gene knockout techniques, are being employed to remove inhibitory signals and improve the metabolic fitness of NK cells. For example, the knockout of the CISH gene has demonstrated promise in enhancing NK cell function and persistence within the tumour microenvironment.[189] There is a massive scientific effort underway investigating novel strategies for augmenting CAR NK cell activity that could lead to substantial clinical advancements.

Considering the critical need for enhancing NK cell-based therapies, I hypothesize that the efficacy of CAR NK cells can be augmented through the overexpression of IL-2Rα. I predict that CAR-IL2Rα NK cells will exhibit an amplified response to IL-2, thereby improving their expansion, persistence, and anti-tumour activity during treatment. Furthermore, this strategy may enhance the NK cells' ability to compete with Tregs for IL-2, thus potentially reducing Treg expansion and mitigating immunosuppression during therapeutic interventions.

10.2 Preliminary Results

In collaboration with the National Research Council of Canada, we received a lentiviral transfer plasmid encoding a conventional CAR construct. Using that plasmid, I cloned a novel multicistronic construct encoding the CAR, an mNeonGreen reporter, and IL-2Rα **(Figure S11A)**. Lentiviral transduction of NK92 cells with this each construct yielded NK cells expressing the CAR and labelled by an mNeonGreen reporter **(Figure S11B)**. NK92 transduced with the novel CAR-IL2Rα construct have increased IL-2Rα expression across IL-2 culture conditions when compared to those transduced with the conventional CAR construct **(Figure S12)**. I found that IL-2Rα expression is inversely related with the IL-2 concentration, as previously shown by Gong et al. I predict that this observation can be explained by increased receptor internalization in high concentrations of IL-2.

To test the functionality of the overexpressed IL-2Rα, we measured phosphorylated signal transducer and activator of transcription 5 (pSTAT5) following overnight stimulation with IL-2 **(Figure S13A)**. CAR- IL2Rα NK92 cells had a greater proportion of pSTAT5 positive cells compared to conventional CAR NK92 cells, with the difference being greatest in 10 and 100U/mL IL-2 conditions **(Figure S13B)**. Next, I predicted that since CAR-IL2Rα cells had more IL-2 signalling, then they should consume more IL-2 from the media. Following 48- or 72-hour culture in different conditions of IL-2, a cytokine bead assay (CBA) was used to measure the amount of IL-2 remaining in the growth medium **(Figure S13C & D)**. This CBA showed that CAR-IL2Rα consume more IL-2 from the media compared to conventional CAR NK cells. After 48-hour cultures in 10 or 100U/mL IL-2, CAR-IL2Rα NK92 cells have around 37% and 27% of the IL-2 signal measured in conventional CAR NK cultures respectively. In high 1000U/mL IL-2 culture, CAR-IL2Rα and conventional CAR NK cells each have abundant IL-2

remaining after 48Hr. These experiments demonstrate that IL-2Rα overexpression on CAR NK92 cells facilitates increased IL-2 signalling and reduction of IL-2 available in the media.

To test the ability of CAR-IL2Rα NK92 cells to compete for IL-2 available in culture, wild-type NK92 cells were mixed with conventional CAR or CAR-IL2Rα NK92 cells in a 7:3 ratio and cultured in various conditions of IL-2 **(Figure S14A)**. During low IL-2 culture, the proportion of CAR-IL2Rα NK92 increased from 30% to between 80-90%. The change in proportion of CAR NK92 cells was measured by the presence of cells positive for the mNeonGreen reporter **(Figure S14B)**. The proportion of conventional CAR NK cells did not change in the same conditions. This finding suggests that IL-2Rα overexpression allows CAR-IL2Rα NK92 to outcompete wild-type NK92 for the limited cytokine available in the media. When cultured at 100U/mL, there is no enrichment of CAR-IL2Rα NK92 cells. Therefore, when IL-2 is present in excess, the 30% CAR-IL2Rα NK92 cells in culture cannot outcompete the 80% wildtype NK92.

Importantly, CAR-IL2Rα NK cells exhibited significantly higher expression levels of Granzyme B and Perforin, compared to conventional CAR NK cells **(Figure S15)**. Granzyme B and Perforin are crucial components of the cytotoxic granules within of NK cells, playing pivotal roles in the induction of target cell apoptosis. This trend of increased expression levels was consistent across all tested IL-2 culture concentrations (1 U/mL, 10 U/mL, 100 U/mL, and 1000 U/mL), indicating that CAR-IL2Rα NK cells maintain their elevated cytotoxic marker expression regardless of IL-2 availability. Furthermore, even in the complete absence of IL-2, CAR-IL2Rα NK cells demonstrated a more pronounced increase in these cytotoxic markers compared to their conventional CAR NK cell counterparts. These results do not quantify the cytotoxic function of these cells, instead they suggest that there are increased cytotoxic molecules within CAR-IL2Rα NK cells, that may provide enhanced cytotoxic potential.

10.3 Discussion

The objective of the project was to enhance CAR NK cell therapy by engineering the overexpression of IL-2Rα. We hypothesize that overexpressing IL-2Rα would improve CAR NK cell expansion, post-transfer persistence and proliferation, and anti-tumor activity while reducing Treg cytokine sequestration.

Preliminary results of this work show that engineered CAR-IL2Rα NK cells have significantly higher IL-2Rα expression and enhanced IL-2 signalling compared to conventional CAR NK cells. They consume more IL-2 from the media, particularly in low IL-2 conditions, and outcompete wild-type NK cells for IL-2 in culture. These findings suggest that IL-2Rα overexpression enhances CAR NK cell responsiveness to IL-2. Future work should focus on addressing the proliferative capacity, cytotoxicity, and persistence of CAR-IL-2Rα NK cells.

When cultured in low concentrations of IL-2, CAR-IL2Rα NK92 cells demonstrated a significant growth advantage over conventional CAR NK92, an effect not observed at higher IL-2 levels. This growth advantage appears to be due to the enhanced ability of CAR-IL2Rα NK92 to sequester low-dose IL-2 from the media, offering a potential proliferative boost to CAR-IL2Rα NK92 and/or inhibiting the growth of conventional CAR NK92 cells. Supporting this observation, Akman et al. engineered primary NK cells with IL-2Rα, confirming their preferential growth in low-dose IL-2 (12.5U/mL).[190] Additionally, they demonstrated that knocking down IL-2Rα in NK92 cells resulted in reduced cell growth in low IL-2 concentrations of 25U/mL and 12.5U/mL, while growth remained unaffected at 50U/mL, underscoring the critical role of IL-2Rα in mediating cellular responses to IL-2 availability.

In-vitro expansion is crucial for NK cell manufacturing, due to its direct impact on the scalability and feasibility of producing a therapeutic product. Therefore, any significant increase or decrease in culture expansion is highly consequential. Therefore, future studies should evaluate the effect of IL-2Rα overexpression on culture expansion of CAR NK cells in various IL-2 conditions. Due to the high IL-2 consumption measured in our CBA assay, careful attention should be made to avoid IL-2 depletion in culture during the expansion process.

Current evidence suggests that persistence and expansion of NK cells post-adoptive transfer is a major determinant of NK cell therapy response.[176] According to my hypothesis, IL-2 administration post adoptive transfer would better activate CAR-IL2Rα NK cells compared to conventional CAR NK cells, leading to improved persistence and proliferation. I recommend future experiments focus on adoptive transfer of IL-2Rα overexpressing NK cells into immunodepleted mice. Subsequently, the persistence and expansion of CAR NK cells should be evaluated at different doses of IL-2 therapy. One major

limitation of this model is that murine Treg IL-2 driven expansion cannot be measured due to limited cross reactivity of human IL-2 on the murine IL-2 receptor. A potentially more ideal pre-clinical experiment would involve an all-mouse CAR NK cell treatment, using murine low dose IL-2 administration for treatment of a murine tumour. However, murine NK cell engineering is presently very challenging. Therefore, most pre-clinical NK cell therapy studies published continue to use immunocompromised adoptive transfer experiments.

Tumour killing is also important to CAR NK cell therapy success. Since pSTAT5 is linked to NK cell cytotoxicity, and we measured improved pSTAT5 in low dose IL-2 cultures, we expect increased cytotoxicity. Furthermore, the increased levels of intracellular granzyme-B and perforin underscore the potential for improved cytotoxicity. Future experiments should evaluate the IFN$\gamma$and CD107α expression of CAR-IL2Rα NK cells following standard co-culture assays in various concentrations of IL-2. In-vivo, one of the best methods for evaluating pre-clinical cell therapy efficacy is longitudinal IVIS monitoring of luciferase expressing tumours in response to CAR NK cell therapy. Any significant modulation to CAR NK cell function would be of critical importance to evaluating the merit of this proposal.

Moreover, it is vital that CAR-IL-2Rα constructs are tested across various NK cell models. This includes the NK92 cell line, primary NK cells isolated from cord or peripheral blood, and iPSC-derived NK cells. Since each of these NK cell sources is being evaluated as therapeutics, understanding any advantage conferred by IL-2Rα overexpression is valuable. IL-2Rα overexpression may enhance the survival, expansion, and efficacy of NK cells, making them more potent and durable when used in clinical settings. By comparing the effects of IL-2Rα overexpression in different NK cell models, researchers can determine the most promising approaches for future clinical applications. This comprehensive evaluation will inform the development of optimized CAR-IL-2Rα NK cell therapies and guide their transition from research to clinical use.

In conclusion, my current evidence is promising regarding potential amelioration of CAR NK cell activity by IL-2Rα overexpression. Further experimentation is necessary for following up on these important preliminary investigations, diving deeper into the potential feasibility and efficacy of this approach. A successful implementation of CAR-IL2Rα NK cell therapy could represent a significant

advancement in cancer immunotherapy. By addressing the limitations of current CAR NK cell therapies, this approach has the potential to improve treatment outcomes for patients with various types of cancer.

10.4 Appendix Methods

10.4.1 Construction of BCMA CAR-IL2Rα Vector

A custom gene fragment containing T2A and the protein-coding sequence of human IL-2Rα (Uniprot ID: P01589) was purchased from Twist Bioscience (Figure 4). Our lab's existing BCMA-CAR vector was obtained initially from collaboration with the National Research Council of Canada. The vector was PCR amplified using high-fidelity Q5 DNA polymerase (NEB) to both linearize it and add complementary sequences to each end that overlap the T2A-IL-2Rα gene fragment. Any remaining circular template plasmid was digested using DpnI (Thermofisher). Then, a Gibson assembly reaction and transformation were performed using the Gibson cloning kit (NEB) and competent E. coli (NEB). Plasmid DNA was extracted from transformed colonies using miniprep (Invitrogen, Thermofisher), and plasmid DNA concentration and purity were assessed using a nanodrop spectrophotometer.

To verify the T2A-IL-2Rα gene fragment was inserted into the vector as intended, miniprep plasmid DNA was digested using EcoRI (ThermoFisher) and PacI (ThermoFisher) restriction enzymes, whose sites were included in the insert. Furthermore, both colony PCR and Sanger sequencing (DNA Sequencing Facility at the Ottawa Hospital Research Institute) confirmed the insertion was made in the correct location without mutations to the protein-coding regions.

10.4.2 Lentivirus Production and Transduction

To produce lentivirus 1.5E6 Lenti-X 293T cells were plated per well on a six-well plate in 2 mL of Opti-MEM medium (31985070; Gibco) containing 5% HI-FBS and 100 mg/mL Pen/Strep. The next day, the Lenti-X 293T cells were transfected using Lipofectamine 3000 (L3000015; Invitrogen). Briefly, 1,200 ng of transfer plasmids encoding the CAR, 1,200 ng of pSPAX2 (gifted from Didier Trono; 12260; Addgene), and 200 ng of BaEV-TR were combined with Lipofectamine 3000 (6 mL of P3000 and 7 mL of Lipofectamine 3000) in 500mL of serum-free Opti-MEM. Then 1 mL of medium was removed from each well and replaced with the Lipofectamine/plasmid mix. After a 4-h incubation, all medium was removed from each well and replaced with fresh, complete Opti-MEM medium. Without concentrating

the LVs, viral supernatant was collected at 48hr and filtered using a low-protein-binding polyethersulfone (PES) filter (83.1826; Sarstedt) and kept at -80C.

5E4 NK92 cells were added to a 96 well U-bottom plate with lentivirus and serum-free RPMI containing 4mg/mL polybrene (TR-1003-G; MilliporeSigma), and 200U/mL IL-2. Spinoculation was performed for 30min at 1,500g 37CC. Then, following a 3.5 hour incubation the transduction media was removed and the pellet was resuspended in complete RP10 culture media containing 200U/mL IL-2. The next day, cells were washed to remove remaining lentivirus.

10.4.3 Cell Culture

NK92 were cultured in RPMI-1640 media (Wisent Inc., Quebec, Canada) supplemented with L-glutamine, Penicillin-Streptomycin Solution (10,000 U/mL Penicillin, 10,000 ug/mL Streptomycin) (Hyclone Laboratories Inc., Utah, USA), 55uM 2- mercaptoethanol (Life Technologies Corp), 1M HEPES (Lonza BioWhittaker), 10% of fetal bovine serum (ThermoFisher) (RP10 medium). This RP10 medium was supplemented with various concentrations IL-2 (NCI Preclinical Repository, USA) depending on the experiment. Lenti-X cells (Takara Bio) were cultured in DMEM (Wisent) with 10% FBS (Thermofisher) and Penicillin Streptomycin solution (10,000 U/mL Penicillin, 10,000 ug/mL Streptomycin).

10.4.4 Flow Cytometry

For all experiments involving NK cell stimulation with various IL-2 concentrations, cells were washed twice in IL-2 free media before resuspension in media containing the specified IL-2 concentrations for the indicated time frames.

For surface antigen staining, cells were washed in a 96 well V-bottom plate with staining buffer (PBS containing 2% HI-FBS), centrifuged at 1500rpm (same speed for all steps unless stated otherwise) for 4 minutes at 4°C, and the supernatant was removed. The cells were then resuspended in staining buffer and incubated with fluorophore-conjugated antibodies for 25 minutes at 4°C. After incubation, cells were washed twice with staining buffer, centrifuged, and resuspended in staining buffer for analysis.

For intracellular proteins (Gzmb and perforin), the Cytofix/Cytoperm kit was employed between surface staining steps. Briefly, following surface staining, cells were washed and centrifuged, then resuspended in BD Cytofix/Cytoperm buffer and incubated for 10-20 minutes at 4°C. Cells were washed

twice with BD Cytoperm Wash buffer and centrifuged. The cells were then incubated with an intracellular antibody cocktail in BD Cytoperm Wash buffer for 25 minutes at 4°C. Following incubation, cells were washed with BD Cytoperm Wash buffer and staining buffer, centrifuged, and resuspended in cold staining buffer for analysis.

For pSTAT5 staining, cells were plated in V-bottom 96-well plates and centrifuged for 5 minutes at 4°C. The supernatant was removed, and cell pellets were resuspended in 100µL BD Cytofix/Cytoperm buffer, pipetted up and down 10 times, and incubated for 20 minutes at 4°C. After centrifugation and removal of the supernatant, the pellets were washed with 200µL freshly prepared BD Cytoperm Wash buffer, centrifuged, and resuspended in 200µL pre-chilled 100% methanol. Following a covered 15-minute incubation on ice, cells were centrifuged at 2000rpm for 5 minutes, washed with cold staining buffer, and resuspended in 50µL staining buffer containing anti-STAT5-PE antibody (15µL per 50µL staining buffer). After a 15-minute incubation at 4°C, cells were washed twice with staining buffer, centrifuged, and resuspended in 200µL cold staining buffer. Samples were acquired immediately post-staining.

Flow cytometry was performed on an Attune NxT flow cytometer (Attune, ThermoFisher) and analyzed using Kaluza (Beckman Coulter).

10.4.5 Cytokine Bead Assay

CAR NK92 cells were incubated in 500uL in a 48 well flat bottom plate for either 48 or 72 hours in RP10 media supplemented with IL-2. Following incubation, 50uL of media was removed and used for the cytokine bead assay (CBA). The experiment was performed using the Human IL-2 CBA assay (BD) following manufactures recommendations, varying the volumes only. Briefly, samples and standards were diluted into a 25uL volume. Next, the mixed 25uL of Capture Beads were added to each well, followed by a covered 1-hour incubation on a plate rocker at room temperature. After the incubation, 25 µL of the mixed PE Detection Reagent was added to each well, which was then gently mixed and incubated for an additional 2 hours at room temperature in the dark, with a short 1min mixing on the plate rocker at the halfway mark.

Following the incubation with the detection reagent, 200 µL of Wash Buffer was added to each well, and the plate was centrifuged at 200g for 5 minutes. The supernatant was carefully aspirated and discarded. To resuspend the beads, 200 µL of Staining Buffer was added to each well, and the plate was briefly vortexed. Samples were then acquired on a flow cytometer on the same day to prevent increased background and reduced sensitivity.

11 Supplemental Figures & Tables

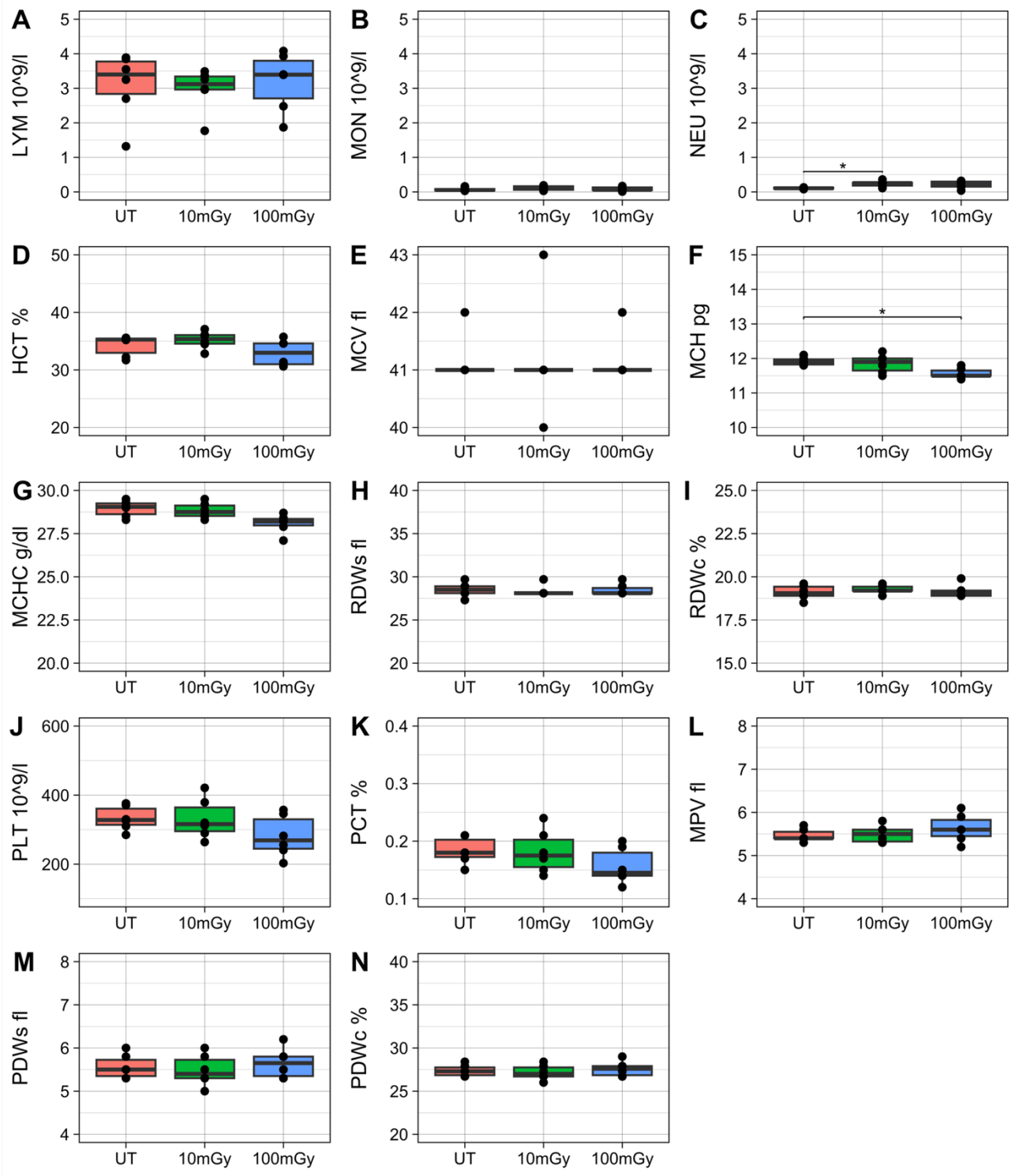

Figure S1. Hematology Analysis. Following the chronic radiation treatment, blood samples were collected and analyzed using an automatic hematology analyzer. Kruskal-Wallis test was used to compare means of each parameter with post-hoc Dunn's tests.

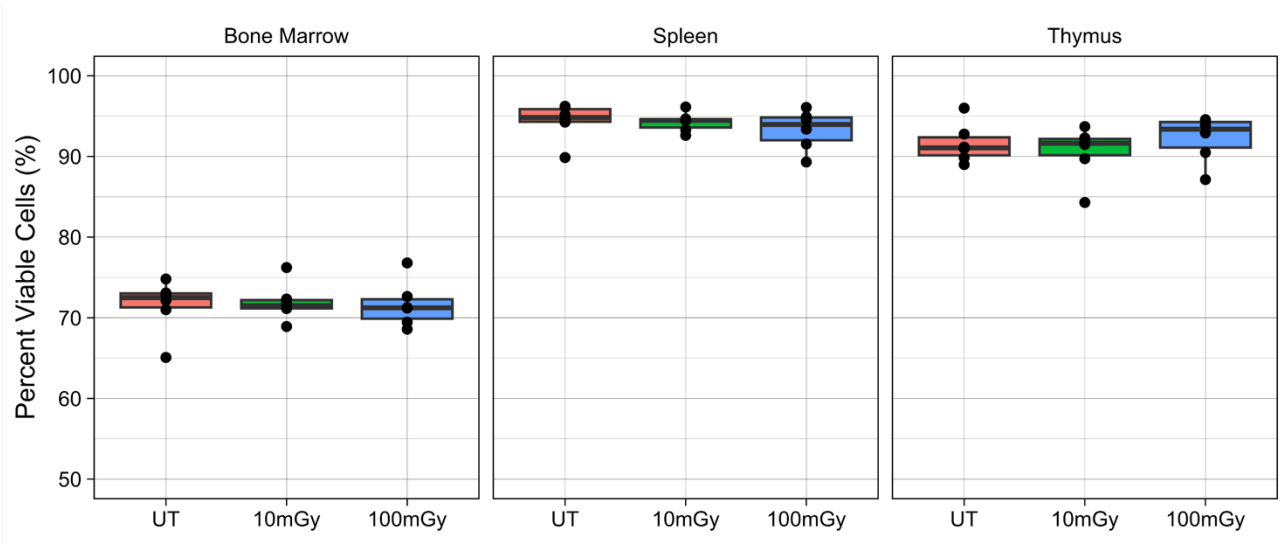

Figure S2. Sample Viability Assessed By Flow Cytometry. Cells isolated from the spleen, bone marrow and thymus were analyzed using flow cytometry. To determine the viability of samples, live cells were gated as those negative for a fixable viability stain. The mean proportion of viable cells was compared across conditions. Kruskal-Wallis test was used to compare means with post-hoc Dunn's tests.

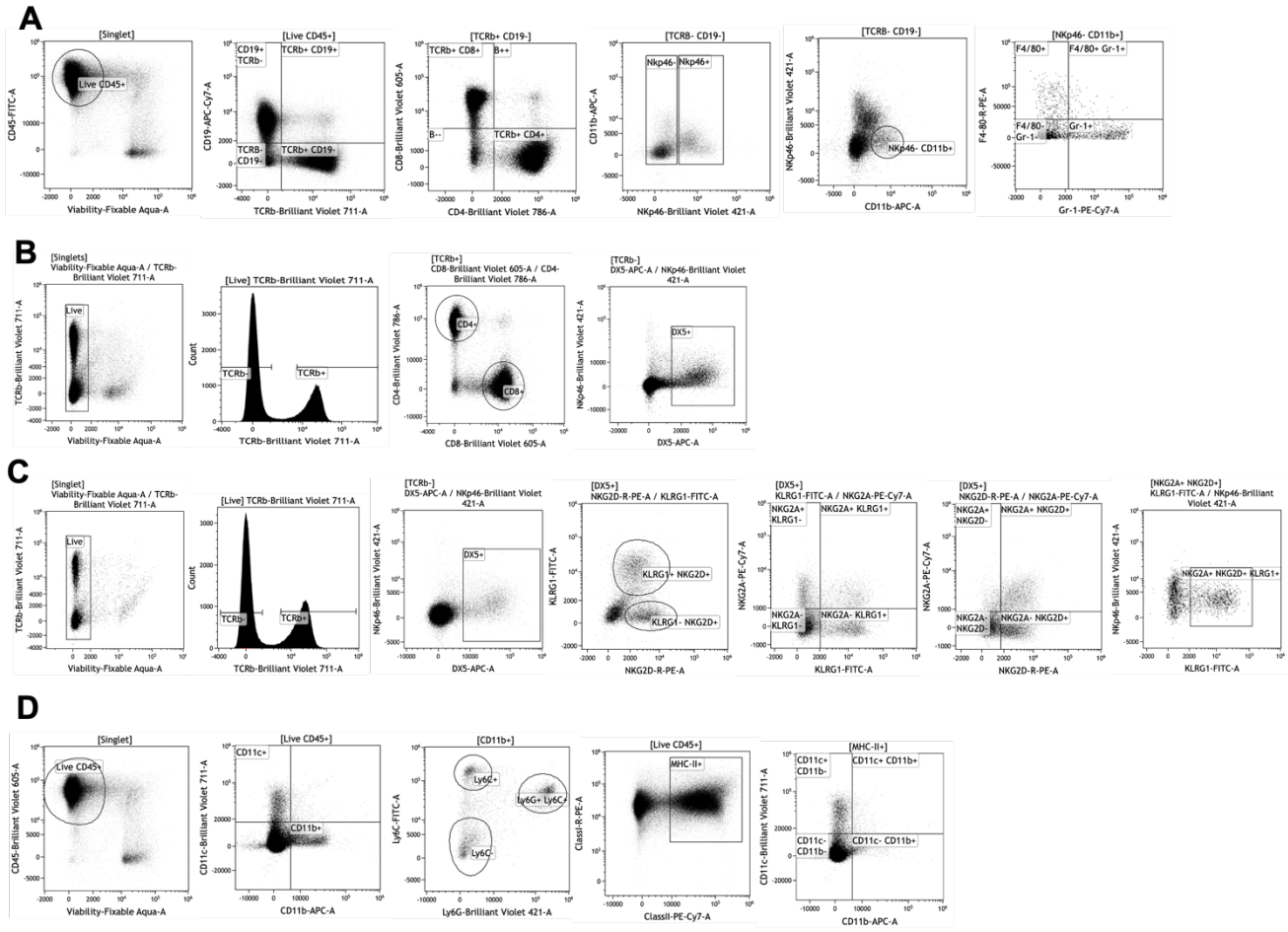

Figure S3. Spleen Gating Strategy. Flow cytometry gating strategy for spleen cell populations using four distinct antibody panels (A-D). Each panel represents a separate set of markers to identify various immune cell subsets within spleen samples. Initial gating was performed to exclude debris and doublets using forward scatter and side scatter parameters. Data represents a single sample. Input gates are titled on top of each plot ([Gate]).

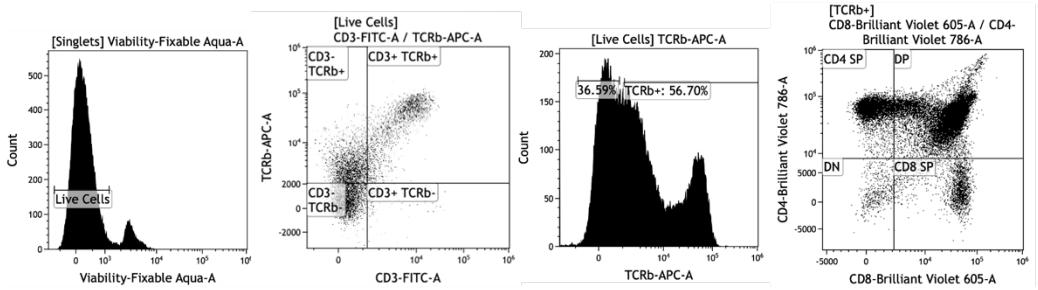

Figure S4. Thymus Gating Strategy. The flow cytometry gating strategy used to analyze thymocytes is depicted. Debris and doublets were first excluded using FSC and SSC parameters. Data represents a single sample. Input gates are titled on top of each plot ([Gate]).

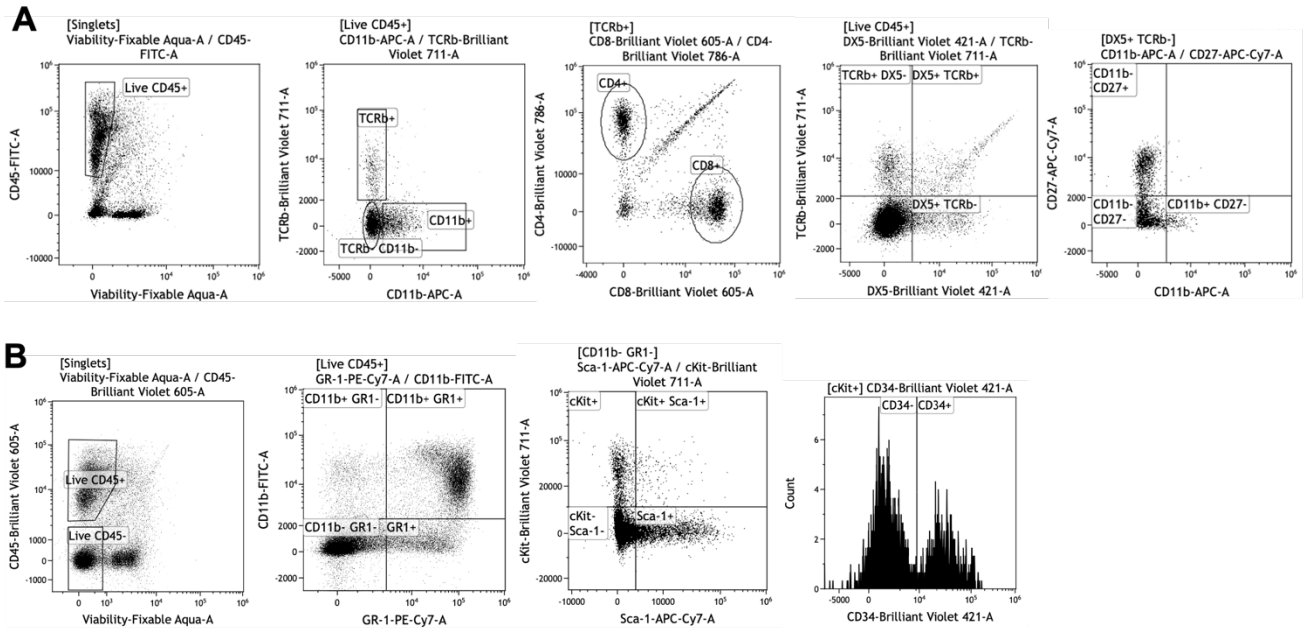

Figure S5. Bone Marrow Gating. The flow cytometry gating strategy used to analyze bone marrow cells is depicted. Two separate sets of antibody panels were used to analyze bone marrow samples (A&B). Initial gating was performed to exclude debris and doublets using forward scatter and side scatter parameters. Data represents a single sample. Input gates are titled on top of each plot ([Gate]).

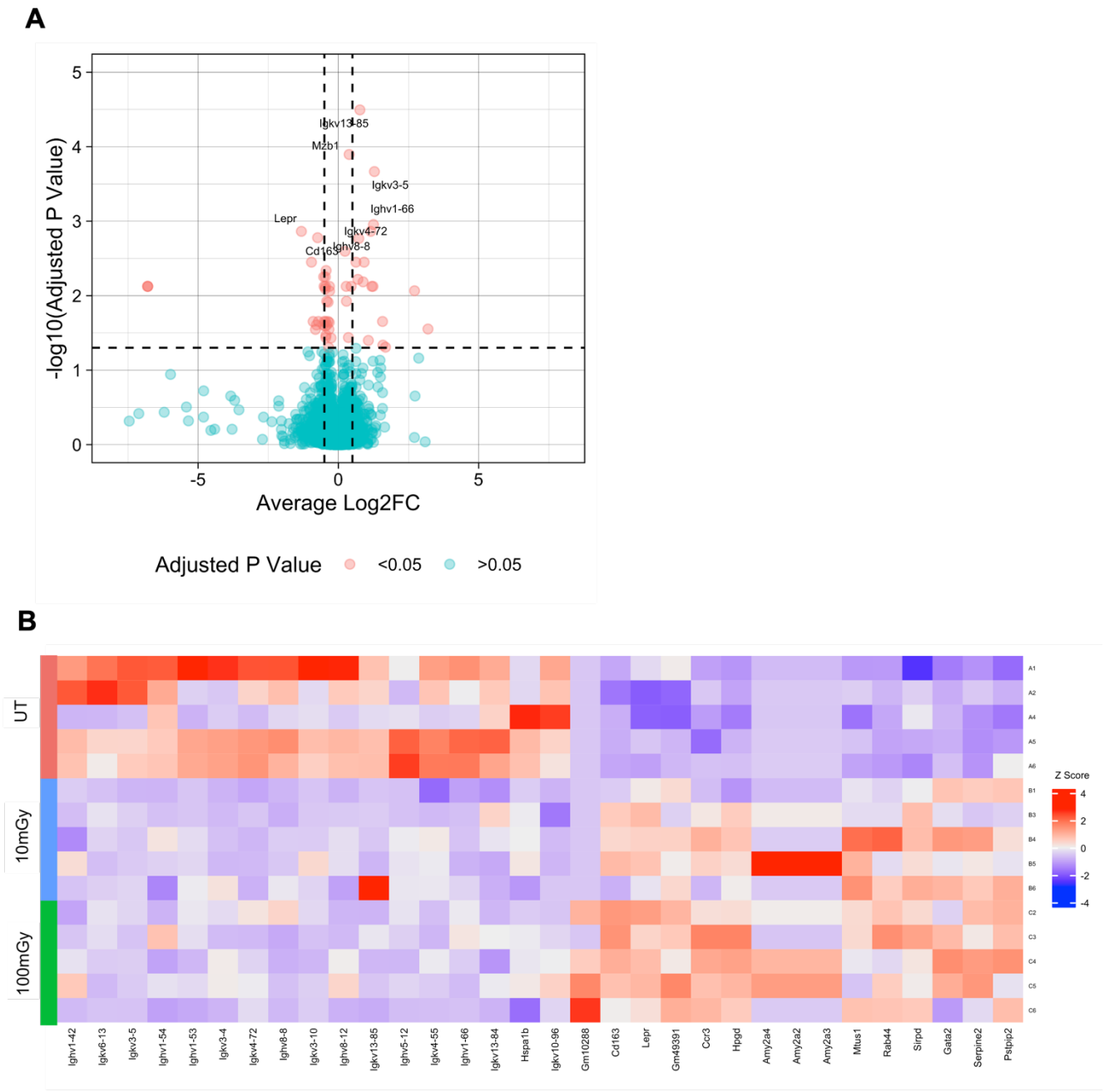

Figure S6. Pooled Differential Expression. Differential expression analysis comparing pooled irradiated (10 mGy and 100 mGy combined) splenocytes to untreated (UT) cells. **(A)** Volcano plot of differentially expressed genes.. Genes with an adjusted p-value < 0.05 are highlighted in red, and those with an absolute log2 fold change > 0.5 are labeled. Dashed lines denote significance thresholds for adjusted p-value and log2 fold change. **(B)** Heatmap of significantly differentially expressed genes (adjusted p-value < 0.05 and absolute log2 fold change > 0.5) obtained from pooled analysis.

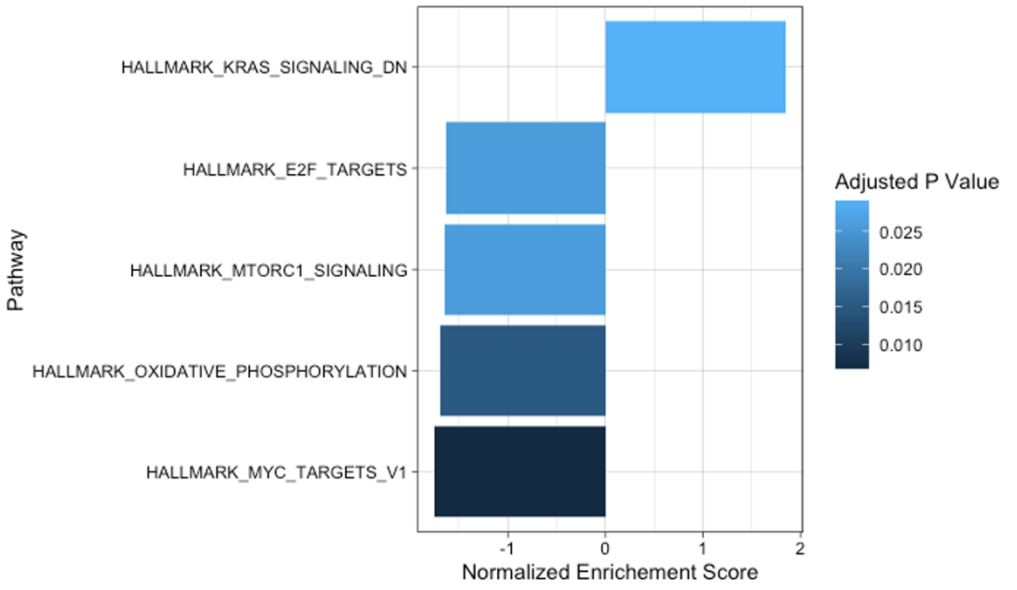

Figure S7. Gene Set Enrichment Analysis. Results comparing untreated samples with 100 mGy-treated spleen cells. GSEA was performed by ranking all DEGs by fold change and comparing them to hallmark pathways from the MSigDB mouse-specific reference. Pathways with significant enrichment (adjusted p-value < 0.05) are displayed, with bar color intensity representing the adjusted p-value. No significant pathways were found for the 10 mGy dose.

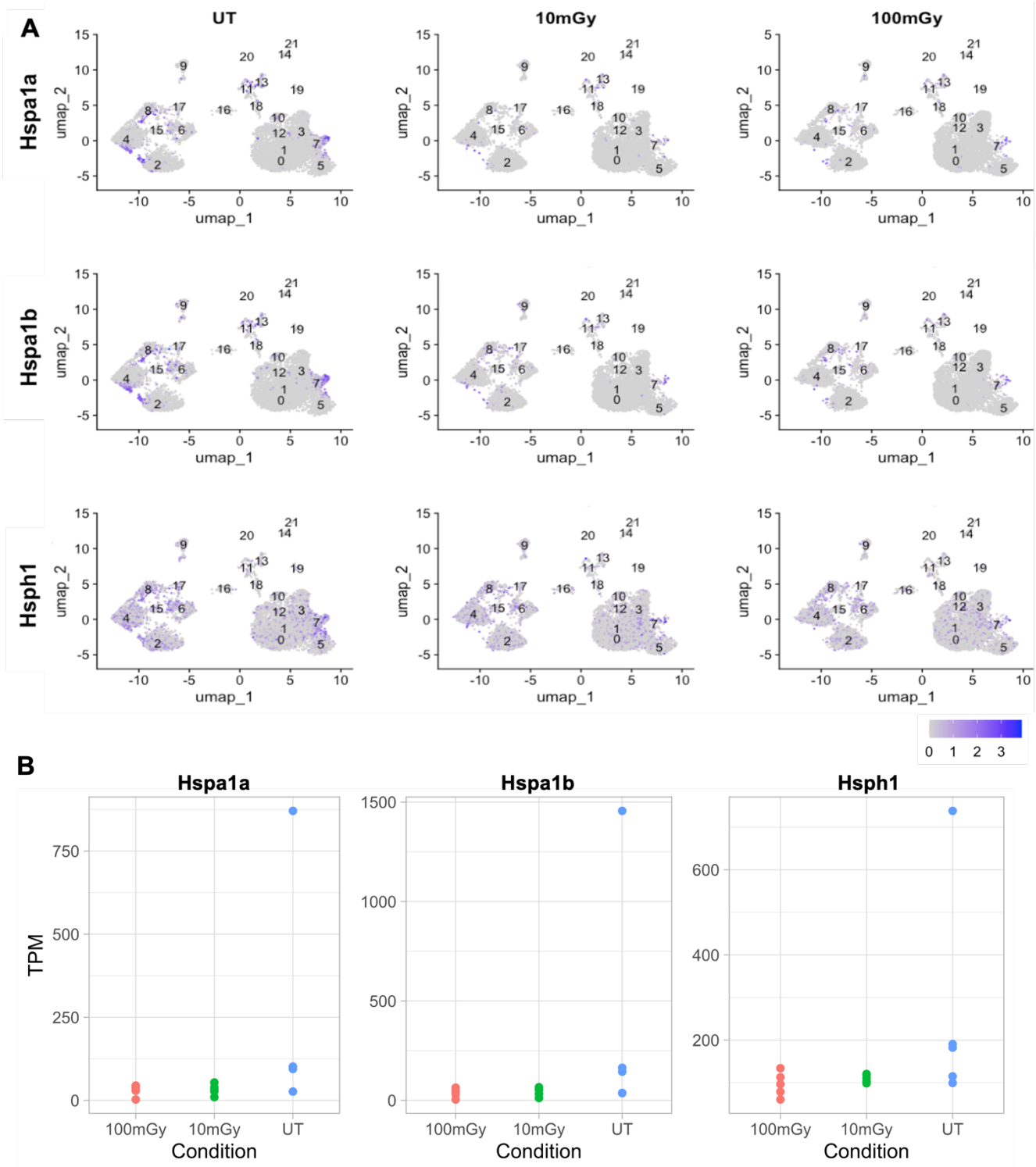

Figure S8. Analysis of heat shock protein markers from scRNA-seq cluster 7. (A) UMAP plots displaying expression levels of Hspa1a, Hspa1b, and Hsph1 across untreated and irradiated conditions. Purple shading intensity represents expression level, with higher expression shown in darker shades. Each plot is labeled by cluster number to indicate spatial expression patterns across clusters, with particular focus on cluster 7. **(B)** Bulk RNA sequencing counts for Hspa1a, Hspa1b, and Hsph1, displayed as TPM values, across the three conditions.

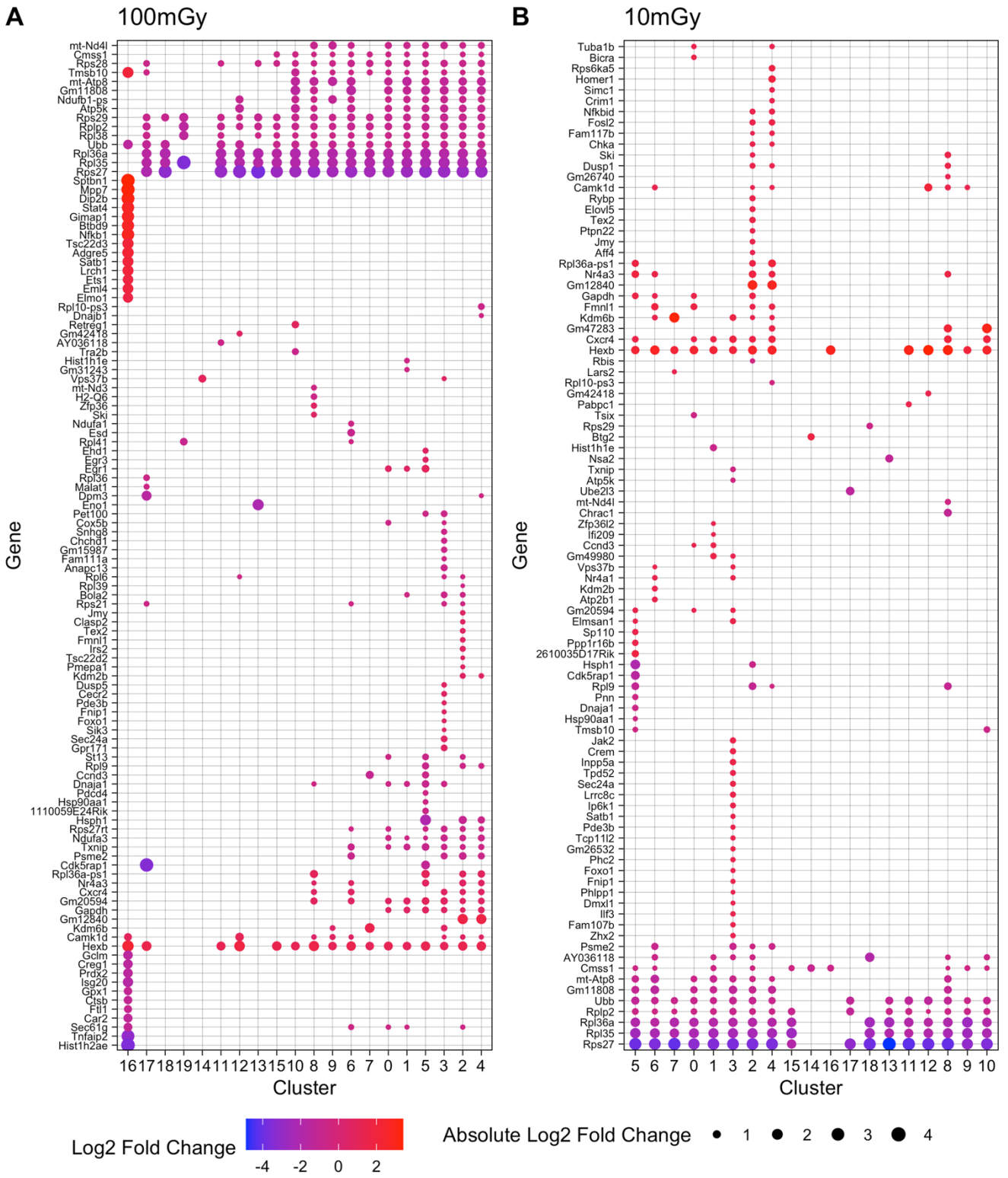

Figure S9. Differentially expressed genes in splenocytes following low-dose radiation exposure. Dot plots display DEGs for each single cell cluster, comparing irradiated samples to untreated controls. **(A)** 100 mGy and **(B)** 10 mGy dose treatments. Only genes with an adjusted p-value < 0.05 and an average absolute log2 fold change > 0.5 are shown. Genes included were expressed in at least 30% of cells within each cluster. Dot color represents log2 fold change, with red indicating upregulation and blue indicating downregulation, while dot size corresponds to the absolute log2 fold change.

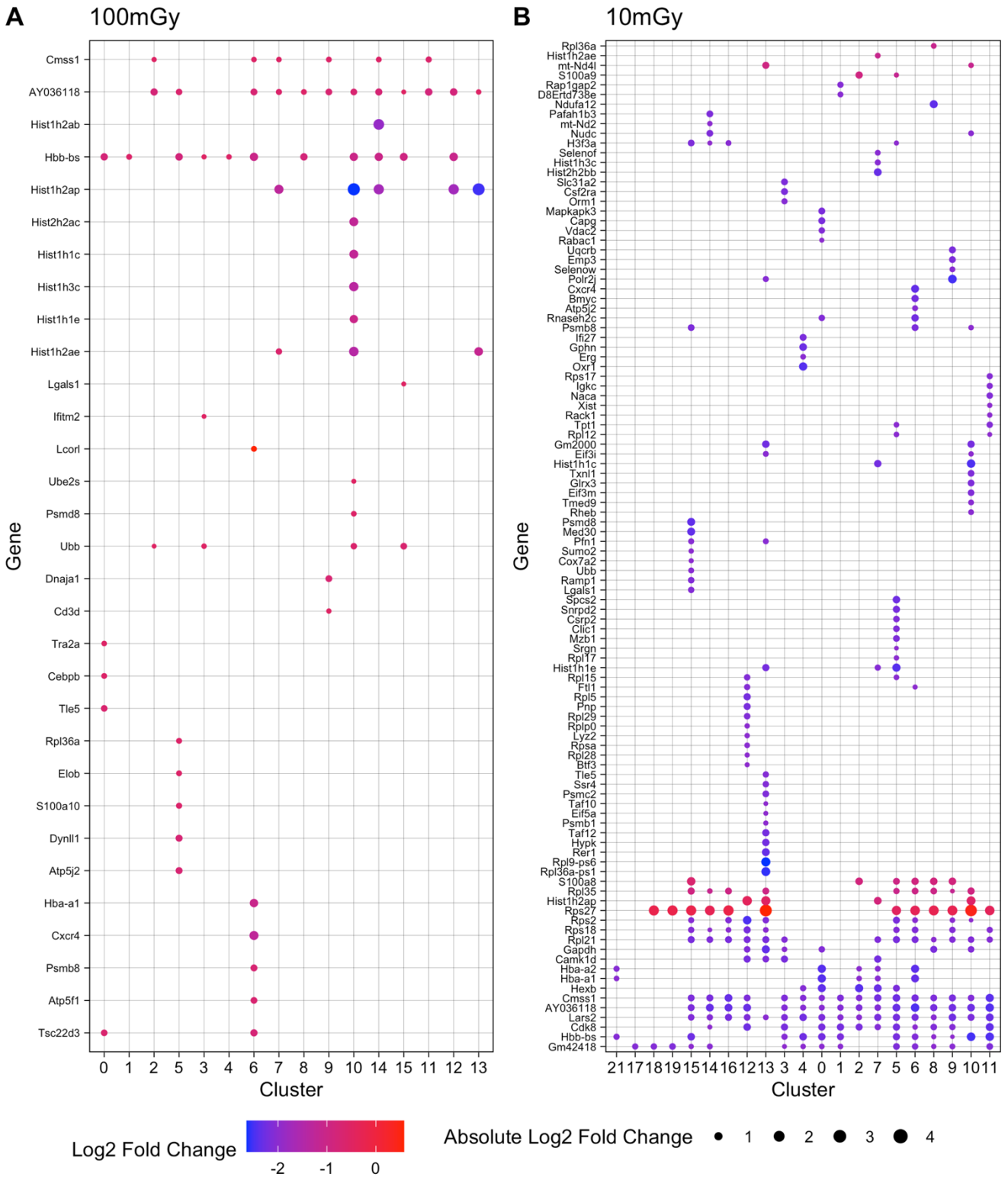

Figure S10. Differentially expressed genes in bone marrow following low-dose radiation exposure. Dot plots display DEGs for each single cell cluster, comparing irradiated samples to untreated controls. **(A)** 100 mGy and **(B)** 10 mGy dose treatments. Only genes with an adjusted p-value < 0.05 and an average absolute log2 fold change > 0.5 are shown. Genes included were expressed in at least 30% of cells within each cluster. Dot color represents log2 fold change, with red indicating upregulation and blue indicating downregulation, while dot size corresponds to the absolute log2 fold change.

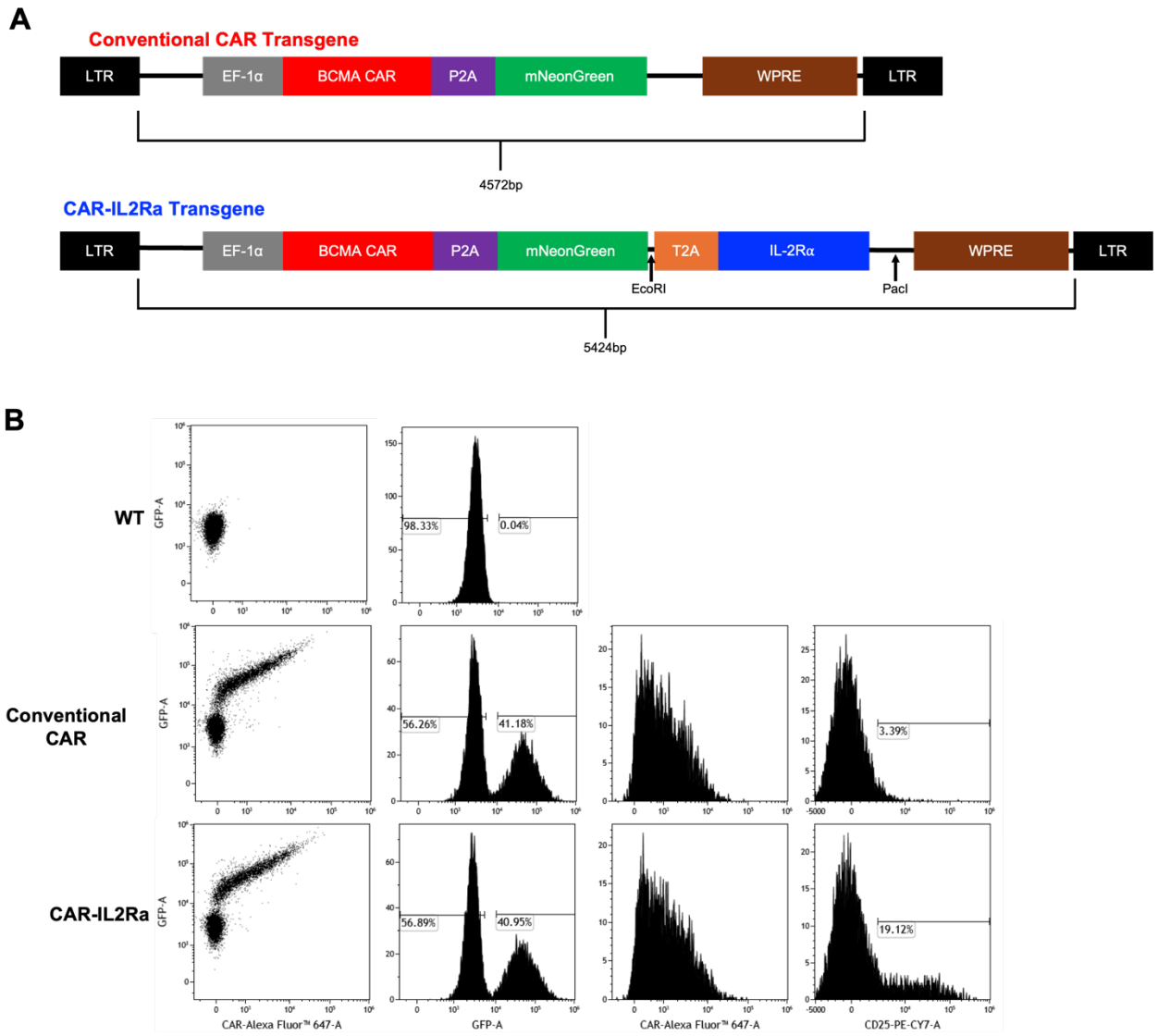

Figure S11. CAR-IL2Rα Transduction. (A) Schematic representation of the two CAR constructs used in this study. The CAR-IL2Rα construct (bottom) was cloned from a conventional BCMA CAR construct (top). Both constructs are driven by an EF-1α promoter, with the CAR-IL2Rα construct including additional T2A and IL-2Ra elements for co-expression. Colony PCR and Restriction enzyme digest (EcoRI and PacI) were used to confirm successful cloning. (B) Transduction efficiency of NK92 cells with each vector. Lentivirus was produced for each construct and used to transduce NK92 cells, with GFP (mNeonGreen) and surface CAR expression confirming successful transduction. Wild-type (WT) NK92 cells are shown as a control for comparison.

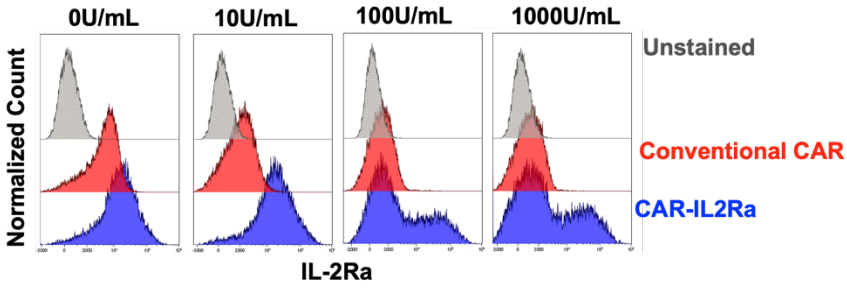

Figure S12. CAR-IL2Rα Cells Have Increased L2Rα Expression. IL2Rα overexpression was validated across various overnight cultures in various concentrations of IL-2 . IL2Rα MFI was inversely related to the IL-2 concentration in culture.

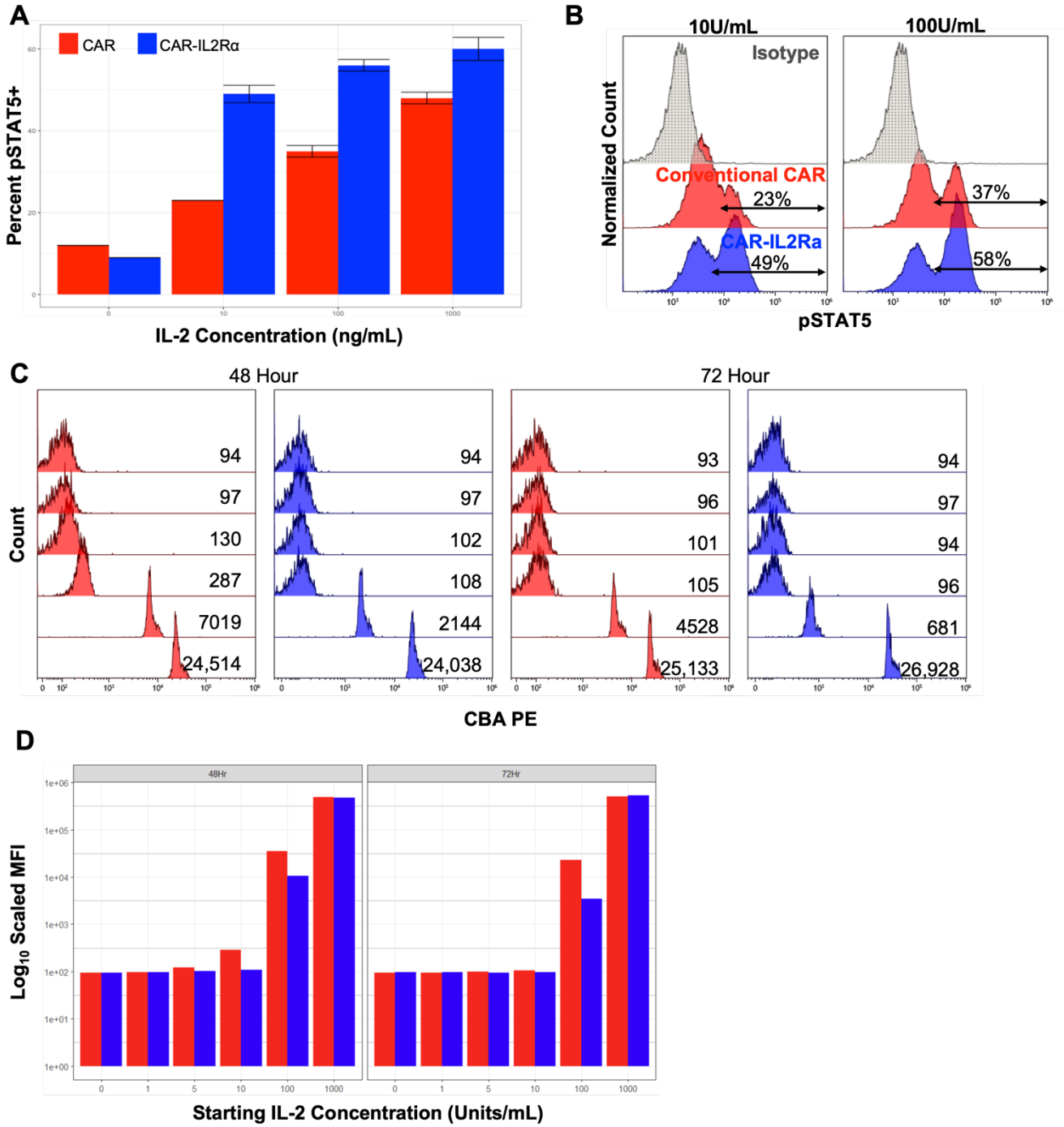

Figure S13. IL-2Rα Overexpression Mediates Increased IL-2 Signaling and Consumption. **(A)** IL-2 signaling was measured by pSTAT5 staining after overnight incubation in various concentrations of IL-2. **(B)** Percent pSTAT5+ cells was gated as shown. **(C)** After 48/72-hour culture in various IL-2 conditions, a cytokine bead assay was used to measure IL-2 available in the media. PE MFI of the IL-2 binding beads is plotted on a log10 scale against the initial IL-2 culture concentration. **(D)** The difference in the IL-2 remaining in culture between CAR-IL2Rα NK and conventional CAR NK is plotted. MFI is scaled using log transformation.

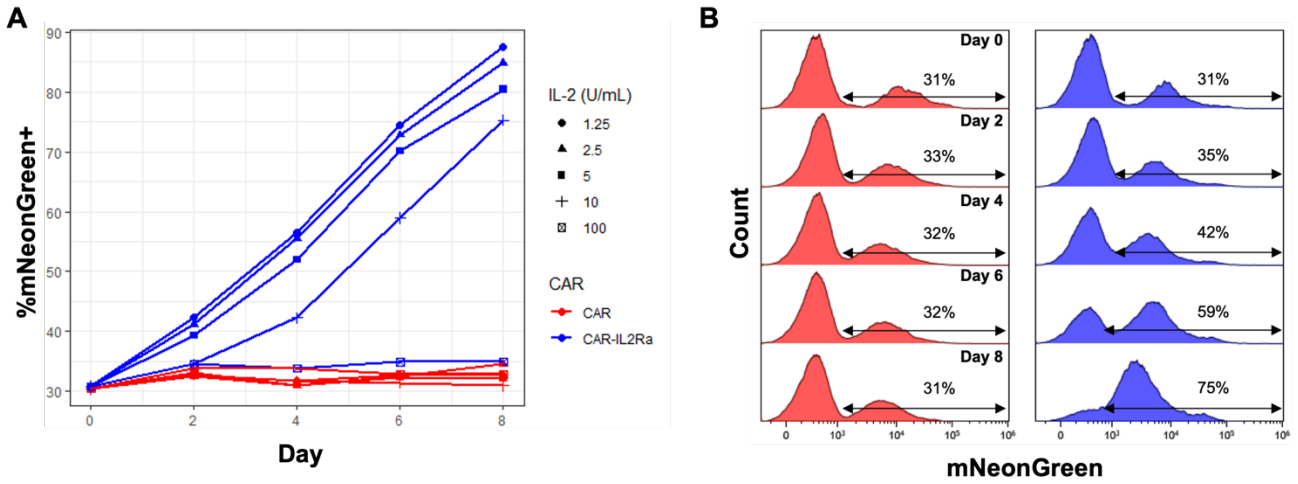

Figure S14. CAR-IL2Rα NK92 Are Enriched in Low IL-2 Co-culture with Wild-type cells. **(A)** CAR NK92 cells were added to untransduced wild-type NK92 in a 3:7 ratio respectively. Media was changed every other day to maintain IL-2 concentration. The proportion of CAR-IL2Rα NK92 became enriched when cultured in 10U/mL IL-2 or under. **(B)** Proportion of CAR NK92 cells in culture was measured overtime using their mNeonGreen reporter. Flow data histograms represent data from 10U/mL IL-2 culture. Red histograms represent cells expressing a conventional CAR, while blue histograms represent cells expressing CAR-IL2Rα. Labelled is the proportion of cells expressing the CAR construct as measured by mNeonGreen expression.

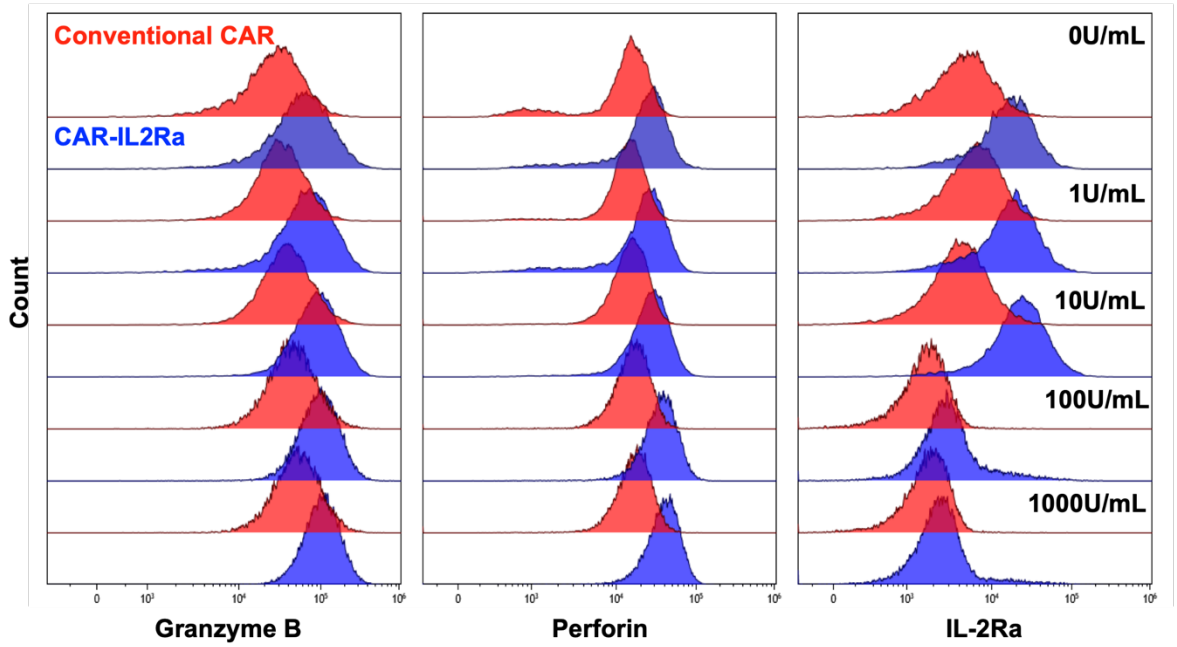

Figure S15. Perforin and Granzyme B expression analysis in CAR-NK. CAR NK92 cells were cultured in varying concentrations of IL-2 (0, 1, 10, 100, 1000 U/mL) and analyzed by flow cytometry. Red histograms represent cells expressing a conventional CAR, while blue histograms represent cells expressing CAR-IL2Rα. GzmB, PFM, and IL2Rα expression levels across IL-2 concentrations. Each row corresponds to a different IL-2 concentration, labeled on the right of Panel C.

Pathway	Test	Gene	Clusters
HALLMARK_TNFα_SIGNALLING_VIA_NFKB	UTv100 mGy	Dusp5	3
HALLMARK_TNFα_SIGNALLING_VIA_NFKB	UTv100 mGy	Egr1	1,0,5
HALLMARK_TNFα_SIGNALLING_VIA_NFKB	UTv100 mGy	Egr3	5
HALLMARK_TNFα_SIGNALLING_VIA_NFKB	UTv100 mGy	Ehd1	5
HALLMARK_TNFα_SIGNALLING_VIA_NFKB	UTv100 mGy	Irs2	2
HALLMARK_TNFα_SIGNALLING_VIA_NFKB	UTv100 mGy	Kdm6b	7,9,3
HALLMARK_TNFα_SIGNALLING_VIA_NFKB	UTv100 mGy	Nfkb1	16
HALLMARK_TNFα_SIGNALLING_VIA_NFKB	UTv100 mGy	Nr4a3	4,6,2,8,5
HALLMARK_TNFα_SIGNALLING_VIA_NFKB	UTv100 mGy	Pmepa1	2
HALLMARK_TNFα_SIGNALLING_VIA_NFKB	UTv100 mGy	Zfp36	8
HALLMARK_TNFα_SIGNALLING_VIA_NFKB	UTv10 mGy	Atp2b1	6
HALLMARK_TNFα_SIGNALLING_VIA_NFKB	UTv10 mGy	Btg2	14
HALLMARK_TNFα_SIGNALLING_VIA_NFKB	UTv10 mGy	Dusp1	4,2,8
HALLMARK_TNFα_SIGNALLING_VIA_NFKB	UTv10 mGy	Fosl2	4,2
HALLMARK_TNFα_SIGNALLING_VIA_NFKB	UTv10 mGy	Kdm6b	4,7,3,6,2
HALLMARK_TNFα_SIGNALLING_VIA_NFKB	UTv10 mGy	Nr4a1	3,6
HALLMARK_TNFα_SIGNALLING_VIA_NFKB	UTv10 mGy	Nr4a3	4,6,2,8,5
HALLMARK_UV_RESPONSE_DN	UTv100 mGy	Nfkb1	16
HALLMARK_UV_RESPONSE_DN	UTv10 mGy	Atp2b1	6
HALLMARK_UV_RESPONSE_DN	UTv10 mGy	Dusp1	4,2,8
HALLMARK_OXIDATIVE_PHOSPHORYLATION	UTv100 mGy	Atp5k	4,1,12,3,6,2,0,8,5,10
HALLMARK_OXIDATIVE_PHOSPHORYLATION	UTv100 mGy	Cox5b	3,0
HALLMARK_OXIDATIVE_PHOSPHORYLATION	UTv100 mGy	Ndufa1	6
HALLMARK_OXIDATIVE_PHOSPHORYLATION	UTv100 mGy	Ndufa3	4,1,3,2,0,5
HALLMARK_OXIDATIVE_PHOSPHORYLATION	UTv10 mGy	Atp5k	3
GOBP_CYTOPLASMIC_TRANSLATION	UTv100 mGy	Rpl36	17
GOBP_CYTOPLASMIC_TRANSLATION	UTv100 mGy	Rpl36a	4,1,7,9,12,3,6,2,0,8,5,13,17,15,11,10,18
GOBP_CYTOPLASMIC_TRANSLATION	UTv100 mGy	Rpl38	19,4,1,7,9,3,6,2,0,8,5,13,17,15,11,10
GOBP_CYTOPLASMIC_TRANSLATION	UTv100 mGy	Rpl39	2
GOBP_CYTOPLASMIC_TRANSLATION	UTv100 mGy	Rpl41	19,6
GOBP_CYTOPLASMIC_TRANSLATION	UTv100 mGy	Rpl6	12,3,2
GOBP_CYTOPLASMIC_TRANSLATION	UTv100 mGy	Rpl9	4,2,5
GOBP_CYTOPLASMIC_TRANSLATION	UTv100 mGy	Rplp2	19,4,1,7,9,12,3,6,2,0,8,5,13,17,15,11,10
GOBP_CYTOPLASMIC_TRANSLATION	UTv100 mGy	Rps21	3,6,2,17
GOBP_CYTOPLASMIC_TRANSLATION	UTv100 mGy	Rps28	4,1,7,9,3,6,2,0,8,5,13,17,15,11,10
GOBP_CYTOPLASMIC_TRANSLATION	UTv100 mGy	Rps29	19,4,1,7,9,12,3,6,2,0,8,5,13,17,15,11,10,18
GOBP_CYTOPLASMIC_TRANSLATION	UTv10 mGy	Rpl36a	4,1,7,9,12,3,6,2,0,8,5,13,15,11,10,18
GOBP_CYTOPLASMIC_TRANSLATION	UTv10 mGy	Rpl9	4,2,8,5
GOBP_CYTOPLASMIC_TRANSLATION	UTv10 mGy	Rplp2	4,1,7,9,12,3,6,2,0,8,5,13,17,15,11,10
GOBP_CYTOPLASMIC_TRANSLATION	UTv10 mGy	Rps29	18

Table S1. Significant Differentially Expressed Genes Involved In GSEA Terms. For selected pathways from the spleen dataset GSEA , genes which contributed to the enrichment (either down or up) are listed. Genes were selected which were differentially expressed when comparing either UT and 10 or 100 mGy, with an adjusted p-value under 0.05 and an absolute log2 fold change greater than 0.5.

12 References

1. Canadian Nuclear Safety Commission. Nuclear power plants. https://www.cnsc-ccsn.gc.ca/eng/reactors/power-plants/ (2024).
2. Serway, R. & Jewett, J. *Physics For Scientists and Engineers with Modern Physics*. (Books/Cole, Boston, 2015).
3. International Atomic Energy Agency. *Radiation Biology: A Handbook for Teachers and Students*. (International Atomic Energy Agency, Vienna, 2010).
4. Baatout, S. *Radiobiology Textbook*. *Radiobiology Textbook* (Springer International Publishing, 2023). doi:10.1007/978-3-031-18810-7.
5. Reisz, J. A., Bansal, N., Qian, J., Zhao, W. & Furdui, C. M. Effects of ionizing radiation on biological molecules - mechanisms of damage and emerging methods of detection. *Antioxidants and Redox Signaling* vol. 21 260–292 Preprint at https://doi.org/10.1089/ars.2013.5489 (2014).
6. Huang, R. X. & Zhou, P. K. DNA damage response signaling pathways and targets for radiotherapy sensitization in cancer. *Signal Transduction and Targeted Therapy* vol. 5 Preprint at https://doi.org/10.1038/s41392-020-0150-x (2020).
7. Ray Chaudhuri, A. & Nussenzweig, A. The multifaceted roles of PARP1 in DNA repair and chromatin remodelling. *Nature Reviews Molecular Cell Biology* vol. 18 610–621 Preprint at https://doi.org/10.1038/nrm.2017.53 (2017).
8. Blackford, A. N. & Jackson, S. P. ATM, ATR, and DNA-PK: The Trinity at the Heart of the DNA Damage Response. *Molecular Cell* vol. 66 801–817 Preprint at https://doi.org/10.1016/j.molcel.2017.05.015 (2017).
9. Li, Q. *et al.* A new wave of innovations within the DNA damage response. *Signal Transduction and Targeted Therapy* vol. 8 Preprint at https://doi.org/10.1038/s41392-023-01548-8 (2023).
10. Santivasi, W. L. & Xia, F. Ionizing radiation-induced DNA damage, response, and repair. *Antioxidants and Redox Signaling* vol. 21 251–259 Preprint at https://doi.org/10.1089/ars.2013.5668 (2014).

11. Brandsma, I. & Van Gent, D. C. *Pathway Choice in DNA Double Strand Break Repair: Observations of a Balancing Act*. http://www.genomeintegrity.com/content/3/1/9 (2012).

12. Zhao, F., Kim, W., Kloeber, J. A. & Lou, Z. DNA end resection and its role in DNA replication and DSB repair choice in mammalian cells. *Experimental and Molecular Medicine* vol. 52 1705–1714 Preprint at https://doi.org/10.1038/s12276-020-00519-1 (2020).

13. Kolesnick, R. & Fuks, Z. Radiation and ceramide-induced apoptosis. *Oncogene* vol. 22 5897–5906 Preprint at https://doi.org/10.1038/sj.onc.1206702 (2003).

14. Aureli, M. *et al.* Exploring the link between ceramide and ionizing radiation. *Glycoconj J* **31**, 449–459 (2014).

15. Chen, Z. *et al.* Cellular senescence in ionizing radiation (Review). *Oncology Reports* vol. 42 883–894 Preprint at https://doi.org/10.3892/or.2019.7209 (2019).

16. Li, M., You, L., Xue, J. & Lu, Y. Ionizing radiation-induced cellular senescence in normal, non-transformed cells and the involved DNA damage response: A mini review. *Frontiers in Pharmacology* vol. 9 Preprint at https://doi.org/10.3389/fphar.2018.00522 (2018).

17. Sinclair, W. K. Cyclic x-ray responses in mammalian cells in vitro. *Radiat Res* **33**, 620–643 (1968).

18. Syljuåsen, R. G. Cell Cycle Effects in Radiation Oncology. *Radiation Oncology* 1–8 (2019) doi:10.1007/978-3-319-52619-5_101-1.

19. Hall, E. & Giaccia, A. *Radiobiology for the Radiologist*. (Wolters Kluwer, Philadelphia, 2019).

20. Pawlik, T. M. & Keyomarsi, K. Role of cell cycle in mediating sensitivity to radiotherapy. *Int J Radiat Oncol Biol Phys* **59**, 928–942 (2004).

21. Vogin, G. & Foray, N. The law of Bergonié and Tribondeau: A nice formula for a first approximation. *Int J Radiat Biol* **89**, 2–8 (2013).

22. Fabbrizi, M. R., Warshowsky, K. E., Zobel, C. L., Hallahan, D. E. & Sharma, G. G. Molecular and epigenetic regulatory mechanisms of normal stem cell radiosensitivity. *Cell Death Discovery* vol. 4 Preprint at https://doi.org/10.1038/s41420-018-0132-8 (2018).

23. Heylmann, D., Badura, J., Becker, H., Fahrer, J. & Kaina, B. Sensitivity of CD3/CD28-stimulated versus non-stimulated lymphocytes to ionizing radiation and genotoxic anticancer drugs: key role of ATM in the differential radiation response. *Cell Death Dis* **9**, (2018).

24. Resnick-Silverman, L. *et al.* In vivo RNA-seq and ChIP-seq analyses show an obligatory role for the C terminus of p53 in conferring tissue-specific radiation sensitivity. *Cell Rep* **42**, (2023).

25. Chistiakov, D. A., Voronova, N. V. & Chistiakov, P. A. Genetic variations in DNA repair genes, radiosensitivity to cancer and susceptibility to acute tissue reactions in radiotherapy-treated cancer patients. *Acta Oncol (Madr)* **47**, 809–824 (2008).

26. Otsuka, K., Koana, T., Tauchi, H. & Sakai, K. *Activation of Antioxidative Enzymes Induced by Low-Dose-Rate Whole-Body γ Irradiation: Adaptive Response in Terms of Initial DNA Damage*. *Source: Radiation Research* vol. 166 (2006).

27. Nagasawa, H. & Little, J. B. Induction of sister chromatid exchanges by extremely low doses of α-particles. *Cancer research (Chicago, Ill.)* **52**, 6394–6396 (1992).

28. Zhang, Z., Li, K. & Hong, M. Radiation-Induced Bystander Effect and Cytoplasmic Irradiation Studies with Microbeams. *Biology* vol. 11 Preprint at https://doi.org/10.3390/biology11070945 (2022).

29. Liu, Z. *et al. A Dose Threshold for a Medium Transfer Bystander Effect for a Human Skin Cell Line*. *Research* vol. 166 https://about.jstor.org/terms (2006).

30. Gh, H. *The Mechanisms of Radiation-Induced Bystander Effect*. *J Biomed Phys Eng* vol. 4 www.jbpe.org (2014).

31. Mothersill, C. & Seymour, C. Low dose radiation mechanisms: The certainty of uncertainty. *Mutat Res Genet Toxicol Environ Mutagen* **876–877**, (2022).

32. Atsdr. *TOXICOLOGICAL PROFILE FOR IONIZING RADIATION*. (1999).

33. History of the Canadian Nuclear Safety Commission. https://www.cnsc-ccsn.gc.ca/eng/about-us/history/.

34. Macià i Garau, M., Lucas Calduch, A. & López, E. C. Radiobiology of the acute radiation syndrome. *Reports of Practical Oncology and Radiotherapy* vol. 16 123–130 Preprint at https://doi.org/10.1016/j.rpor.2011.06.001 (2011).

35. Kamiya, K. *et al. From Hiroshima and Nagasaki to Fukushima 1 Long-Term Eff Ects of Radiation Exposure on Health*. *www.thelancet.com* vol. 386 www.thelancet.com (2015).

36. Douple, E. B. *et al.* Long-term radiation-related health effects in a unique human population: Lessons learned from the atomic bomb survivors of Hiroshima and nagasaki. *Disaster Medicine and Public Health Preparedness* vol. 5 Preprint at https://doi.org/10.1001/dmp.2011.21 (2011).

37. Richardson, D. *et al.* Ionizing radiation and leukemia mortality among Japanese atomic bomb survivors, 19502000. *Radiat Res* **172**, 368–382 (2009).

38. Ozasa, K. *et al.* Studies of the mortality of atomic bomb survivors, report 14, 1950-2003: An overview of cancer and noncancer diseases. *Radiation Research* vol. 177 229–243 Preprint at https://doi.org/10.1667/RR2629.1 (2012).

39. Jeggo, P. The Role of the DNA Damage Response Mechanisms after Low-Dose Radiation Exposure and a Consideration of Potentially Sensitive Individuals. *Radiat Res* **174**, 825–832 (2010).

40. National Academies of Sciences, E. and M. *Leveraging Advances in Modern Science to Revitalize Low-Dose Radiation Research in the United States*. *Leveraging Advances in Modern Science to Revitalize Low-Dose Radiation Research in the United States* (National Academies Press, Washington DC, 2022). doi:10.17226/26434.

41. Natural background radiation. https://www.cnsc-ccsn.gc.ca/eng/resources/fact-sheets/natural-background-radiation/.

42. Canadian Nuclear Safety Commission. Radiation doses. https://www.cnsc-ccsn.gc.ca/eng/resources/radiation/radiation-doses/.

43. World Nuclear Association. Radiation Pocket Guide. Preprint at (2015).

44. Boice, J. D. *et al.* Mortality from leukemia, cancer and heart disease among U.S. nuclear power plant workers, 1957–2011. *Int J Radiat Biol* **98**, 657–678 (2022).

45. Nuclear Safety Commission. *Radiation Protection Regulations*. (Canada, 2000).

46. National Research Council. *Health Risks from Exposure to Low Levels of Ionizing Radiation: BEIR VII Phase 2*. (2006).

47. International Commission on Radiological Protection (ICRP). *The 2007 Recommendations of the International Commission on Radiological Protection*. (2007).

48. Asaithamby, A. & Chen, D. J. Cellular responses to DNA double-strand breaks after low-dose γ-irradiation. *Nucleic Acids Res* **37**, 3912–3923 (2009).

49. Rothkamm, K. & Lö, M. *Evidence for a Lack of DNA Double-Strand Break Repair in Human Cells Exposed to Very Low x-Ray Doses*. www.pnas.orgcgidoi10.1073pnas.0830918100 (2003).

50. Halm, B. M. *et al.* γ-H2AX foci are increased in lymphocytes in vivo in young children 1 h after very low-dose X-irradiation: a pilot study. *Pediatric Radiology 2014 44:10* **44**, 1310–1317 (2014).

51. Golfier, S. *et al.* Dicentric chromosomes and γ-H2AX foci formation in lymphocytes of human blood samples exposed to a CT scanner: a direct comparison of dose response relationships. *Radiat Prot Dosimetry* **134**, 55–61 (2009).

52. Schanz, S. *et al.* Accumulation of DNA damage in complex normal tissues after protracted low-dose radiation. *DNA Repair (Amst)* **11**, 823–832 (2012).

53. Rothkamm, K. & Lö, M. *Evidence for a Lack of DNA Double-Strand Break Repair in Human Cells Exposed to Very Low x-Ray Doses*. www.pnas.orgcgidoi10.1073pnas.0830918100 (2003).

54. Grudzenski, S., Raths, A., Conrad, S., Rübe, C. E. & Löbrich, M. Inducible response required for repair of low-dose radiation damage in human fibroblasts. *Proc Natl Acad Sci U S A* **107**, 14205–14210 (2010).

55. Belov, O. *et al.* Dose-Dependent Shift in Relative Contribution of Homologous Recombination to DNA Repair after Low-LET Ionizing Radiation Exposure: Empirical Evidence and Numerical Simulation. *Curr Issues Mol Biol* **45**, 7352–7373 (2023).

56. Mladenov, E., Mladenova, V., Stuschke, M. & Iliakis, G. New Facets of DNA Double Strand Break Repair: Radiation Dose as Key Determinant of HR versus c-NHEJ Engagement. *International Journal of Molecular Sciences* vol. 24 Preprint at https://doi.org/10.3390/ijms241914956 (2023).

57. Mladenov, E. *et al.* Strong suppression of gene conversion with increasing DNA double-strand break load delimited by 53BP1 and RAD52. *Nucleic Acids Res* **48**, 1905–1924 (2020).

58. Soni, A., Murmann-Konda, T., Siemann-Loekes, M., Pantelias, G. E. & Iliakis, G. Chromosome breaks generated by low doses of ionizing radiation in G2-phase are processed exclusively by gene conversion. *DNA Repair (Amst)* **89**, (2020).

59. Maccallum, D. E., Hall, P. A. & Wright, E. G. *The Trp53 Pathway Is Induced In Vivo by Low Doses of Gamma Radiation*. *Source: Radiation Research* vol. 156 https://about.jstor.org/terms (2001).

60. Shimura, T., Nakashiro, C., Narao, M. & Ushiyama, A. Induction of oxidative stress biomarkers following whole-body irradiation in mice. *PLoS One* **15**, (2020).

61. Sampadi, B. *et al.* Divergent Molecular and Cellular Responses to Low and High-Dose Ionizing Radiation. *Cells* **11**, (2022).

62. Khan, M. G. M. & Wang, Y. Advances in the Current Understanding of How Low-Dose Radiation Affects the Cell Cycle. *Cells* vol. 11 Preprint at https://doi.org/10.3390/cells11030356 (2022).

63. Yunis, R., Albrecht, H., Kalanetra, K. M., Wu, S. & Rocke, D. M. Genomic characterization of a three-dimensional skin model following exposure to ionizing radiation. *J Radiat Res* **53**, 860–875 (2012).

64. Wang, Y. *et al.* A comparative study on the dose–effect of low-dose radiation based on microdosimetric analysis and single-cell sequencing technology. *Sci Rep* **14**, (2024).

65. Soon Kim, C. *et al. Low-Dose Radiation Stimulates the Proliferation of Normal Human Lung Fibroblasts Via a Transient Activation of Raf and Akt*. *Mol. Cells* vol. 24.

66. Mothersill, C., Seymour, C., Cocchetto, A. & Williams, D. Factors Influencing Effects of Low-dose Radiation Exposure. *Health-Physics* **126**, (2024).

67. Shin, E. *et al.* Organ-Specific Effects of Low Dose Radiation Exposure: A Comprehensive Review. *Frontiers in Genetics* vol. 11 Preprint at https://doi.org/10.3389/fgene.2020.566244 (2020).

68. Cullings, H. M. *et al. Dose Estimation for Atomic Bomb Survivor Studies: Its Evolution and Present Status*. *Research* vol. 166 https://about.jstor.org/terms (2006).

69. Richardson, D. B. *et al.* Cancer mortality after low dose exposure to ionising radiation in workers in France, the United Kingdom, and the United States (INWORKS): Cohort study. *BMJ* (2023) doi:10.1136/bmj-2022-074520.

70. Richardson, D. B. *et al.* Risk of cancer from occupational exposure to ionising radiation: Retrospective cohort study of workers in France, the United Kingdom, and the United States (INWORKS). *The BMJ* **351**, (2015).

71. Leuraud, K. *et al.* Ionising radiation and risk of death from leukaemia and lymphoma in radiation-monitored workers (INWORKS): An international cohort study. *Lancet Haematol* **2**, e276–e281 (2015).

72. Rühm, W., Laurier, D. & Wakeford, R. Cancer risk following low doses of ionising radiation – Current epidemiological evidence and implications for radiological protection. *Mutat Res Genet Toxicol Environ Mutagen* **873**, (2022).

73. Gillies, M. *et al.* Mortality from circulatory diseases and other non-cancer outcomes among nuclear workers in France, the United Kingdom and the United States (inworks). *Radiat Res* **188**, 276–290 (2017).

74. Zhang, W., Haylock, R. G. E., Gillies, M. & Hunter, N. Mortality from heart diseases following occupational radiation exposure: Analysis of the National Registry for Radiation Workers (NRRW) in the United Kingdom. *Journal of Radiological Protection* **39**, 327–353 (2019).

75. Luarent, O. *et al.* Updated Mortality Analysis of SELTINE, the French Cohort of Nuclear Workers, 1968–2014. *Cancers (Basel)* **15**, (2022).

76. Abalo, K. D. *et al.* Early life ionizing radiation exposure and cancer risks: systematic review and meta-analysis. doi:10.1007/s00247-020-04803-0/Published.

77. Meulepas, J. M. *et al.* Radiation exposure from pediatric CT scans and subsequent cancer risk in the Netherlands. *J Natl Cancer Inst* **111**, 256–263 (2019).

78. Hauptmann, M. *et al.* Epidemiological studies of low-dose ionizing radiation and cancer: Summary bias assessment and meta-analysis. *J Natl Cancer Inst Monogr* **2020**, 188–200 (2020).

79. Shore, R. E. *et al.* Implications of recent epidemiologic studies for the linear nonthreshold model and radiation protection. *Journal of Radiological Protection* vol. 38 1217–1233 Preprint at https://doi.org/10.1088/1361-6498/aad348 (2018).

80. Protecting workers. https://www.cnsc-ccsn.gc.ca/eng/resources/radiation/protecting-workers/.

81. Boice, J. D., Cohen, S. S., Mumma, M. T. & Ellis, E. D. The Million Person Study, whence it came and why. *International Journal of Radiation Biology* vol. 98 537–550 Preprint at https://doi.org/10.1080/09553002.2019.1589015 (2022).

82. Boice, J. D. *et al.* Mortality among medical radiation workers in the United States, 1965–2016. *Int J Radiat Biol* **99**, 183–207 (2023).

83. Doss, M. Comment on 'Implications of recent epidemiologic studies for the linear nonthreshold model and radiation protection'. *Journal of Radiological Protection* vol. 39 650–654 Preprint at https://doi.org/10.1088/1361-6498/ab076a (2019).

84. Vaiserman, A., Koliada, A., Zabuga, O. & Socol, Y. Health Impacts of Low-Dose Ionizing Radiation: Current Scientific Debates and Regulatory Issues. *Dose-Response* vol. 16 Preprint at https://doi.org/10.1177/1559325818796331 (2018).

85. Scott, B. R. Radiation-hormesis phenotypes, the related mechanisms and implications for disease prevention and therapy. *J Cell Commun Signal* **8**, 341–352 (2014).

86. Janiak, M. K. & Waligórski, M. P. R. Can Low-Level Ionizing Radiation Do Us Any Harm? *Dose-Response* vol. 21 Preprint at https://doi.org/10.1177/15593258221148013 (2023).

87. Shibamoto, Y. & Nakamura, H. Overview of biological, epidemiological, and clinical evidence of radiation hormesis. *International Journal of Molecular Sciences* vol. 19 Preprint at https://doi.org/10.3390/ijms19082387 (2018).

88. Dawood, A., Mothersill, C. & Seymour, C. Low dose ionizing radiation and the immune response: what is the role of non-targeted effects? *International Journal of Radiation Biology* vol. 97 1368–1382 Preprint at https://doi.org/10.1080/09553002.2021.1962572 (2021).

89. Dawood, A. Immune System Modulation by Low Dose Ionizing Radiation. (McMaster University, Hamilton, ON, 2021).

90. Acute Death Due to Radiation – Radiation Effects Research Foundation (RERF). https://www.rerf.or.jp/en/programs/roadmap_e/health_effects-en/early-en/death_en/.

91. Wu, Y. Q. *et al.* Single-Cell Transcriptomics Reveals Early Effects of Ionizing Radiation on Bone Marrow Mononuclear Cells in Mice. *Int J Mol Sci* **25**, 9287 (2024).

92. Ghandhi, S. A. *et al.* Longitudinal multi-omic changes in the transcriptome and proteome of peripheral blood cells after a 4 Gy total body radiation dose to Rhesus macaques. *BMC Genomics* **24**, (2023).

93. Paganetti, H. A review on lymphocyte radiosensitivity and its impact on radiotherapy. *Front Oncol* **13**, (2023).

94. Rathmell, J. C. & Thompson, C. B. *Review Pathways of Apoptosis in Lymphocyte Development, Homeostasis, and Disease*. *Cell* vol. 109 (2002).

95. Durum, S. K. & Gengozian, N. The comparative radiosensitivity of t and b lymphocytes. *Int J Radiat Biol* **34**, 1–15 (1978).

96. Moreno-Villanueva, M. *et al.* Single-cell RNA-sequencing identifies activation of TP53 and STAT1 pathways in human T lymphocyte subpopulations in response to ex vivo radiation exposure. *Int J Mol Sci* **20**, (2019).

97. Zhang, Z. *et al.* scRNA-seq transcriptomic profiling of irradiated mouse skin reveals altered cell types, pathways, and cell-cell interactions. *Radiat Med Prot* **5**, 185–193 (2024).

98. Rosen, E. M., Fan, S., Rockwell, S. & Goldberg, D. *The Molecular and Cellular Basis of Radiosensitivity: Implications for Understanding How Normal Tissues and Tumors Respond to Therapeutic Radiation*. *Cancer Investigation* vol. 17 (1999).

99. Liu, Y. G. *et al.* NLRP3 inflammasome activation mediates radiation-induced pyroptosis in bone marrow-derived macrophages. *Cell Death & Disease 2017 8:2* **8**, e2579–e2579 (2017).

100. Najafi, M. *et al.* Mechanisms of inflammatory responses to radiation and normal tissues toxicity: clinical implications. *International Journal of Radiation Biology* vol. 94 335–356 Preprint at https://doi.org/10.1080/09553002.2018.1440092 (2018).

101. Zhu, M. *et al.* Immunogenic Cell Death Induction by Ionizing Radiation. *Frontiers in Immunology* vol. 12 Preprint at https://doi.org/10.3389/fimmu.2021.705361 (2021).

102. Ma, L. *et al.* A Study on the Radiosensitivity of Radiation-Induced Lung Injury at the Acute Phase Based on Single-Cell Transcriptomics. *Front Immunol* **13**, (2022).

103. Lu, H. *et al.* Single-cell map of dynamic cellular microenvironment of radiation-induced intestinal injury. *Commun Biol* **6**, (2023).

104. Lorimore, S. A., Coates, P. J., Scobie, G. E., Milne, G. & Wright, E. G. *In¯ammatory-Type Responses after Exposure to Ionizing Radiation in Vivo: A Mechanism for Radiation-Induced Bystander E□ects?* www.nature.com/onc.

105. Straub, J. M. *et al.* Radiation-induced fibrosis: mechanisms and implications for therapy. *Journal of Cancer Research and Clinical Oncology 2015 141:11* **141**, 1985–1994 (2015).

106. Yashavarddhan, M. H. *et al.* Development of hematopoietic syndrome mice model for localized radiation exposure. *Sci Rep* **11**, (2021).

107. Lumniczky, K. *et al.* Low dose ionizing radiation effects on the immune system. *Environ Int* **149**, (2021).

108. Frey, B. *et al.* Whole body low dose irradiation improves the course of beginning polyarthritis in human TNF-transgenic mice. *Autoimmunity* **42**, 346–348 (2009).

109. Deloch, L. *et al.* Low-dose radiotherapy ameliorates advanced arthritis in hTNF-α tg mice by particularly positively impacting on bone metabolism. *Front Immunol* **9**, (2018).

110. Nakatsukasa, H., Tsukimoto, M., Tokunaga, A. & Kojima, S. Repeated gamma irradiation attenuates collagen-induced arthritis via up-regulation of regulatory T cells but not by damaging lymphocytes directly. *Radiat Res* **174**, 313–324 (2010).

111. Seegenschmiedt, M. H., Micke, O. & Muecke, R. Radiotherapy for non-malignant disorders: State of the art and update of the evidence-based practice guidelines. *British Journal of Radiology* **88**, (2015).

112. Micke, O. *et al.* Low-Dose Radiation Therapy for Benign Painful Skeletal Disorders: The Typical Treatment for the Elderly Patient? *Int J Radiat Oncol Biol Phys* **98**, 958–963 (2017).

113. Rodríguez-Tomàs, E. *et al.* Effect of Low-Dose Radiotherapy on the Circulating Levels of Paraoxonase-1-Related Variables and Markers of Inflammation in Patients with COVID-19 Pneumonia. *Antioxidants 2022, Vol. 11, Page 1184* **11**, 1184 (2022).

114. Hess, C. B. *et al.* Low-dose whole-lung radiation for COVID-19 pneumonia: Planned day 7 interim analysis of a registered clinical trial. *Cancer* **126**, 5109–5113 (2020).

115. Sanmamed, N. *et al.* Low-dose Radiation Therapy in the Management of COVID-19 Pneumonia (LOWRAD-Cov19). Final results of a prospective phase I–II trial: LOWRAD-Cov19. Final report. *Radiotherapy and Oncology* **171**, 25–29 (2022).

116. Le Reun, E. & Foray, N. Low-Dose Radiation Therapy (LDRT) against Cancer and Inflammatory or Degenerative Diseases: Three Parallel Stories with a Common Molecular Mechanism Involving the Nucleoshuttling of the ATM Protein? *Cancers* vol. 15 Preprint at https://doi.org/10.3390/cancers15051482 (2023).

117. Li, X. H. *et al.* Effects of low-to-moderate doses of gamma radiation on mouse hematopoietic system. *Radiat Res* **190**, 612–622 (2018).

118. Puukila, S. *et al.* Transcriptomic response in the spleen after whole-body low-dose X-ray irradiation. *Radiat Res* **196**, 66–73 (2021).

119. Puukila, S. *et al.* Acute pulmonary and splenic response in an in vivo model of whole-body low-dose X-radiation exposure. *Int J Radiat Biol* **95**, 1072–1084 (2019).

120. Hayashi, T. *et al.* Long-term effects of radiation dose on inflammatory markers in atomic bomb survivors. *American Journal of Medicine* **118**, 83–86 (2005).

121. Jangiam, W. *et al.* Late Effects of Low-Dose Radiation on the Bone Marrow, Lung, and Testis Collected From the Same Exposed BALB/cJ Mice. *Dose-Response* **16**, (2018).

122. Candéias, S. M. *et al.* Low-dose radiation accelerates aging of the T-cell receptor repertoire in CBA/Ca mice. *Cellular and Molecular Life Sciences* **74**, 4339–4351 (2017).

123. Liu, X. *et al.* Effects of low dose radiation on immune cells subsets and cytokines in mice. *Toxicol Res (Camb)* **9**, 249–262 (2020).

124. Song, K. H. *et al.* Analysis of immune cell populations and cytokine profiles in murine splenocytes exposed to whole-body low-dose irradiation. *Int J Radiat Biol* **91**, 795–803 (2015).

125. Shin, S. C. *et al.* Alteration of cytokine profiles in mice exposed to chronic low-dose ionizing radiation. *Biochem Biophys Res Commun* **397**, 644–649 (2010).

126. Bogdándi, E. N. *et al.* Effects of Low-Dose Radiation on the Immune System of Mice after Total-Body Irradiation. *Source: Radiation Research* **174**, 480–489 (2010).

127. Courtade, M., Caratero, A., Jozan, S., Pipy, B. & Caratero, C. Influence of continuous, very low-dose gamma-irradiation on the mouse immune system. *Int J Radiat Biol* **77**, 587–592 (2001).

128. Guo, C. Y. *et al.* Sensitivity and dose dependency of radiation-induced injury in hematopoietic stem/progenitor cells in mice. *Sci Rep* **5**, 8055 (2015).

129. Yanai, T. *et al.* Long-term effects of continuous low dose-rate gamma-ray irradiation on mouse hematopoietic cells. *Radiat Prot Dosimetry* **200**, 1603–1607 (2024).

130. Pandey, R., Shankar, B. S., Sharma, D. & Sainis, K. B. Low dose radiation induced immunomodulation: Effect on macrophages and CD8+ T cells. *Int J Radiat Biol* **81**, 801–812 (2005).

131. Braga-Tanaka, I. *et al.* Experimental studies on the biological effects of chronic low dose-rate radiation exposure in mice: overview of the studies at the Institute for Environmental Sciences. *International Journal of Radiation Biology* vol. 94 423–433 Preprint at https://doi.org/10.1080/09553002.2018.1451048 (2018).

132. Cheda, A. *et al. Single Low Doses of X Rays Inhibit the Development of Experimental Tumor Metastases and Trigger the Activities of NK Cells in Mice*. *Research* vol. 161 https://www.jstor.org/stable/3581036?seq=1&cid=pdf- (2004).

133. Song, K. H. *et al.* Evaluation of anti-tumor effects of whole-body low-dose irradiation in metastatic mouse models. *Cancers (Basel)* **12**, (2020).

134. Cancer immunotherapy- how low-level ionizing radiation can play a key role | Enhanced Reader.

135. Mathias, D. *et al.* Low-dose irradiation affects expression of inflammatory markers in the heart of ApoE -/- Mice. *PLoS One* **10**, (2015).

136. Kusunoki, Y. *et al. Flow Cytometry Measurements of Subsets of T, B and NK Cells in Peripheral Blood Lymphocytes of Atomic Bomb Survivors*. *Source: Radiation Research* vol. 150 https://www.jstor.org/stable/3579858 (1998).

137. Yamaoka, M. *et al. Decreases in Percentages of Naïve CD4 and CD8 T Cells and Increases in Percentages of Memory CD8 T-Cell Subsets in the Peripheral Blood Lymphocyte Populations of A-Bomb*. *Source: Radiation Research* vol. 161 https://www.jstor.org/stable/3581031 (2004).

138. Kusunoki, Y., Akiyama, M., Kyoizumi, S., Bloom, E. T. & Makinodan, T. Age-related alteration in the composition of immunocompetent blood cells in atomic bomb survivors. *Int J Radiat Biol* **53**, 189–198 (1988).

139. Kusunoki, Y. *et al. T-Cell Responses to Mitogens in Atomic Bomb Survivors: A Decreased Capacity to Produce Interleukin 2 Characterizes the T Cells of Heavily Irradiated Individuals*. *Source: Radiation Research* vol. 155 https://about.jstor.org/terms (2001).

140. Kusunoki, Y. & Hayashi, T. Long-lasting alterations of the immune system by ionizing radiation exposure: Implications for disease development among atomic bomb survivors. *International Journal of Radiation Biology* vol. 84 1–14 Preprint at https://doi.org/10.1080/09553000701616106 (2008).

141. Gyuleva, I., Djounova, J. & Rupova, I. Impact of low-dose occupational exposure to ionizing radiation on T-cell populations and subpopulations and humoral factors included in the immune response. *Dose-Response* **16**, (2018).

142. Rees, G. S. *et al.* Occupational exposure to ionizing radiation has no effect on T- and B-cell total counts or percentages of helper, cytotoxic and activated T-cell subsets in the peripheral circulation of male radiation workers. *Int J Radiat Biol* **80**, 493–498 (2004).

143. Godekmerdan, A. *et al.* Diminished cellular and humoral immunity in workers occupationally exposed to low levels of ionizing radiation. *Arch Med Res* **35**, 324–328 (2004).

144. Kłuciński, P. *et al.* Assessment of selected B cells populations in the workers of X-ray departments. *Int J Occup Med Environ Health* **27**, 467–473 (2014).

145. Attar, M., Molaie Kondolousy, Y. & Khansari, N. *Effect of High Dose Natural Ionizing Radiation on the Immune System of the Exposed Residents of Ramsar Town, Iran*. *IRANIAN JOURNAL OF ALLERGY, ASTHMA AND IMMUNOLOGY. All rights reserved. Iran J Allergy Asthma Immunol* vol. 6 (2007).

146. Li, K. *et al.* Long-term immune effects of high-level natural radiation on Yangjiang inhabitants in China. *Int J Radiat Biol* **95**, 764–770 (2019).

147. Jain, V. & Das, B. Global transcriptome profile reveals abundance of DNA damage response and repair genes in individuals from high level natural radiation areas of Kerala coast. *PLoS One* **12**, (2017).

148. Wang, Y. *et al.* Low-dose radiobiology program at Canadian nuclear laboratories: past, present, and future. *Int J Radiat Biol* **95**, 1361–1371 (2019).

149. Zhang, X. *et al.* Kctd9 Deficiency Impairs Natural Killer Cell Development and Effector Function. *Front Immunol* **10**, 744 (2019).

150. Osorio, D. & Cai, J. J. Systematic determination of the mitochondrial proportion in human and mice tissues for single-cell RNA-sequencing data quality control. *Bioinformatics* **37**, 963–967 (2021).

151. Germain, P. L., Robinson, M. D., Lun, A., Garcia Meixide, C. & Macnair, W. Doublet identification in single-cell sequencing data using scDblFinder. *F1000Res* **10**, 979 (2022).

152. Hafemeister, C. & Satija, R. Normalization and variance stabilization of single-cell RNA-seq data using regularized negative binomial regression. *Genome Biol* **20**, (2019).

153. Analysis, visualization, and integration of Visium HD spatial datasets with Seurat • Seurat. https://satijalab.org/seurat/articles/cell_cycle_vignette#alternate-workflow.

154. Heng, T. S. P. *et al.* The Immunological Genome Project: networks of gene expression in immune cells. *Nature Immunology 2008 9:10* **9**, 1091–1094 (2008).

155. Delano, M. J. *et al.* Neutrophil Mobilization from the Bone Marrow during Polymicrobial Sepsis Is Dependent on CXCL12 Signaling. *The Journal of Immunology* **187**, 911–918 (2011).

156. Ueda, Y., Cain, D. W., Kuraoka, M., Kondo, M. & Kelsoe, G. IL-1R Type I-Dependent Hemopoietic Stem Cell Proliferation Is Necessary for Inflammatory Granulopoiesis and Reactive Neutrophilia. *The Journal of Immunology* **182**, 6477–6484 (2009).

157. Baschant, U. *et al.* Effects of dietary iron deficiency or overload on bone: Dietary details matter. *Bone* **184**, (2024).

158. Luo, X. *et al.* Pathway-based analyses of gene expression profiles at low doses of ionizing radiation. *Frontiers in Bioinformatics* **4**, (2024).

159. Cho, S. J., Kang, H., Hong, E. H., Kim, J. Y. & Nam, S. Y. Transcriptome analysis of low-dose ionizing radiation-impacted genes in CD4+ T-cells undergoing activation and regulation of their expression of select cytokines. *J Immunotoxicol* **15**, 137–146 (2018).

160. Fang, F. *et al.* Transcriptomic profiling reveals gene expression in human peripheral blood after exposure to low-dose ionizing radiation. *J Radiat Res* **63**, 8–18 (2022).

161. McComb, S. *et al.* Programmable Attenuation of Antigenic Sensitivity for a Nanobody-Based EGFR Chimeric Antigen Receptor Through Hinge Domain Truncation. *Front Immunol* **13**, (2022).

162. Abramson, J. S. *et al.* Lisocabtagene maraleucel as second-line therapy for large B-cell lymphoma: primary analysis of the phase 3 TRANSFORM study. *Blood* **141**, 1675–1684 (2023).

163. Wang, M. *et al.* Three-Year Follow-Up of KTE-X19 in Patients With Relapsed/Refractory Mantle Cell Lymphoma, Including High-Risk Subgroups, in the ZUMA-2 Study. *J Clin Oncol* **41**, 555–567 (2023).

164. Westin, J. R. *et al.* Survival with Axicabtagene Ciloleucel in Large B-Cell Lymphoma. *New England Journal of Medicine* **389**, 148–157 (2023).

165. Awasthi, R., Maier, H. J., Zhang, J. & Lim, S. Kymriah® (tisagenlecleucel) - An overview of the clinical development journey of the first approved CAR-T therapy. *Hum Vaccin Immunother* **19**, 2210046 (2023).

166. Mitra, A. *et al.* From bench to bedside: the history and progress of CAR T cell therapy. *Front Immunol* **14**, (2023).

167. Cappell, K. M. & Kochenderfer, J. N. Long-term outcomes following CAR T cell therapy: what we know so far. *Nat Rev Clin Oncol* **20**, 359–371 (2023).

168. Palen, K., Zurko, J., Johnson, B. D., Hari, P. & Shah, N. N. Manufacturing chimeric antigen receptor T cells from cryopreserved peripheral blood cells: time for a collect-and-freeze model? *Cytotherapy* **23**, 985–990 (2021).

169. Cohet, G. *et al.* Failure and out of Specification Manufacturing of Autologous CAR-T Cells Could be Associated with a High Concentration of Total Nucleated Cells, CD3 + Cells and Neutrophils in the Apheresis Product. *Blood* **142**, 3520–3520 (2023).

170. Topp, M. & Feuchtinger, T. Management of Hypogammaglobulinaemia and B-Cell Aplasia. *The EBMT/EHA CAR-T Cell Handbook* 147–149 (2022) doi:10.1007/978-3-030-94353-0_28.

171. Brudno, J. N. & Kochenderfer, J. N. Toxicities of chimeric antigen receptor T cells: recognition and management. *Blood* **127**, 3321–3330 (2016).

172. Hunter, B. D. & Jacobson, C. A. CAR T-Cell Associated Neurotoxicity: Mechanisms, Clinicopathologic Correlates, and Future Directions. *J Natl Cancer Inst* **111**, 646–654 (2019).

173. Caruso, S. *et al.* Safe and effective off-the-shelf immunotherapy based on CAR.CD123-NK cells for the treatment of acute myeloid leukaemia. *J Hematol Oncol* **15**, (2022).

174. Romanski, A. *et al.* CD19-CAR engineered NK-92 cells are sufficient to overcome NK cell resistance in B-cell malignancies. *J Cell Mol Med* **20**, 1287–1294 (2016).

175. Tang, X. *et al.* First-in-man clinical trial of CAR NK-92 cells: safety test of CD33-CAR NK-92 cells in patients with relapsed and refractory acute myeloid leukemia. *Am J Cancer Res* **8**, 1083–1089 (2018).

176. Marin, D. *et al.* Safety, efficacy and determinants of response of allogeneic CD19-specific CAR-NK cells in CD19+ B cell tumors: a phase 1/2 trial. *Nat Med* **30**, 772–784 (2024).

177. Leong, J. W. *et al.* Preactivation with IL-12, IL-15, and IL-18 induces cd25 and a functional high-affinity il-2 receptor on human cytokine-induced memory-like natural killer cells. *Biology of Blood and Marrow Transplantation* **20**, 463–473 (2014).

178. Gasteiger, G. *et al.* IL-2-dependent tuning of NK cell sensitivity for target cells is controlled by regulatory T cells. *Journal of Experimental Medicine* **210**, 1065–1068 (2013).

179. Lee, S.-H., Fragoso, M. F. & Biron, C. A. Cutting Edge: A Novel Mechanism Bridging Innate and Adaptive Immunity: IL-12 Induction of CD25 To Form High-Affinity IL-2 Receptors on NK Cells. *The Journal of Immunology* **189**, 2712–2716 (2012).

180. Stauber, D. J., Debler, E. W., Horton, P. A., Smith, K. A. & Wilson, I. A. *Crystal Structure of the IL-2 Signaling Complex: Paradigm for a Heterotrimeric Cytokine Receptor*. www.pnas.orgcgidoi10.1073pnas.0511161103 (2006).

181. Dutcher, J. P. *et al.* High dose interleukin-2 (Aldesleukin) - expert consensus on best management practices-2014. *Journal for ImmunoTherapy of Cancer* vol. 2 Preprint at https://doi.org/10.1186/s40425-014-0026-0 (2014).

182. Shimasaki, N., Jain, A. & Campana, D. NK cells for cancer immunotherapy. *Nature Reviews Drug Discovery 2020 19:3* **19**, 200–218 (2020).

183. Geller, M. A. *et al.* A phase II study of allogeneic natural killer cell therapy to treat patients with recurrent ovarian and breast cancer. *Cytotherapy* **13**, 98–107 (2011).

184. Bachanova, V. *et al.* Allogeneic natural killer cells for refractory lymphoma. *Cancer Immunol Immunother* **59**, 1739–1744 (2010).

185. Pahl, J. H. W., Cerwenka, A. & Ni, J. Memory-Like NK cells: Remembering a previous activation by cytokines and NK cell receptors. *Front Immunol* **9**, 417507 (2018).

186. Leong, J. W. *et al.* Preactivation with IL-12, IL-15, and IL-18 induces CD25 and a functional high-affinity IL-2 receptor on human cytokine-induced memory-like natural killer cells. *Biol Blood Marrow Transplant* **20**, 463–473 (2014).

187. Ni, J., Miller, M., Stojanovic, A., Garbi, N. & Cerwenka, A. Sustained effector function of IL-12/15/18–preactivated NK cells against established tumors. *Journal of Experimental Medicine* **209**, 2351–2365 (2012).

188. Romee, R. *et al.* Cytokine-induced memory-like natural killer cells exhibit enhanced responses against myeloid leukemia. *Sci Transl Med* **8**, (2016).

189. Daher, M. *et al.* Targeting a cytokine checkpoint enhances the fitness of armored cord blood CAR-NK cells. *Blood* **137**, 624–636 (2021).

190. Akman, B. *et al.* PRDM1 decreases sensitivity of human NK cells to IL2-induced cell expansion by directly repressing CD25 (IL2RA). *J Leukoc Biol* **109**, 901–914 (2021).